UNIVERSITY OF CALIFORNIA,
IRVINE

Epigenetic Regulation of White-Opaque Switching in *Candida albicans*

DISSERTATION

submitted in partial satisfaction of the requirements
for the degree of

DOCTOR OF PHILOSOPHY

in Biomedical Sciences

by

Zhiyun Guan

Dissertation Committee:
Professor Haoping Liu, Chair
Professor Peter Kaiser
Professor Suzanne Sandmeyer
Professor Kyoko Yokomori

2014

DEDICATION

To my family
For their constant support and inspiration

TABLE OF CONTENTS

LIST OF FIGURES

LIST OF TABLES

Page

ACKNOWLEDGMENTS

This dissertation owes its completion to the help and support of many people. First and foremost, I would like to thank my advisor, Dr. Haoping Liu. As a mentor, Dr. Liu has been a constant source of guidance and inspiration since I joined her lab, and has been patient and supportive of my research over the years, and through many unexpected findings and challenges. Her engaging approach and passionate for science has helped me grow as a more critical thinker and disciplined, curious scientist. None of this would have been possible without her.

I thank the current and former members of the Liu lab for their support, knowledge, and camaraderie. Our lab manager, Shelley Lane, has offered invaluable suggestions on my projects, as well as technical training and support, over the years. I would also like to thank my current fellow graduate students, Selma Alkafeef and Ohimai Unoje, for always being available to discuss scientific questions, lend a helping hand, as well as for making the lab a livelier and more enjoyable place. I also thank Dr. Yang Lu, Dr. Su Chang, Dr. Fuqiang Wang and Dr. Lianjuan Yang for their assistance and helpful discussions. Our former lab members, Dr. Brian Mochon, Dr. Allen Wang, Dr. John Stevenson, and Will Baker were also extremely helpful in years past in helping me get started on studying white-opaque switching, and for instilling an indomitable spirit in our lab culture that persists to this day, and I am grateful to everyone.

I would like to thank my committee members, Drs. Peter Kaiser, Suzanne Sandmeyer, and Kyoko Yokomori for their involvement and immensely helpful suggestions and questions regarding my projects. My thanks also extends to other faculty and current and former students in the Department of Biological Chemistry, for training on technical procedures and shared

equipment, and for always providing a welcome, intellectually engaging atmosphere. In particular, I thank Stacey Borrego and Dr. Kristina Clemens for help and training with polysome profiling. I also thank Dr. Qing Nie in the Department of Mathematics, and his current and former lab members, for collaborative projects and helpful discussions, and I also thank Dr. Nie for serving on my advancement committee. I thank the Institute for Genomics and Bioinformatics and the Center for Complex Biosciences at UCI for opportunities to learn about computational biology and think about my project in a different way as well as sharing my work with others. In particular, I am grateful for the opportunity to have participated in the Biomedical Informatics Training grant through IGB.

I thank the Biological Chemistry department staff for making life in the department easier and more friendly for everyone. I would also like to thank the mentors I worked with prior to coming to UCI, Dr. Judith Campbell at Caltech and Dr. Miriam Polne-Fuller at UCSB, for inspiring and supporting my interest in research.

I owe much thanks to my friends currently or formerly at UCI for friendship, encouragement, and always being available to talk science. I also thank my friends that I met before UCI for always being there through the years. Finally, I thank my family for their unconditional love and support, and for inspiring and encouraging a love of learning for as long as I could remember.

This research was supported by the National Institutes of Health grants (R01GM/AI55155 and R01AI099190) to Dr. Haoping Liu and a National Library of Medicine Biomedical Informatics Training grant (5T15LM007443) to Zhiyun Guan.

CURRICULUM VITAE

Zhiyun Guan

EDCUATION

Doctor of Philosophy in Biomedical Sciences 2014
University of California, Irvine Irvine, California

Bachelor of Science in Biology 2008
California Institute of Technology Pasadena, California

RESEARCH EXPERIENCE

Graduate Student Researcher 2008-2014
University of California, Irvine Irvine, California
Advisor: Dr. Haoping Liu
Department of Biological Chemistry
Project: Regulation of white-opaque switching in *Candida albicans*

Undergraduate Research Fellow 2005 - 2008
California Institute of Technology Pasadena, California
Advisor: Dr. Judith Campbell
Department of Biology and Chemistry
Project: The S-phase checkpoint in *Saccharomyces Cerevisiae*

PUBLICATIONS

Lou H, Komata M, Katou Y, **Guan Z**, Reis C, Budd M, Shirahige K, Campbell JL. (2008) Mrc1 and DNA polymerase ε function together in linking DNA replication and the S phase checkpoint. Molecular Cell. 32, 106-117.

WORKS IN PROGRESS

Guan Z, Liu H. The *WOR1* 5'untranslated region regulates white-opaque switching in *Candida albicans* by reducing translational efficiency. 2014. *Manuscript in review.*

Guan Z, Liu H. Overlapping functions between *SWR1* deletion and H3K56 acetylation in *Candida albicans* . 2014. *Manuscript in preparation.*

TEACHING EXPERIENCE

Teaching Assistant 2010
University of California, Irvine Irvine, California
BIO SCI D111L: Developmental & Cell Lab Spring 2010

HONORS AND FELLOWSHIPS

UCI Biomedical Informatics Training Program Fellow 2010-2012
UCI Center for Complex Biological Systems Opportunity Award 2010
Caltech Summer Undergraduate Research Fellowship (SURF) 2007-2005
Howard Hughes Medical Institute Fellow 2007
Michael Mathis Endowed Scholarship 2006

MEETINGS ATTENDED

12th American Society for Microbiology Conference on Candida & Candidiasis
New Orleans, LA. March 2014
Poster presentation
Abstract title: Deposition of H2A.Z by SWR1 regulates epigenetic switching and interacts with H3K56 acetylation in *Candida albicans*.

The Center for Complex Biological Systems Annual Retreat, UC Irvine. March 2011
Oral presentation
An integrated approach to the epigenetic regulation of feedback in white-opaque switching in *Candida albicans.*

The Center for Complex Biological Systems Annual Retreat, UC Irvine March 2010
Poster presentation
A temporal profile of *WOR1*, a major regulator of the white-opaque switch in *Candida albicans*, reveals negative autoregulation during switching.

ABSTRACT OF THE DISSERTATION

Epigenetic Regulation of White-Opaque Switching in *Candida albicans*

By

Zhiyun Guan

Doctor of Philosophy in Biomedical Sciences

University of California, Irvine, 2014

Professor Haoping Liu, Chair

Candida albicans, a significant human fungal pathogen, switches between two phenotypic states, white and opaque. The white-opaque switch is a unique and tractable system for the study of epigenetic regulation of gene expression. Switching is controlled by a transcriptional regulatory network of interlocking feedback loops on the master regulator *WOR1*. Translational regulation of the network, as well as chromatin-level regulation of *WOR1*, have not been extensively explored. This dissertation investigates the means through which *WOR1* expression and the white-opaque phenotype are epigenetically regulated, and identifies several novel mechanisms.

The long 5' untranslated region of *WOR1* was identified as a translational regulator of the white-opaque transition. Deletion of the *WOR1* 5'UTR promoted white-opaque switching and stabilized opaque state. Transcripts containing the *WOR1* 5'UTR show reduced translational efficiency and lower polysome association, and this repressive effect may exist for additional key regulators of cell fate and morphology with long 5'UTR.

The role of the histone variant H2A.Z in chromatin-level epigenetic regulation of switching was investigated. Deletion of *SWR1*, the major subunit of the SWR1 complex depositing H2A.Z into

chromatin, promoted white-opaque switching. Deletion of *YNG2*, a subunit of NuA4 histone acetyltransferase complex that targets SWR1 activity, produced a similar switching phenotype. Through nucleosome mapping, SWR1 was demonstrated to be required for proper nucleosome positioning and stability on the *WOR1* promoter, with effects differing in white and opaque cells. Furthermore, H2A.Z was enriched at the *WOR1* promoter in white cells, suggesting stabilization of a repressive chromatin state. An interaction was discovered between *swr1* and elevated H3K56ac resulting in a severe synthetic growth defect on nicotinamide, as well as a synergistic effect on white-opaque switching, suggesting altered nucleosome turnover from this interaction.

Finally, the role of the long promoter of *WOR1* was investigated. Truncation of the promoter to a 3 kb region, while sufficient to drive opaque-specific gene expression, abrogated switching to opaque, pointing to *cis*-regulatory elements further upstream. The studies described in this dissertation identify novel translational as well as nucleosome-level regulations of *WOR1* expression and white-opaque switching, with further implications for epigenetic regulation.

Chapter 1

Introduction

The diploid yeast *Candida albicans* is associated with humans as a commensal as well as a major fungal pathogen. In healthy individuals, *C. albicans* exists as a harmless commensal, and is found on the skin, oral-pharyngeal, gastrointestinal, and urogenital tract (Calderone & Fonzi, 2001). The commensal form of *C. albicans* may be carried by 50% to 90% of healthy individuals (Odds, 1987). As a pathogen, *C. albicans* can cause localized infection of mucosal membranes, as well as systemic infection known as candidiasis, particularly in immunocompromised patients. The mortality rate of systemic infections is up to 50%, and is a particularly serious concern as a hospital-acquired infection (Wey *et al.*, 1988). The phenotypic plasticity of *C. albicans* contributes to its success as a commensal and pathogen. *C. albicans* can switch between a budding yeast form to a filamentous hyphal form, and this transition is important to its virulence (Lo *et al.*, 1997).

White-opaque switching in *Candida albicans*

In addition to the yeast-hyphal transition, *C. albicans* also undergoes switching between two epigenetically heritable phenotypic states, white and opaque. The white-opaque transition was

first described in the clinical isolate WO-1 (Slutsky *et al.*, 1987). Cell and colony morphology differ between white and opaque state: white cells appear round and form smooth, glossy, domed colonies, while opaque cells are elongated and form larger, flatter, dull colonies. Spontaneous switching between the two states is stochastic and reversible, and occurs approximately every 10^4 to 10^5 generations (Rikkerink *et al.*, 1988). White-to-opaque switching can be induced by environmental conditions, such as genotoxic stresses, N-acetyl-glucosamine (GlcNAc) as a carbon source, anaerobic conditions, and high CO_2 concentration (Huang *et al.*, 2010, Ramirez-Zavala *et al.*, 2008, Alby & Bennett, 2009). Growth at 37^{o}C converts opaque cells to white (Bergen *et al.*, 1990). White and opaque cells exhibit distinct gene expression profiles, with 1306 genes transcribed differentially between the two states (Tuch *et al.*, 2010). In addition, white and opaque cells adapt to host defenses differently, with white cells more capable of causing infections in the bloodstream, while opaque cells are more efficient in colonizing skin, and in escaping macrophage detection (Kvaal *et al.*, 1999, Lachke *et al.*, 2003, Lohse & Johnson, 2008). Opaque cells are mating-competent, and *MTL**a*** or *MTLα* opaque cells mate with 10^6 greater efficiency compared to white cells. In *MTL**a**/α* cells, the **a**1-α2 heterodimer represses opaque formation (Miller & Johnson, 2002). Although the majority of natural *C. albicans* isolates are *MTL**a**/α*, a recent study has shown that passage through the mammalian gut promotes a phenotypic switch of *MTL**a**/α* cells to opaque-like cells that are more fit for GI colonization and commensalism (Pande *et al.*, 2013). In addition, *MTL**a**/α* cells are capable of opaque formation under high CO_2 and with GlcNAc as a carbon source, conditions that mimic the host environment (Xie *et al.*, 2013). These findings support the notion that white-opaque switching can occur in a majority of *C. albicans* strains and is highly relevant to *Candida*-host interactions. The white-opaque switch is a promising model for epigenetic regulation.

Regulation of the white-opaque transition by *WOR1*

The master regulator of white-opaque switching is *WOR1* (White-Opaque Regulator 1), which is highly expressed in opaque cells but not white cells (Figure 1.1). *WOR1* is required for switching to opaque and its ectopic expression converts cells from white to opaque state, even in *MTL**a**/α* cells. (Huang *et al.*, 2006, Srikantha *et al.*, 2006, Zordan *et al.*, 2006). White-opaque switching and *WOR1* transcription are regulated by a circuit of interlocking transcriptional feedback loops, consisting of regulators *WOR1*, *EFG1*, *CZF1*, *WOR2*, *WOR3*, and *AHR1* (Downs *et al.*, 2004, Zordan *et al.*, 2007, Levchenko & Jackson, 2004, Lohse *et al.*, 2013, Hernday *et al.*, 2013). Wor1 protein has been shown to contain a novel DNA-binding domain, and promotes its own expression by binding to the *WOR1* promoter up to 8kb upstream of the coding sequence (Zordan *et al.*, 2007, Lohse *et al.*, 2010). *EFG1* represses *WOR1* transcription and promotes white state, and deletion of EFG1 promotes opaque state (Sonneborn *et al.*, 1999). *CZF1* contributes to opaque state formation, while *WOR2* is necessary for opaque stability (Zordan *et al.*, 2007). Feedback between these regulators make up the core circuitry of white-opaque regulation (Figure 1.2). More recently, *WOR3* has been identified to promote opaque formation and stability (Lohse *et al.*, 2013), and *AHR1* to repress the white-opaque transition (Wang *et al.*, 2011). All of the identified key regulators have been found to bind to the promoters of other regulators in the network, forming a complex circuitry of transcriptional feedback regulating white and opaque state (Hernday *et al.*, 2013).

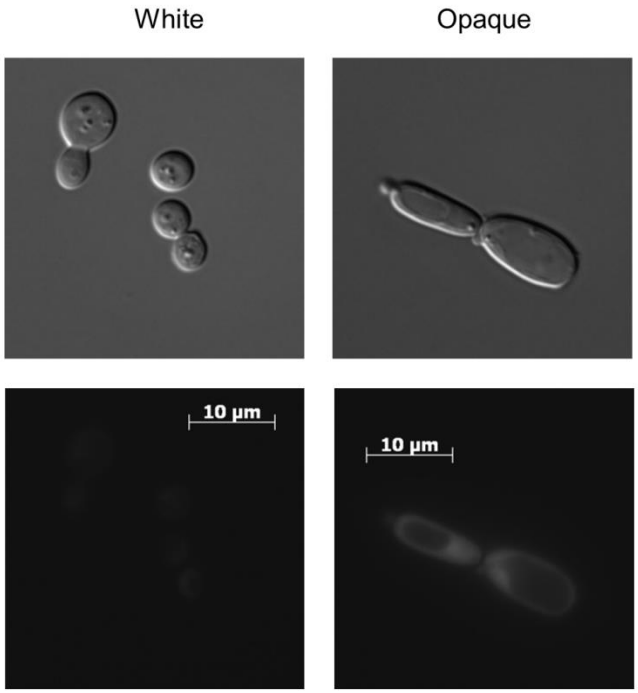

Figure 1.1. White and opaque cells of *C. albicans* show opaque-specific *WOR1* expression
DIC and fluorescence microscopy images of white and opaque *C. albicans* cells of genotype WT + p*WOR1-GFP* (HLY3555), where GFP fluorescence is a reporter of *WOR1* expression.

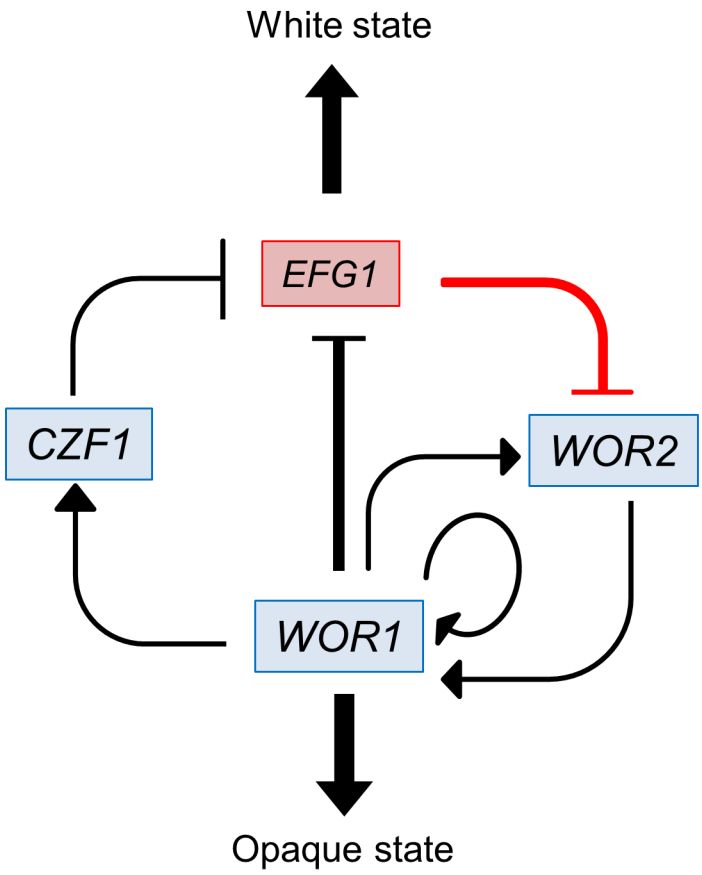

Figure 1.2**:** The core white-opaque transcriptional regulation circuitry. The core transcriptional network regulating white and opaque cell states, consists of *WOR1*, *EFG1*, *CZF1*, and *WOR2*.

Epigenetic regulation of *WOR1* expression

While the transcriptional regulation of *WOR1* has been extensively characterized, additional mechanisms behind the epigenetic regulation of white and opaque state through *WOR1* expression remain to be explored. In particular, the translational regulation of *WOR1*. Notably, *WOR1*, as well as other transcriptional regulators in the white-opaque circuit, have long 5' untranslated regions (5'UTR) (Bruno *et al.*, 2010, Tuch *et al.*, 2010). In numerous higher eukaryotes, the 5'UTR has been characterized to regulate translation through various mechanisms such as upstream ORFs, internal ribosome entry sites, RNA-binding proteins, and secondary structures (Gilbert *et al.*, 2007, Hellen & Sarnow, 2001, Morris & Geballe, 2000, Gray & Hentze, 1994, Pickering & Willis, 2005). The *WOR1* 5'UTR is thus a promising target for regulation of white-opaque switching through *WOR1* translation. Chapter 3 of this dissertation identifies a role for the *WOR1* 5'UTR in reducing translational efficiency of *WOR1*, as well as exploring its implications for regulation of white-opaque switching and other morphological transitions in *C. albicans*.

Chromatin-level regulation of epigenetic phenomena has been extensively studied in eukaryotic organisms. In *C. albicans*, Histone 3 Lysine 56 acetylation has been shown to promote white-opaque switching (Stevenson & Liu, 2011). Much remains to be explored on the regulation of *WOR1* on a chromosomal level, particularly as relating to nucleosomal stability and dynamics. In Chapter 4 of this dissertation, the role of deposition by the histone variant H2A.Z by the chromatin remodeling complex SWR1 on the regulation of *WOR1* and white-opaque switching, as well as its interaction with H3K56 acetylation, are discussed. Finally, in addition to a long

5’UTR, *WOR1* also has a long 8 kb promoter crucial to its regulation and the binding of its regulators. In Chapter 5 of this dissertation, the role of the promoter in phase-specific *WOR1* expression and opaque formation is discussed.

Chapter 2

Materials and Methods

Strains and culturing conditions

Strains used in this study are listed in Tables 2.1 through 2.3. For liquid culture, strains were grown in YEP (1% yeast extract, 2% peptone) + 2% dextrose or maltose, or SCD (synthetic complete + 2% dextrose) media unless otherwise described. Colonies were maintained on YEP agar at room temperature for opaque cells or 30 ℃ for white cells.

Strain construction

For Chapter 3, plasmid p*MAL2*-*WOR1*-HA was constructed in this lab as described by Huang et al (Huang *et al.*, 2006). Plasmid *WOR1*p-Δ5'*WOR1*-HA was modified from p*MAL2*-*WOR1*-HA by replacing the *MAL2* promoter with a fragment of the *WOR1* promoter 5081 to 1975 base pairs upstream of the start codon, which does not include the 5'UTR sequence. *WOR1p-Δ5'WOR1-HA* was digested with ClaI for integration at the ClaI site 4647 bp upstream of the *WOR1* start codon, and transformed into the strain *WOR1/wor1::HIS1* to produce 5'UTR-*WOR1*/Δ5'-*WOR1*, or *wor1Δ* to produce Δ5'-*WOR1/wor1*. Transformants were selected for growth on SCD-ura.

Integration of Δ5'-*WOR1* into the correct allele in the *WOR1/wor1::HIS1* background was verified by Southern blotting. To construct the Δ5'-*WOR1/* Δ5'-*WOR1* strain, the *URA3* marker in Δ5'-*WOR1/wor1* was replaced with the *SAT1* marker to confer nourseothiricin (NAT) resistance. The *SAT1* marker driven by the *ACT1* promoter was amplified from plasmid pNIM1(Ramirez-Zavala *et al.*, 2008), with flanking sequences homologous to *URA3* introduced during amplification, then transformed into Δ5'-*WOR1/wor1* . NAT^R and *ura3*- strains were selected from colonies capable of growth on YPD + 200mM NAT and incapable of growth on SCD-ura, then transformed again with plasmid *WOR1*p-Δ5'*WOR1*-HA, resulting in the Δ5'-*WOR1/* Δ5'-*WOR1* strain. Nourseothiricin was obtained as ClonNAT from WERNER BioAgents. The *MAL2p-5'UTR-WOR1-HA* plasmid was constructed by inserting a PCR amplification product containing the *WOR1* 5'UTR into the XbaI site at the 5' end of *WOR1* in p*MAL2-WOR1*-HA.

The *MAL2p-myc-GFP* plasmid was modified from the *MAL2p-myc-HGC* plasmid (Levchenko *et al.*, 2005), by replacement of *HGC* with a 700 bp *GFP* fragment (Wunsch & Jackson, 2005). The *MAL2p-5'UTR-GFP* plasmid was modified from the *MAL2p-myc-GFP* plasmid by excision of the 13-myc tag via digestion with XbaI and MluI, and replacement with a PCR product containing the *WOR1* 5'UTR. All plasmids containing the *MAL2* promoter described in this study were digested with AscI for integration at the *ADE2* locus for transformation into *C. albicans*. The WT + *WOR1p-GFP* + *MAL2p-WOR1* strain was constructed as described in (van Daal & Elgin, 1992).

The *ago1* mutant was constructed by deleting *AGO1* from the wild-type strain SN148 using the two-step PCR deletion method described by Noble and Johnson (Noble & Johnson, 2005). One copy of *AGO1* was replaced with *Candida dubliniensis HIS1* from pSN52. Due to difficulty of directing replacing the second copy, a *MAL2p-AGO1-URA3* plasmid was transformed into the resulting *AGO1/ago1* strain and integrated at the *ADE2* locus. Subsequently, the remaining copy of *AGO1* at its native locus was replaced with *Candida maltosa LEU2* amplified from pSN40, and the *MAL2p-AGO1-URA3* insert eliminated by growth on 5'FOA. Complete deletion of *AGO1* was verified by PCR. The *MAL2p-AGO1-URA3* plasmid was modified from BES116 (Jackson, 1987).

In Chapter 4, *SWR1* was deleted using the deletion cassettes described by Noble & Johnson (Noble & Johnson, 2005). PCR amplification of *Candida dubliniensis HIS1* from plasmid pSN52, or *Candida dubliniensis ARG4* from plasmid pSN69, was performed using long primers containing flanking sequences to *SWR1*, such that the PCR product flanked by 90 bp sequences homologous to flanking sequences of *SWR1*. The PCR product was then transformed into WT (JYC1) *C. albicans* to replace *SWR1* by homologous recombination. Transformants were selected for survival on SCD-his and –arg media, and deletion of *SWR1* was verified by PCR.

H2A.Z (*HTA3*) was HA-tagged by PCR amplification of the *HTA3* coding sequence with 3x-HA tag at the 5' of the sequence, with HindIII and PstI sites introduced 5' and 3' of the amplicon respectively. The *HTA3* promoter was amplified in a separate reaction, flanked by XhoI and HindIII sites. Subsequently, the HA-*HTA3* and *HTA3* promoter sequences were inserted into the p*WOR1-GFP-SAT1* plasmid (Stevenson & Liu, 2011), replacing the *GFP* and *WOR1* promoter

sequences respectively. The plasmid was digested with MscI prior to transformation into WT or *swr1* strains.

In Chapter 5, the p*WOR1-GFP-URA* plasmid (Huang *et al.*, 2006) was integrated at the *ADE2* locus by digestion with AscI to produce the WT + 3kb *pWOR1-GFP* strain. To generate a plasmid with *GFP* driven by a 2.4kb version of the *WOR1* promoter, the p*WOR1-GFP-URA* plasmid was digested to MulI and ClaI to excise the 3.0 kb to 2.4 kb fragment. The remaining large fragment was extracted using the QiaQuick Gel Extraction Kit, and Klenow was used to fill in 5' overhangs. The blunt-ended fragment was then ligated to itself using T4 DNA Ligase, producing the 2.4kb-p*WOR1-GFP-URA* plasmid, which was used to generate the WT + 2.4kb *pWOR1-GFP* strain.

To construct the 3kb-promoter-*WOR1/wor1* strain, the p*WOR1-GFP* plasmid carrying the 3kb *WOR1* promoter fragment was digested at the BglII site 1.4kb upstream of the *WOR1* start codon. Subsequently, the digestion product was transformed into the *WOR1/wor1* strain. Integration of the 3kb *WOR1* promoter upstream of the intact copy of *WOR1* was verified by PCR using primers homologous to the pBluescript sequence of the base plasmid, and the 5' sequence of *WOR1*. Integration of the 3 kb *WOR1* promoter upstream of *wor1::HIS1* resulted in the strain used as full-promoter-*WOR1/wor1* control.

All primers used in strain construction, and for other assays except qPCR and nucleosome mapping, are listed in Table 2.4.

Candida albicans transformation

Strains were grown overnight at 30 ℃ in liquid YPD medium, then diluted 1:50 into 25 ml fresh YPD medium. After 6 hours of growth at 30 ℃, 2 ml of cell culture was pelleted, and washed once with TEL buffer (10mM Tris-HCl pH=7.5, 1mM EDTA, 0.1M LiAcetate). Pellets were resuspended in 100ul TEL buffer, and 15 µl boiled salmon sperm DNA and up to 60 µl transforming DNA added. Samples were incubated with rotation for 30 minutes at 30 ℃. 700 µl of 40% PEG-TEL were added, and samples were further incubated with rotation overnight. Subsequently, samples were heat-shocked at 42 ℃ for 1 hour with inversion every 15 minutes, washed once in water, resuspended in 5 ml YPD, and incubated 1 to 2 hours at 30 ℃. Finally, cells were washed and plated to selective medium.

Switching assays

Stable white or opaque cells from log-phase cultures were plated at density of 100 cells/plate, using 100 µl of a dilution of 1000 cells/ml, to SCD agar plates. Colony morphology was scored after 7 days. Both whole-colony and sectored switching events were counted. For white-opaque switching assays, plates were incubated at 25 ℃. For opaque stability assays, plates were incubated at 25 and 37 ℃.

To assay switching in CO_2 or on GlcNAc in Chapters 3 and 4, stable white or opaque cells from log-phase cultures were spread to agarose plates of Lee's medium (modified from (Manning & Mitchell, 1980)) supplemented with 25 µg/ml uridine and 50 µg/ml arginine, with 1.25%

dextrose or N-acetyl-D-Glucosamine (Spectrum Chemical) as carbon source. For CO_2 assay, plates were incubated in a Thermo Forma Series II Water Jacketed CO_2 incubator at 25C with 5% CO_2. Colony morphology was scored after 7 days. Both whole-colony and sectored switching events were counted.

Northern blotting

RNA was extracted from log-phase cultures using the Qiagen RNeasy kit. Northern blotting was conducted as described in (Chen *et al.*, 2002). A 500 bp PCR product of *WOR1* or *GFP* was used to probe for RNA containing the region of interest. Loading was assessed using a fragment of *ACT1* as probe, or with visualization of ribosomal RNA. Primers used for amplification of the *WOR1* probe are listed as WOR1probeF/R in (Huang *et al.*, 2006).

Western blotting

Protein extraction was modified from (Meimoun *et al.*, 2000). After precipitation with TCA as described, samples were washed once with acetone and boiled 5 min with equivolume urea buffer (8M urea, 4M 2-mercaptoethanol, 125mM Tris pH 6.8, and 10% SDS), then centrifuged 5 min at 13 krpm. The supernatant was mixed with equivolume 20% glycerol + bromophenol blue, and run on SDS-PAGE gels for Western blotting. The HA tag was detected with monoclonal rabbit anti-HA antibody from Abcam. GFP was detected with Living Colors monoclonal mouse anti-GFP antibody from Clontech. PSTAIRE (Cdc28) antibody was obtained from Invitrogen. Secondary IgG antibodies (anti-mouse or anti-rabbit) were obtained from BioRad.

Polysome profiling

Polysome profiling was modified from Masek et al (Masek *et al.*, 2011). *C. albicans* cultures were grown to OD_{600} = 0.6, treated with 1mg/ml cycloheximide, and incubated at 4℃ for 5 minutes. 50 ml of culture were collected for each sample. Extraction buffer as described by Masek et al was supplemented with 1mg/ml cycloheximide. 7-47% sucrose gradients were prepared by stepwise freezing of 2.4 ml each of 7%, 17%, 27%, 37%, and 47% sucrose in Beckman Coulter polyallomer centrifuge tubes at -80℃, then thawing at 4℃ overnight. Lysate samples were applied to gradients and centrifuged at 35,000 rpm at 4℃ for 2.5 hours in a Beckman SW41 rotor. Gradients were fractionated, absorbance was read at 254nm, and polysome profile was created using the ISCO Gradient Fractionator (Teledyne). Fractions were collected using the Foxy Jr Fraction Collector. Fractions of 500 µl each were added to 800 µl 8M guanidine HCl and 700 µl 100% EtOH, and placed at -20℃ overnight for RNA precipitation. Pellets were washed with 70% EtOH and resuspended in 30 µl RNase-free water for subsequent use in RT-qPCR.

Quantitative PCR

cDNA was synthesized from 2µg total RNA using the BioRad iScript Reverse Transcription Kit. Quantitative PCR using the BioRad SYBR Green mix was performed on the BioRad iCycler. Cycle conditions were 95℃ for 1 minute, then 39 cycles of 95℃ for 10 seconds, 56℃ for 45 seconds, 68℃ for 20 seconds. Melt curve was taken starting at 50℃ with 0.5℃ increments for

5s, 90 cycles. All reactions were carried out in triplicate. Primers used for qPCR are listed in Table 2.5.

Splint ligation for qSL-RT-PCR

10 µg total RNA, 20 pmol of DNA splint, and 30pmol of RNA anchor were mixed and incubated at 70 ℃, 60 ℃, 42 ℃, and 25 ℃, for 5 minutes at each step. 20 U T4 DNA ligase (Invitrogen), T4 DNA ligase buffer, and 20 U RNase Inhibitor Plus (Promega) were then added, and ligation allowed to proceed overnight at 15 ℃. Ligase was omitted for control samples. Reactions were then treated with DNase using the Qiagen DNAse kit and protocols described therein. RNA was extracted using phenol/chloroform, precipitated with 1ml 100% EtOH and 0.3M sodium acetate for 2 hours at -20 ℃, and washed once with 70% EtOH. RNA was then resuspended in 13.3 µl RNase-free water, and used for RT-qPCR.

Fluorescence Activated Cell Sorting (FACS)

FACS was conducted using the BD FACSCalibur system. FL1-H channel was used for GFP detection, and 10,000 cells were counted per sample. Results were analyzed with FlowJo cytometry analysis software.

Nucleosome mapping

Micrococcal nuclease (MNase) digestion was modified from (Kent & Mellor, 1995) and (Bai *et al.*, 2010). Cells were grown to OD_{600} = 2, then crosslinked with 2% formaldehyde at growth temperature for 30 min before treatment with zymolase to spheroplast cells. Spheroplasts were then treated with a titration of 2 to 8 units of *Staphylococcus aureus* MNase from Signma Aldrich, and digested samples were visualized by electrophoresis on 2% agarose gel. Samples with a distinct mononuclesome and dinucleosome band pattern were selected for further analysis. DNA from these samples was isolated using phenol/chloroform extraction and used for qPCR for nucleosome mapping. Nucleosomal enrichment was normalized to values for the -1 nucleosome at *BUD2*. A full list of the primers used for mapping the *WOR1* promoter is available in Table 2.6. Chromatin immunoprecipitation was performed on mononucleosomal DNA as described in (Lu *et al.*, 2011). Anti-HA antibody (Abcam) was used for immunoprecipitation of HA-tagged H2A.Z.

Spot assays

C. albicans strains were grown in liquid YPD medium to log phase and diluted to OD_{600} = 0.1, after which 5 additional 5-fold serial dilutions were made into ddH_2O a 96-well plate. An 8-channel multipipettor was used to transfer 2.5µl of each dilution onto YPD agarose plates. For drug treatment plates, nicotinamide and MMS were obtained from Sigma Aldrich. Plates were incubated for 3 days at 30℃ and colony growth imaged with Fujifim LAS-4000 imager.

Sorbose assay for aneuploidy

Cells from log-phase liquid culture were plated at a density of 100 cells/plate onto Lee's medium with 2% L-sorbose or dextrose as a carbon source and incubated at 30℃ for 6 days. Survival was calculated as the ratio of colonies formed on sorbose to those formed on dextrose.

H2A-phosphorylation assay

To assay phosphorylation of H2A, 0.2% MMS or 50mM NAM was added to cells growing at log phase in YPD liquid medium at 30℃ for 1 hour. Cells were then collected for Western blotting to detect H2A-γ using anti- H2A-γ antibody from Abcam. To assay clearance of H2A-γ, cells were first treated with MMS or NAM as described, then washed 3x with ddH2O before resuspension into the same volume of YPD without drug, and allowed to continue to incubate. Samples were taken for Western blotting at 1, 2, and 4 hours after reinoculation.

Doxycycline treatment

For conditional repression in GRACE strains in Chapter 4, cells were grown on solid medium containing 50 μM doxycycline from Sigma Aldrich. For induction of the TET1 promoter in Chapter 5, cells were incubated in liquid medium with 50 μM doxycycline. In all cases, cell cultures were kept from direct light due to the light sensitivity of doxycycline.

Table 2.1: *C. albicans* strains used in Chapter 3 for *WOR1* 5'UTR studies

Name	Description	Genotype	Source
JYC1	WT	*MTL**a**/**a** ura3::imm434/ura3::imm434 his1::hisG/his1::hisG arg4::hisG/arg4::hisG*	Chen *et a.l*, 2002
JYC5	WT	*MTL**a**/**a** ura3::imm434/ura3::imm434*	Chen *et al.*, 2002
HLY3903 (NO605-13-13)	5'UTR-*WOR1/wor1*	*MTL**a**/**a** ura3::imm434/ura3::imm434 his1::hisG/his1::hisG arg4::hisG/ arg4::hisG WOR1/wor1::HIS1*	J. Chen; derived from CAH1 from Huang *et al.*, 2006
HLY3570 (CAH3)	*wor1Δ*	*MTL**a**/**a** ura3::imm434/ura3::imm434 his1::hisG/his1::hisG arg4::hisG/ arg4::hisG wor1::ARG4/wor1:: HIS1*	Huang *et al.*, 2006
HLY4212	5'UTR-*WOR1*/Δ5'-*WOR1*	*MTL**a**/**a** ura3::imm434/ura3::imm434 his1::hisG/his1::hisG arg4::hisG/ arg4::hisG WOR1/wor1::HIS1::Δ5'WOR1-URA3*	this study
HLY4213	Δ5'-*WOR1/wor1*	*MTL**a**/**a** ura3::imm434/ura3::imm434 his1::hisG/his1::hisG arg4::hisG/ arg4::hisG wor1::ARG4/wor1:: HIS1::Δ5'WOR1-URA3*	this study
HLY4214	Δ5'-*WOR1*/Δ5'-*WOR1*	*MTL**a**/**a** ura3::imm434/ura3::imm434 his1::hisG/his1::hisG arg4::hisG/ arg4::hisG wor1::ARG4::Δ5'WOR1-SAT1/wor1:: HIS1::Δ5'WOR1-URA3*	this study
HLY4215	JYC5 + *MAL2p-5'UTR-WOR1-HA*	*MTL**a**/**a** ura3::imm434/ura3::imm434 ADH1/adh1::pMAL2-5'UTR-WOR1-3XHA-URA3*	this study
HLY3569	JYC5 + *MAL2p-WOR1-HA*	*MTL**a**/**a** ura3::imm434/ura3::imm434 ADH1/adh1::pMAL2-WOR1-3XHA-URA3*	Huang *et al.*, 2006
HLY4216	JYC5 + *MAL2p-WOR1 5'UTR-GFP*	*MTL**a**/**a** ura3::imm434/ura3::imm434 ADH1/adh1::pMAL2-(WOR1)5'UTR-GFP-URA3*	this study
HLY4217	JYC5 + *MAL2p-GFP*	*MTL**a**/**a** ura3::imm434/ura3::imm434 ADH1/adh1::pMAL2-13myc-GFP-URA3*	this study
HLY3673	*ago1*	*MTL**a**/**a** his1Δ/his1Δ ura3Δ::imm434/ura3Δ::imm434 iro1Δ::imm434/iro1Δ::imm434 ago1::C. dubliniensis HIS1/ago1::C. maltosa LEU2*	this study
HLY4218	*ago1 + MAL2p-WOR1-5'UTR-GFP*	*MTL**a**/**a** his1Δ/his1Δ ura3Δ::imm434/ura3Δ::imm434 iro1Δ::imm434/iro1Δ::imm434 ago1::C. dubliniensis HIS1/ago1::C. maltosa LEU2 ADH1/adh1::pMAL2-(WOR1)5'UTR-GFP-URA3*	this study
HLY4219	*ago1+ MAL2p-GFP*	*MTL**a**/**a** his1Δ/his1Δ ura3Δ::imm434/ura3Δ::imm434 iro1Δ::imm434/iro1Δ::imm434 ago1::C. dubliniensis HIS1/ago1::C. maltosa LEU2ADH1/adh1::pMAL2-13myc-GFP-URA3*	this study
HLY4220	*ssd1*	*MTL**a**/α ura3::imm434/ura3::imm434 his1::hisG/his1::hisG arg4::hisG/arg4::hisG ssd1::HIS1/ssd1::ARG4*	Gank *et al*., 2008
HLY4221	*ssd1 + MAL2p-WOR1-5'UTR-GFP*	*MTL**a**/α ura3::imm434/ura3::imm434 his1::hisG/his1::hisG arg4::hisG/arg4::hisG ssd1::HIS1/ssd1::ARG4 ADH1/adh1::pMAL2-(WOR1)5'UTR-GFP-URA3*	this study

HLY4222	*ssd1+ MAL2p-GFP*	*MTL**a**/α ura3::imm434/ura3::imm434 his1::hisG/his1::hisG arg4::hisG/arg4::hisG ssd1::HIS1/ssd1::ARG4 ADH1/adh1::pMAL2-13myc-GFP-URA3*	this study
HLY4055	JYC5 + *WOR1p-GFP + MAL2p-WOR1*	*MTL**a**/**a** ura3::imm434/ura3::imm434 WOR1/wor1::pWOR1-GFP-URA3-WOR1 ADH1/adh1::pMAL2-WOR1-3XHA-SAT1*	Stevenson & Liu, 2013

Table 2.2: *C. albicans* strains used in Chapter 4 for study of *SWR1*

Name	Description	Genotype	Source
JYC1	WT	*MTL**a/a** ura3::imm434/ura3::imm434 his1::hisG/his1::hisG arg4::hisG/arg4::hisG*	Chen *et al*., 2002
HLY4235	*SWR1/swr1*	*MTL**a/a** ura3::imm434/ura3::imm434 his1::hisG/his1::hisG arg4::hisG/arg4::hisG SWR1/swr1::HIS1*	this study
HLY4233	*swr1*	*MTL**a/a** ura3::imm434/ura3::imm434 his1::hisG/his1::hisG arg4::hisG/arg4::hisG swr1::HIS1/swr1::ARG4*	this study
HLY3555	WT + *pWOR1-GFP*	*MTL**a/a** ura3::imm434/ura3::imm434 his1::hisG/his1::hisG arg4::hisG/arg4::hisG ADH1/adh1::pWOR1-GFP-URA3*	Huang *et al*., 2006
HLY4234	*swr1 + pWOR1-GFP*	*MTL**a/a** ura3::imm434/ura3::imm434 his1::hisG/his1::hisG arg4::hisG/arg4::hisG swr1::HIS1/swr1::ARG4 ADH1/adh1::pWOR1-GFP-URA3*	this study
HLC54/ HLY3600	*efg1 + pWOR1-GFP*	*ura3::1 imm434/ura3::1 imm434 efg1::hisG/efg1::hisG + ADH1/adh1::pWOR1-GFP-URA3*	Lo *et al*., 1997
HLY4238	WT + *HTA1-HA*	*MTLa/a ura3::imm434/ura3::imm434 HTA3/3xHA-HTA3-SAT1 ADH1/adh1::pMAL2-WOR1-URA3*	this study
HLY4236	*swr1 + HTA1-HA*	*MTL**a/a** ura3::imm434/ura3::imm434 his1::hisG/his1::hisG arg4::hisG/arg4::hisG swr1::HIS1/swr1::ARG4 ADH1/adh1::pWOR1-GFP-URA3 HTA3/3xHA-HTA3-SAT1 ADH1/adh1::pMAL2-WOR1-URA3*	this study
HLY3993	*HST3/hst3*	*MTLa/a ade2/ade2 ura3::ADE2/ura3::ADE2 HST3/hst3::FRT*	Stevenson & Liu, 2013
HLY3997	*rtt109*	*MTLa/a rtt109::FRT/rtt109::FRT*	Stevenson & Liu, 2013
CLY4	*yng2*	*MTLa/a ura3::1 imm434/ura3::1 imm434 yng2::hisG/yng2::hisG*	Lu *et al*., 2008
HLY3886	*yng2 + YNG2*	*MTLa/a ura3::1 imm434/ura3::1 imm434 yng2::hisG/yng2::hisG + YNG2-URA3*	Lu *et al*., 2008
SWR1: #2061	*SWR1/swr1* (GRACE)	modified CAI4	Roemer *et al*., 2003

Table 2.3: *C. albicans* strains used in Chapter 5 for study of the *WOR1* promoter

Name	Description	Genotype	Source
HLY3555	WT + (full promoter) p*WOR1-GFP*	*MTL**a/a** ura3::imm434/ura3::imm434 his1::hisG/his1::hisG arg4::hisG/arg4::hisG WOR1/wor1::pWOR1-GFP-URA3 WOR1*	Huang *et al.*, 2006
HLY3550	WT + 3kb p*WOR1-GFP*	*MTL**a/a** ura3::imm434/ura3::imm434 his1::hisG/his1::hisG arg4::hisG/arg4::hisG ADH1/adh1::pWOR1-GFP-URA3*	Huang *et al.*, 2006
HLY3895	WT + 2.4kb p*WOR1-GFP*	*MTL**a/a** ura3::imm434/ura3::imm434 his1::hisG/his1::hisG arg4::hisG/arg4::hisG ADH1/adh1:: 2.4kb pWOR1-GFP-URA3*	this study
HLY4239	3kb *WOR1* promoter-*WOR1/wor1* + p*WOR1-GFP*	*MTL**a/a** ura3::imm434/ura3::imm434 his1::hisG/his1::hisG arg4::hisG/ arg4::hisG 3kb-WOR1pro-WOR1 WOR1pro-GFP/wor1::HIS1*	this study
HLY4240	full promoter *WOR1/wor1* + 3kb p*WOR1-GFP*	*MTL**a/a** ura3::imm434/ura3::imm434 his1::hisG/his1::hisG arg4::hisG/ arg4::hisG WOR1/wor1::pWOR1-GFP-URA3 HIS1*	this study
HLY4241	3kb *WOR1* promoter-*WOR1/wor1* + p*WOR1-GFP* + *TET1-WOR1*	*MTL**a/a** ura3::imm434/ura3::imm434 his1::hisG/his1::hisG arg4::hisG/ arg4::hisG 3kb-WOR1pro-WOR1 WOR1pro-GFP/wor1::HIS1 ADH1/adh1::pTET1-WOR1-SAT1*	this study
HLY4242	full promoter *WOR1/wor1* + 3kb p*WOR1-GFP + TET1-WOR1*	*MTL**a/a** ura3::imm434/ura3::imm434 his1::hisG/his1::hisG arg4::hisG/ arg4::hisG WOR1/wor1::pWOR1-GFP-URA3 HIS1 ADH1/adh1::pTET1-WOR1-SAT1*	this study

Table 2.4: List of primers used for cloning and other experiments

Name	Sequence	Purpose
URA3_ACT1pSAT1_F	CCAACCAGCATCTCTATACCTTTTACCTTCAATATCTGGATCTCTTCCTTTACCAAACAATCCTCTACCA	amplifies from pNIM1 the *SAT1* marker with *URA3*-homologous sequences
URA3_SAT1_R	CCAACCAGCATCTCTATACCTTTTACCTTCAATATCTGGATCTCTTCCTTTACCAAACAATCCTCTACCATTAGGCGTCATCCTGTGCTC	amplifies from pNIM1 the *SAT1* marker with *URA3*-homologous sequences
UTR_F	CGTCTAGAAATTCTCAAAGTTTTGATTTCTATT	cloning the *WOR1* 5'UTR with XbaI site
UTR_R	CCTCTAGAAAGCTTTGCTTAATATTGAATTGAATTATAC	cloning the *WOR1* 5'UTR with XbaI and HindIII sites
UTR_del_F	CCTGCGGCCGCTGTAAACACTACACTACCAGC	for making the *WOR1*p-Δ*5*'-*WOR1* construct. 5081bp upstream of the *WOR1 ATG*.
UTR_del_R	CCGTCTAGAAAGCTTAAAAAATAGAAATCAAAACTTTGAG	for making the *WOR1*p-Δ*5*'-*WOR1* construct. 1975 bp upstream of the *WOR1* ATG.
AGO1 primer1	CTATATTCTGTTACGACGGCC	Primers 1-6 for deletion method described by Noble & Johnson
Uni primer2	CCGCTGCTAGGCGCGCCGTGACCAGTGTGATGGATATCTGC	
AGO1 primer3	CACGGCGCGCCTAGCAGCGGGATTGTTAAATAGCCAGAGACG	
AGO1 primer4	GTCAGCGGCCGCATCCCTGCTTCTTCTTCATCATCTCCTTCG	
Uni primer5	GCAGGGATGCGGCCGCTGACAGCTCGGATCCACTAGTAACG	
AGO1 primer6	TTGAAGTGAAAAATGTTCAATTGG	
XbaIAGO1_F	GCTCTAGAATGAGTGATTTGGTTAAATTTTC	cloning *MAL2p-AGO1*
MluIAGO1_R	CGACGCGTAATATAAAACATGGTGTTTTTAATAC	cloning *MAL2p-AGO1*
AGO1 up	GTAGTAGTTTATGTTGATAACGC	checking deletion of *AGO1*
AGO1 down	CTGGGCCAATTTCTGAGGC	checking deletion of *AGO1*
AGO1 INTF	CAATGAAATTGGGTATTATTGC	checking *AGO1* internal sequence
AGO1 INTR	ACATTGATCTTCAGTTTTGGC	checking *AGO1* internal sequence
GFP NF	CAACCTTAGTCACTACTTTCG	*GFP* probe for Northern blotting
GFP NR	CATACCATGGGTAATACCAGC	*GFP* probe for Northern blotting
SWR1D-F	CGATTTATTTAATTACAATTTCGGAAATTAAATCTCATCTTGCAGATCCAGCAAACACATCAAGCATATTCTCACAAGAAAACCAGAAATGCCAGAGAATGGAACCAGTGTGATGGATATCTGC	*SWR1* deletion

SWR1D-R	AGACTTATCCTTGATGTCTGTACTAGTACCAACGATACGCAAGAGA TTTTTATAAAAGAAAGGGCCATTTGCTTAATATGTAATACAAGGAG TGATACCATATAGCTCGGATCCACTAGTAACG	*SWR1* deletion
SWR1outsideF	TGTTTACACTGTAATTTTCTGC	for checking integration of deletion cassette at *SWR1* locus
SWR1outsideR	ACTATA CGATAT GGTATCCGT	
C.dubHIS-F	AACACAACTGCACAATCTGG	*C. dubliniensis HIS1* check
C.dubHIS-R	ATTAGATACGTTGGTGGTTC	*C. dubliniensis HIS1* check
C.dubARG-F	ACGGAGTACCACATACGATG	*C. dubliniensis ARG4* check
C.dubARG-R	ACACAGAGATACCTTGTACT	*C. dubliniensis ARG4* check
SWR1internalF	CTAATTCCAATATCCACCAAGC	*SWR1* internal sequence check, 963 bp from 3'
SWR1internalR	GACCTTGTGATATAACTTTCG	*SWR1* internal, 1134 bp from 5' of coding sequence
HTA3F3	CCGCTCGAGTGATGTCAAAGTTCCTACAAAG	*HTA3* promoter
HTA3R3	CCCAAGCTTTGCATAGTCCGGGACGTCATAGGGATAGCCCGCATA GTCAGGAACATCGTATGGGTACATTGTAGTGTTTGTTGTGGTTTCG	*HTA3* promoter
HTA3F4	CCCAAGCTTGGATCCTATCCATATGACGTTCCAGATTACGCTGCTA TGTCTGGGAAGGGAAAAGTGC	HA-*HTA3*
HTA3R4	GCAACTGCAGACCGCCACTAAATAGAGAGC	HA-*HTA3*
BScheck	CGAGGTCGACGGTATCGAT	for checking 3kb-promoter-*WOR1/wor1*
WOR1Rcheck	CACTTCCAGAAACTATAAGCA	for checking 3kb-promoter-*WOR1/wor1*

Table 2.5: List of primers used for quantitative PCR

Name	**5' to 3' Sequence**	**Target/purpose**
WOR1 UTR_F	CCCTGACATCACCTTTGTTG	5'UTR-*WOR1*
WOR1 UTR_R	TTCCCTTCCGTTAAATAACCC	5'UTR-*WOR1*
WOR1-HA F	TCTAATACCAGTGGTAATATTG	Δ5' *WOR1*-HA
WOR1-HA R	GGTACCGCATGCCTAAGCG	Δ5' *WOR1*-HA
ACT1_F	TGGAAGCTGCTGGTATTGAC	*ACT1*
ACT1_R	TTCAGCAATACCTGGGAACA	*ACT1*
CZF1_F	ACATT TACAACCCAT TTATTACG	*CZF1*
CZF1_R	AACGATAGTCTGTAACAATTTCT	*CZF1*
NRG1_F	ATTA TAATTAACCC CTCCTTGC	*NRG1*
NRG1_R	AATATTGGAAAATAGTAACCTGG	*NRG1*
EFG1_F	CAAGCAAACAAACGACCAAA	*EFG1*
EFG1_R	CAAGGGACACAAAGGGGTTA	*EFG1*
FLO8_F	CAAA AGTTTTGATT GATAAATTGC	*FLO8*
FLO8_R	CTGCCTTTAATGTCAGTTTGC	*FLO8*
RFG1_F	TAAT ATAGAAGGTT TTCCTTATAC	*RFG1*
RFG1_R	TATTTTCACAATTAAACCTTCAAG	*RFG1*
GFP1_F	GGAAGATCTCCTCTAAAGGTGAAGAATT	*GFP1*
GFP1_R	TAACCTTCTGGCATGGCAG	*GFP1*
RDN18_F	AAGA TGATCAGATA CCGTCG	*RDN18* (40S)
RDN18_R	GATTTCTCGTAAGGTGCCG	*RDN18* (40S)
RDN25_F	TCGAACGGCC TCTAGTGC	*RDN25* (60S)
RDN25_R	CCAACTGCTGTTGACATGG	*RDN25* (60S)
Anchor	GCUGAUGGCGAUGAAUGAACACUGCGUUUGCUGGCUUUGAUG	RNA Anchor for splint ligation
Splint-WOR1	AGAATAAATTCAAAACCTAAAAAATCAAAACATCAAAGCCAGCAAAC GCAGTGTTCATTC	Splint with homology to Anchor and *WOR1* 5'UTR
Splint-ACT1	TTTCTAAGAAAGAAAGAAAACCAGGAGTGACATCAAAGCCAGCAAAC GCAGTGTTCATTC	Splint with homology to Anchor and *ACT1*
Anchor_F	GGCGATGAATGAACACTGC	Amplifies ligation product
WOR1_SL-R	GTTAAGTGATCTAATTGATAGTAG	Amplifies ligated *WOR1*
ACT1_SL-R	CCGTCCATTTTGAATGATTATAT	Amplifies ligated *ACT1*

Table 2.6: List of primers used in Chapter 4 for nucleosome mapping of the *WOR1* promoter

Name/target amplicon location (bp upstream of *WOR1* ATG)	Sequence
ZG10F:3640-3540	TATACAGCCCATTGCTAGATC
ZG11F:3600-3500	AGAATGTCAAATGACATAATAAGA
ZG12F:3560-3460	GTAGAACCTGTACACTCTTTG
ZG13F:3520-3420	TATTTTTTTGCATTCTAGTTGCG
ZG14F:3480-3380	CTTTATTATTATCATTGTATGGTTT
ZG15F:3440-3340	CTAATGAATCCCGATAAATATATA
ZG16F:3400-3300	GAATCTTGTTTAAGTGATAGATT
ZG17F:3360-3260	AAAAAGTTTGTATCAGTTTCACTA
ZG18F:3320-3220	AATTACTGTTCAATCCCCAGAA
ZG19F:3280-3180	AAATCAACAGACTAACTACAAAC
ZG20F:3240-3140	TGAAAAATAAAAGGACAAAACAAG
ZG21F:3200-3100	TGGACTCTTCACTGTTTTGAAA
ZG22F:3160-3060	TATTTTCGTGAATATTTTTCCTTC
ZG23F:3120-3020	CTATTTTCAAGAAATTTCCACTT
ZG24F:3080-2980	TGTCCCCGTATTTGAGATATT
ZG25F:3040-2940	CTGAAATTTCCTGCTAGAGAG
ZG26F:3000-2900	TTATTCAAAATCTTGATACCCTAT
ZG27F:2960-2860	ATAGACTTTGATAGTTCATGATT
ZG28F:2920-2820	GTGCTTAATTCTAATTTTGCCA
ZG29F:2880-2780	GATCAAAAACAAAAAAAAAGAAAAT
ZG30F:2840-2740	ATGTCTATCTATATTCAAGTATC
ZG31F:2800-2700	GTAACTATAAAGGTTGTCTTGTA
ZG32F:2760-2660	TAACGTCATCTCATCTCAAATTT
ZG33F:2720-2620	AAACCAAAAAAAATTCTTAACTTTG
ZG34F:2680-2580	TTGTCGTCTTTGCTATAGTTAG
ZG35F:2640-2540	TTTCCTTTTTTTTGTCAATATCTC
ZG36F:2600-2500	TAGTATCAATATTACTGATCTTG
ZG37F:2560-2460	TGGCACTACCAAATGTAATAAT
ZG38F:2520-2420	AAATTTCGGGAGTTTAGTGATA
ZG39F:2480-2380	GGAAAAAAAAACAGGGAATTAC
ZG40F:2440-2340	GTATAGTCTGTGCAGACTTTG
ZG41F:2400-2300	CCTTGCATTTACAAAAGTTTAAAT
ZG42F:2360-2260	CTTTATTTAAAAACAAAAAAACAAAC
ZG43F:2320-2220	GGGAAACAAGGAACACAGTTA

ZG44F:2280-2180	GTTTATAGGCGGGTCTACATT
ZG45F:2240-2140	AAGAAAAAAAAACAACAATTACCAA
ZG46F:2200-2100	CCATTGTAACCATAAAGAAGTAT
ZG47F:2160-2060	AAGAAAAACCACTGGGTGTAAA
ZG48F:2120-2020	CAGATAGACATTTCATTTAAGCA
ZG97F:2080-1980	AGAGAGAAAACGAGAGAAGAAA
ZG98F:2040-1940	TTGAATTATTTAACACAACTTTGAA
ZG99F:2000-1900	CTCAAAGTTTTGATTTCTATTTTTT
ZG100F:1960-1860	TGAATTTATTCTTATTATTTTAACTC
ZG101F:1920-1820	CTATCAATTAGATCACTTAACTAT
ZG102F:1880-1780	TTTGCTGTTACTGCTACCACT
ZG103F:1840-1740	TTTTAAATTAAGTGAATTACCCC
ZG104F:1800-1700	GTCTTTTAAATTCAGGACACTAA
ZG105F:1760-1660	CGACCAACACTTTTTCTGATTT
ZG106F:1720-1620	CTCAGAAGTTCAATCACCGTT
ZG107F:1680-1580	ATAGGAGATTCCAGTTATCATT
ZG10R:3640-3540	AAAGAGTGTACAGGTTCTACT
ZG11R:3600-3500	GCAACTAGAATGCAAAAAAATAAT
ZG12R:3560-3460	CATACAATGATAATAATAAAGAAAA
ZG13R:3520-3420	TATTTATCGGGATTCATTAGCTT
ZG14R:3480-3380	CTATCACTTAAACAAGATTCGAA
ZG15R:3440-3340	AACTGATACAAACTTTTTCCTTT
ZG16R:3400-3300	TGGGGATTGAACAGTAATTGT
ZG17R:3360-3260	TGTAGTTAGTCTGTTGATTTACT
ZG18R:3320-3220	TTTTGTCCTTTTATTTTTCACAG
ZG19R:3280-3180	TCAAAACAGTGAAGAGTCCAC
ZG20R:3240-3140	GAAAAATATTCACGAAAATAATAGA
ZG21R:3200-3100	TGGAAATTTCTTGAAAATAGTAAC
ZG22R:3160-3060	ATATCTCAAATACGGGGACATT
ZG23R:3120-3020	TCTCTAGCAGGAAATTTCAGG
ZG24R:3080-2980	GGTATCAAGATTTTGAATAATAATA
ZG25R:3040-2940	CATGAACTATCAAAGTCTATGC
ZG26R:3000-2900	GCAAAATTAGAATTAAGCACCT
ZG27R:2960-2860	CTTTTTTTTTGTTTTTGATCAAAGT
ZG28R:2920-2820	ACTTGAATATAGATAGACATCAC
ZG29R:2880-2780	AAGACAACCTTTATAGTTACAATT
ZG30R:2840-2740	TTTGAGATGAGATGACGTTATAT
ZG31R:2800-2700	TTAAGAATTTTTTTTGGTTTTGTTC
ZG32R:2760-2660	AACTATAGCAAAGACGACAAAAA
ZG33R:2720-2620	TATTGACAAAAAAAAGGAAATGAC

ZG34R:2680-2580	GATCAGTAATATTGATACTACTAA
ZG35R:2640-2540	TATTACATTTGGTAGTGCCAGA
ZG36R:2600-2500	TCACTAAACTCCCGAAATTTCT
ZG37R:2560-2460	TTCCCTGTTTTTTTTTCCTTTTA
ZG38R:2520-2420	GTCTGCACAGACTATACACAA
ZG39R:2480-2380	TTAAACTTTTGTAAATGCAAGGAT
ZG40R:2440-2340	TTTTTTGTTTTTAAATAAAGTCAAAG
ZG41R:2400-2300	GTTTTTTTGTTTTTAAATAAAGTCAA
ZG42R:2360-2260	ATGTAGACCCGCCTATAAACA
ZG43R:2320-2220	AATTGTTGTTTTTTTTTCTTTGTCT
ZG44R:2280-2180	CTTCTTTATGGTTACAATGGTTT
ZG45R:2240-2140	TACACCCAGTGGTTTTTCTTA
ZG46R:2200-2100	TTAAATGAAATGTCTATCTGACAT
ZG47R:2160-2060	TCTTCTCTCGTTTTCTCTCTG
ZG48R:2120-2020	AGTTGTGTTAAATAATTCAATATTTA
ZG97R:2080-1980	ATAGAAATCAAAACTTTGAGATTTA
ZG98R:2040-1940	AAATAATAAGAATAAATTCAAAACCT
ZG99R:2000-1900	TTAAGTGATCTAATTGATAGTAGA
ZG100R:1960-1860	GTGGTAGCAGTAACAGCAAA
ZG101R:1920-1820	GTAATTCACTTAATTTAAAAGTTATA
ZG102R:1880-1780	GTGTCCTGAATTTAAAAGACAAA
ZG103R:1840-1740	ATCAGAAAAAGTGTTGGTCGTT
ZG104R:1800-1700	ACGGTGATTGAACTTCTGAGT
ZG105R:1760-1660	TGATAACTGGAATCTCCTATG
ZG106R:1720-1620	TTTGCCACAATGGAAAAAGTG
ZG107R:1680-1580	CCTGCTTTATTGAACACACAAT
BUD2 -350F	AGACAGACAGCCCTCAATC
BUD2-350R	CTGAAATAAATTTTGGTATTGGA
BUD2-200F	CAGTTCTATCCTATATATAATATA
BUD2-200R	GATTAATTTTTTTTGGGGTATAAA
BUD2-50F	TCCACATTTTTAAATTAAAACTAT
BUD2-50R	CACGAGAAATGATTTTATGAAAT

Chapter 3

The *WOR1* 5'untranslated region regulates white-opaque switching by reducing translational efficiency

Introduction

WOR1, the master regulator of white-opaque switching, is part of a network of transcriptional feedback loops that governs switching and white-opaque phenotype. Notably, most of the regulatory genes in this circuit have a long 5' untranslated region (5'UTR): for example, the *WOR1* 5'UTR is 1997 bp, *EFG1* 1139 bp, *CZF1* 1662 bp. In contrast, 5'UTRs of other *C. albicans* genes that are not in the regulatory circuits for cell fate or yeast-hyphal regulation, are mostly under 100 bp in length (Tuch *et al.*, 2010, Bruno *et al.*, 2010). Most yeasts, such as *Saccharomyces cerevisiae*, do not have genes with long 5'UTRs (Nagalakshmi *et al.*, 2008, Bruno *et al.*, 2010). Although the transcriptional regulation of *WOR1* and white-opaque switching has been extensively studied, functions of and regulation by long 5'UTRs remain to be explored.

While long 5'UTRs are rare in yeasts, they are common in higher eukaryotes and in viral genes, and are frequently linked to translational regulation, in particular translational repression. A

common mechanism for translational repression at the 5'UTR is through RNA-binding proteins. For example, a developmentally regulated translational control at 5'UTR by a meiosis-specific RNA-binding protein is critical for establishing the meiotic chromosome segregation pattern in *S. cerevisiae* (Berchowitz *et al.*, 2013). Additional elements that have been shown to control translational efficiency at 5'UTRs include upstream ORFs (uORFs), upstream ATGS, and internal ribosome entry sites (IRES) (Morris & Geballe, 2000, Hellen & Sarnow, 2001). In *S. cerevisiae*, cap-independent translation at IRESs in the 5'UTR of a small subset of genes is required for invasive growth (Gilbert *et al.*, 2007). Recently, an example of gene expression regulation through a uORF has been identified in *C. albicans* (Sundaram & Grant, 2014). The length and structure of the 5'UTR also affect microRNA-mediated translational repression (Meijer *et al.*, 2013). Finally, secondary structures in the 5'UTR can inhibit translation by stalling translational initiation (Jackson *et al.*, 1996, Jackson & Gorovsky, 2000). In *C. albicans*, translational inhibition by a long 5'UTR has been observed for the hyphal-specific transcriptional regulator *UME6* (Childers *et al.*, 2014). The long 5'UTR of *WOR1* makes it a promising candidate as a cis-regulatory element of *WOR1* translation, and therefore of white-opaque switching.

In this study, we find that the *WOR1* 5'UTR regulates the white-opaque phenotype by reducing translational efficiency of *WOR1*. We demonstrate that the 5'UTR is repressive toward both opaque formation and stability. Deletion of the 5'UTR greatly increases white-to-opaque switching while reducing opaque-to-white switching. Contribution of this translational regulation to cell fate commitment and stability will be discussed. We further show that transcriptional repression at long 5'UTR is pervasive and is observed for many genes with long 5'UTR. As

those genes play pivotal roles in yeast-hyphal and/or white-opaque transitions, we speculate that translational regulation at their 5'UTR may also play an important role in cell fate commitment and maintenance.

Results

Deletion of the *WOR1* 5'UTR enhances white-opaque switching and opaque stability

In order to examine the role of the *WOR1* 5'UTR in white-opaque switching, we constructed strains in which the 5'UTR was deleted, as shown in Figure 3.1A and described in detail in Chapter 2. In brief, the *WOR1p-Δ5'WOR1-HA* plasmid was constructed, in which a 3 kb region of the *WOR1* promoter was placed directly upstream of the *WOR1* coding sequence without the 5'UTR sequence. To generate a 5'UTR-*WOR1*/Δ5'-*WOR1* strain, *WOR1p-Δ5'WOR1-HA* was transformed into a *WOR1* heterozygous deletion (5'UTR-*WOR1/wor1*) and integrated at the *WOR1* promoter upstream of the *wor1*Δ locus. Δ5'-*WOR1/*Δ5'-*WOR1* and Δ5'-*WOR1/wor1* strains were generated by transforming *WOR1p-Δ5'WOR1-HA* into the *wor1Δ/wor1*Δ strain once and twice, respectively (see Chapter 2). These Δ5'-*WOR1* strains were compared to 5'UTR-*WOR1* strains for white-opaque switching frequency and opaque phase stability. White cells were grown on SCD plates at room temperature to assay spontaneous switching to opaque. After 7 days, all strains carrying Δ5'-*WOR1* displayed increased white-to-opaque switching, compared to corresponding strains carrying the same copy number of 5'UTR-*WOR1* (Figure 3.1B). The switching rate of 5'UTR-*WOR1*/Δ5'-*WOR1* approached 100%, in contrast to 2% for wild type

cells of 5'UTR-*WOR1*/5'UTR-*WOR1* strain. Switching of 5'UTR-*WOR1*/Δ5'-*WOR1* occurred as multiple opaque sectors per white colony, with entire colonies becoming opaque by 7 days. Intriguingly, the Δ5'-*WOR1*/Δ5'-*WOR1* strain had the 35.7% white-opaque switching rate, still substantially elevated from wild type but lower than 5'UTR-*WOR1*/Δ5'-*WOR1*. Notably, the highest switching rate appeared to be conferred by heterozygosity for the *WOR1* 5'UTR, suggesting both a positive and negative role for the 5'UTR in regulation of switching. For cells carrying only one copy of *WOR1*, the absence of the 5'UTR still conferred a higher switching rate. Compared to 5'UTR-*WOR1/wor1*, which has a switching rate of only 1%, Δ5'-*WOR1/wor1* is able to switch to opaque at 12%. However, this is much lower than the Δ5'-*WOR1*/Δ5'-*WOR1* strain that carries two copies of *WOR1* (Figure 3.1B). The high white-opaque switching frequency raised the question of whether opaque state itself is more stably maintained in Δ5'-*WOR1* strains. Stability was assayed by incubating opaque cells of control and Δ5'-*WOR1* strains on solid media at room temperature or 37°C. We find that the presence of Δ5'-*WOR1* enhances opaque stability and reduces opaque-to-white switching (Figure 3.1C). 5'UTR-*WOR1*/Δ5'-*WOR1* and Δ5'-*WOR1*/Δ5'-*WOR1* showed less spontaneous opaque-white switching at room temperature than wild type, while Δ5'-*WOR1/wor1* also switched to white less frequently than 5'UTR-*WOR1/wor1*. At 37℃, where opaque wild-type and 5'UTR-*WOR1/wor1* cells switched *en masse* to white, nearly all 5'UTR-*WOR1*/Δ5'-*WOR1* cells as well as 65.7% of Δ5'-*WOR1*/Δ5'-*WOR1* cells remained opaque after 7 days. However, all Δ5'-*WOR1/wor1* cells switched to white (Figure 3.1C). The highly opaque-switching and opaque-stable phenotype of cells carrying Δ5'-*WOR1* appears to be enhanced by increased copy number of *WOR1*, and in particular by having both 5'UTR-*WOR1* and Δ5'-*WOR1*.

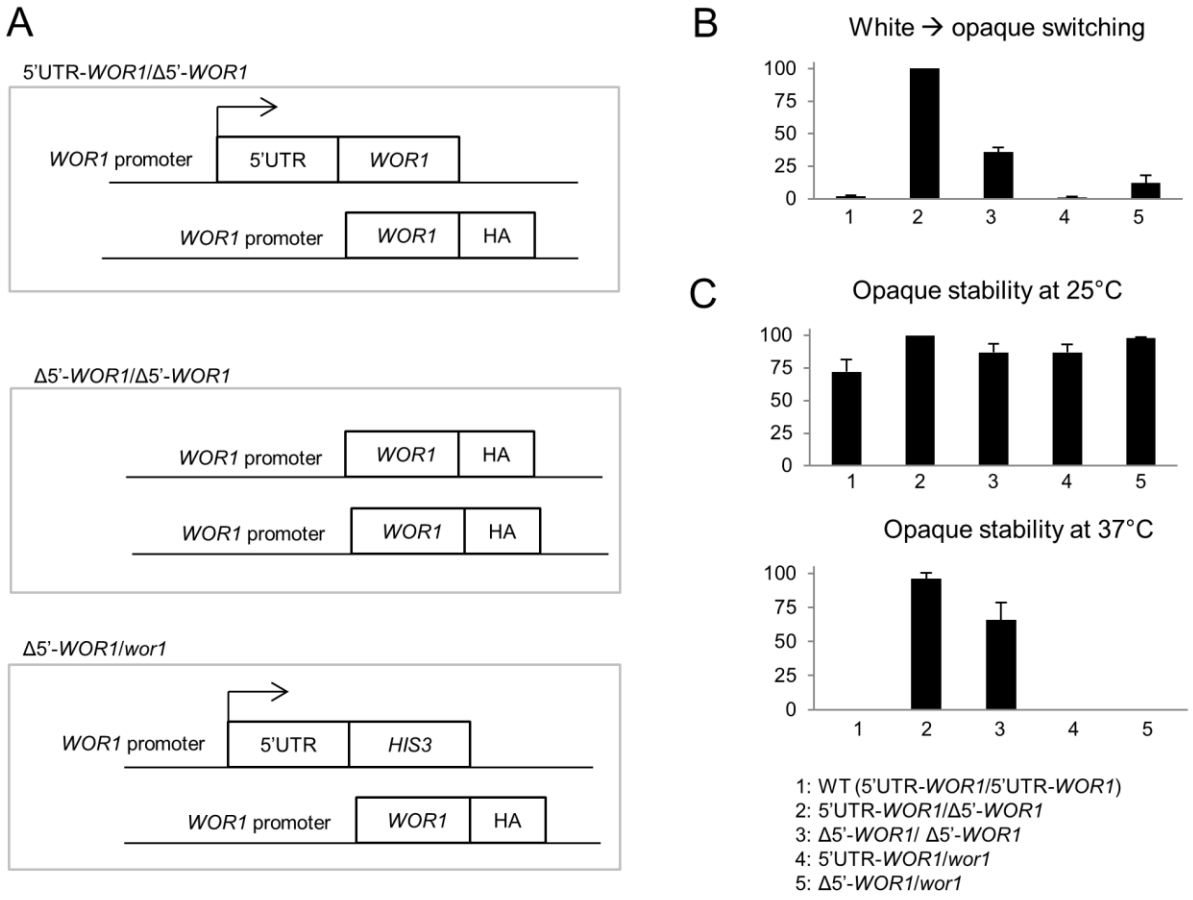

Figure 3.1: Deletion of the 5'UTR of *WOR1* promotes white-opaque switching and opaque stability. (A) Schematics of *WOR1* loci of the Δ5'-*WOR1* strains constructed for this study: 5'UTR-*WOR1*/Δ5'-*WOR1*, Δ5'-*WOR1*/ Δ5'-*WOR1*, and Δ5'-*WOR1/wor1*. (B) Percentage of spontaneous white-opaque switching in the following strains; 1: 5'UTR-*WOR1*/5'UTR-*WOR1* (wild type; JYC1), 2: 5'UTR-*WOR1*/Δ5'-*WOR1* (HLY4212), 3: Δ5'-*WOR1*/ Δ5'-*WOR1* (HLY4214), 4: 5'UTR-*WOR1/wor1*(HLY3903), and 5: Δ5'-*WOR1/wor1* (HLY4213) . White cells grown at 30 ℃ were plated to SCD media and grown at room temperature (25 ℃) for 7 days before colony phenotype was scored. (C) Opaque stability of the strains described in (B). Opaque cells grown at 25 ℃ were plated to SCD media and grown at 25 ℃ and 37 ℃ for 7 days. Stability of opaque state was measured as percentage of colonies that stay in opaque.

Deletion of the *WOR1* 5'UTR stabilizes *WOR1* positive feedback at 37°C

As *WOR1* transcription reflects the white-opaque phenotypic state of the cell, *WOR1* expression in strains carrying Δ5'-*WOR1* could illuminate the processes behind the higher opaque stability of Δ5'-*WOR1* strains. We examined the effects of the 5'UTR on *WOR1* transcript levels under conditions where wild-type opaque cells switch to white, but Δ5'-*WOR1* opaque cells remain mostly in opaque. To this end, we incubated at 37℃ opaque cells of two strains that carry only one copy of *WOR1*: 5'UTR-*WOR1/wor1* and Δ5'-*WOR1/wor1*. Northern blotting probing for *WOR1* was performed to compare transcript level in these two strains, sampled every 4 hours (Fig. 2A). Cells from each time point were plated and grown on YPD plates at room temperature to determine percent of opaque cells. Prior to transfer to 37℃, *WOR1* transcript was more abundant in opaque Δ5'-*WOR1/wor1* cells than in 5'UTR-*WOR1/wor1*. After cells were incubated at 37℃, *WOR1* transcript disappeared from the 5'UTR-*WOR1/wor1* strain immediately, but persisted for longer in the Δ5'-*WOR1/wor1* strain, with some transcript detectable 12 hours after temperature shift (Figure 3.2A). The opaque stability of cells removed from 37°C during the experiment was also higher for Δ5'-*WOR1/wor1* (Figure 3.2A). The elevated level of Δ5'-*WOR1* transcript even at high temperature presents two possibilities: either a heightened transcript stability or translation efficiency from the Δ*5'-WOR1* that in turn promotes *WOR1* transcription through positive feedback of Wor1. To further examine the effect of the Δ*5'-WOR1* on *WOR1* positive feedback, we conducted Northern blotting under the same conditions on strains carrying two copies of *WOR1*: 5'UTR-*WOR1/*5'UTR-*WOR1* and 5'UTR-*WOR1*/Δ5'-*WOR1* (Figure 3.2B). At room temperature, 5'UTR-*WOR1* transcript levels were similar in opaque cells of both strains. In the 5'UTR-*WOR1*/Δ5'-*WOR1* strain, Δ5'-*WOR1* was

present at a lower level than 5'UTR-*WOR1*. This result suggested that the 5'UTR of *WOR1* does not reduce its transcript level, and in fact is correlated with more stable transcript. Upon shifting to 37℃, *WOR1* transcript rapidly disappears in wild-type 5'UTR-*WOR1/5*'UTR-*WOR1* cells, while both 5'UTR-*WOR1* and Δ5'-*WOR1* persist strongly for 8 or more hours in 5'UTR-*WOR1*/Δ5'-*WOR1*, and are still detectable at 12 hours (Figure 3.2B). Consistent with persistent *WOR1* transcription, high percentage of cells remained opaque after treatment at 37℃ compared to the wild-type control. We suggest that the stronger and more stable expression of *WOR1* in the 5'UTR-*WOR1/*Δ5'-*WOR1* strain is due to a stronger positive feedback from Wor1 protein, which is likely translated more efficiently from Δ5'-*WOR1* than from *5'UTR-WOR1*.

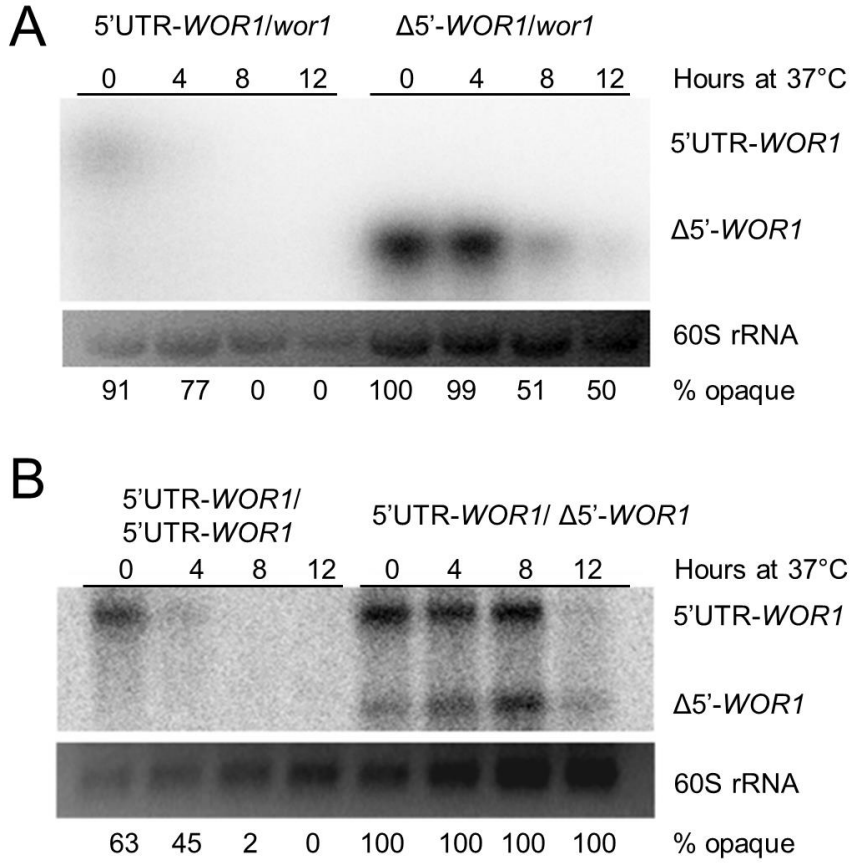

Figure 3.2: Stabilization of *WOR1* expression at 37°C in Δ5'-*WOR1* strains. (A) Northern blot probing for a 500 bp region of the *WOR1* coding sequence against total RNA of opaque 5'UTR-*WOR1/wor1* and Δ5'-*WOR1/wor1* cells. (B) Northern blot probing for a 500 bp region of the *WOR1* coding sequence in opaque wild type (5'UTR-*WOR1*/5'UTR-*WOR1*) or 5'UTR-*WOR1*/ Δ5'-*WOR1* cells. Strains were grown to log phase at 25℃, then transferred to 37℃. RNA was extracted every 4 hours for Northern blotting, and white-opaque phenotype was assessed by removing cells to SCD plates, incubating at 25℃, then scoring colony phenotype after 4 days.

5'UTR-*WOR1* transcripts are enriched in monosome

We suspected that 5'UTR-*WOR1* is less efficiently translated than Δ5'-*WOR1*. Transcripts that are actively translated in the cell are associated with multiple ribosomes (polysomes), while those with stalled or less efficient translation are associated with ribosomal subunits or single 80S ribosomes (monosomes). Polysomes can be isolated by sedimentation of cell lysates (McQuillen *et al.*, 1959, Warner *et al.*, 1963). To determine the effect of the *WOR1* 5'UTR on translational efficiency, we conducted a polysome gradient assay on the 5'UTR-*WOR1*/Δ5'-*WOR1* strain, using opaque cells in which *WOR1* is expressed. Whole cell extract was separated by centrifugation on a sucrose gradient into fractions enriched for monosomes or polysomes, and absorbance taken to visualize polysomal peaks (Figure 3.3A). RT-qPCR was then performed on RNA extracted from each fraction to determine the level of monosomal and polysomal association of 5'UTR-*WOR1* and Δ5'-*WOR1* transcripts. As Δ5'-*WOR1* is tagged at the 3' end with –HA in this strain, primers amplifying a region extending from the 3' end of the *WOR1* coding sequence to the –HA tag were used for detection of Δ5'-*WOR1* transcript. Primers amplifying a region of the *WOR1* 5'UTR were used for detection of 5'UTR-*WOR1* transcript. We found 5'UTR-*WOR1* most enriched in the monosome fraction, and present at lower levels in the polysomal fractions. Conversely, Δ5'-*WOR1* transcript level was low in monosome and high in polysome association (Figure 3.3B). The polysome association of Δ5'-*WOR1* was similar to that of *ACT1*. These results suggest less efficient translation of *WOR1* transcripts bearing the 5'UTR, while Δ5'-*WOR1* transcripts are bound by multiple ribosomes and actively translated like *ACT1*.

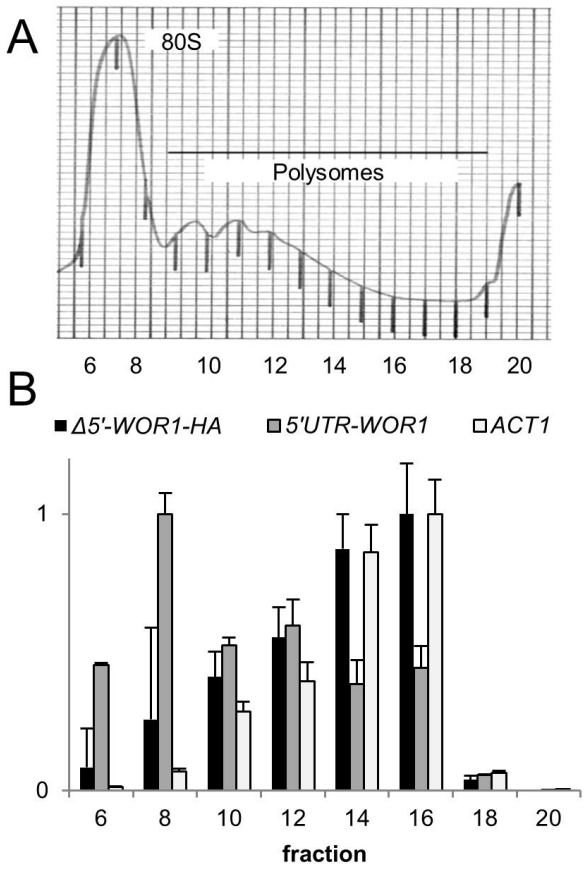

Figure 3.3. 5'UTR-*WOR1* transcripts are enriched in monosomes, while Δ5'-*WOR1* transcripts are enriched in polysomes. (A) Polysome profile of 5'UTR-*WOR1*/Δ5'-*WOR1* opaque cells grown to log phase at room temperature (25 ℃). Cell lysate was applied to a sucrose gradient and centrifuged to separate monosomal and polysomal fractions. Fractions were collected in order of least to most density on ISCO gradient fractionator, and absorbance profile taken at A254 nm.(B) Relative abundance of 5'UTR-*WOR1*, Δ5'-*WOR1*-HA, and *ACT1* transcripts in each gradient fraction as determined by RT-qPCR. All experiments were performed in triplicate. For each transcript, values were normalized to the fraction containing the highest value, set as 1. Error bars represent standard deviation.

The *WOR1* 5'UTR reduces translational efficiency

Having established that transcripts containing the *WOR1* 5'UTR are enriched in monosomes and less translated, we next sought to demonstrate that less Wor1 protein is made from the *5'UTR-WOR1* transcript than the *WOR1* transcript without the 5'UTR. To this end, the *WOR1* gene with or without its 5'UTR was tagged with –HA and placed under the maltose-inducible *MAL2* promoter, resulting in the *MAL2p-5'UTR-WOR1-HA* or *MAL2p-WOR1-HA plasmid*. This allows for conditional expression without positive feedback of Wor1 onto its own promoter. Cells of WT + *MAL2p-5'UTR-WOR1-HA* or WT + *MAL2p-WOR1-HA* were transferred from dextrose to maltose to turn on expression from the *MAL2* promoter, upon which *WOR1* mRNA levels were assayed by RT-qPCR, and HA-tagged Wor1 protein by Western blotting (Figure 3.4). At the transcript level, little difference was observed between 5'UTR-*WOR1* or *WOR1*, indicating that the 5'UTR did not function to reduce transcription. As the *MAL2* promoter is more active at higher temperature, transcript levels were elevated at 37℃, but again this was observed for both the 5'UTR-*WOR1* and *WOR1* constructs (Figure 3.4A). At the protein level, however, much higher levels of Wor1 were detected from *MAL2p-WOR1-HA* than *MAL2p-5'UTR-WOR1-HA*, pointing to significantly reduced translation when the 5'UTR is present (Figure 3.4B).

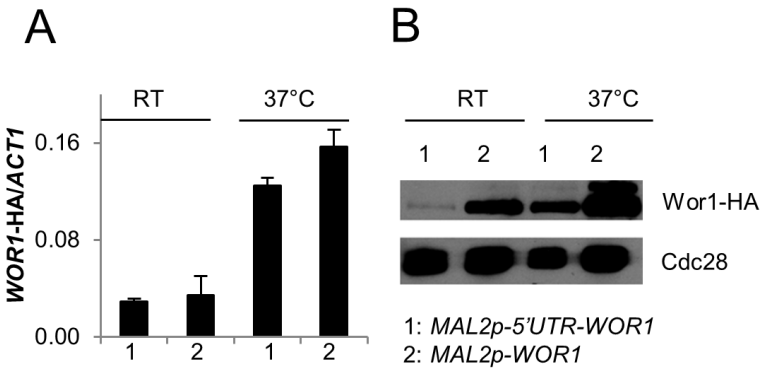

Figure 3.4. *MAL2*-driven 5'UTR-*WOR1* produces less Wor1 protein than *MAL2*-driven *WOR1*. (A) RT-qPCR of *WOR1*, and (B) Western blot detecting HA-tagged Wor1, in WT carrying *MAL2p-5'UTR-WOR1-HA* (HLY4215) or *MAL2p-WOR1-HA* (HLY3569). White cells were grown to log phase in YEP + dextrose, then inoculated to YEP + maltose to induce transcription from the *MAL2* promoter for 4 hours at RT (25 ℃) or 37 ℃. For qPCR, all experiments were performed in triplicate, and values were normalized to *ACT1* signal.

To determine whether the *WOR1* 5'UTR was sufficient for the observed translational inhibition effect and the *WOR1* coding region did not contribute, we cloned (*WOR1*) 5'UTR-*GFP* under the *MAL2* promoter to produce the *MAL2p-5'UTR-GFP* plasmid. A *MAL2p-myc-GFP* plasmid was used as a 5'UTR-less control. White and opaque wild-type cells transformed with either plasmid were again transferred from dextrose to maltose to turn on expression from the *MAL2* promoter. Transcript levels of GFP with and without the *WOR1* 5'UTR were similar, as shown by qPCR (Figure 3.5A). The *MAL2* promoter is not entirely shut off in dextrose in the *MAL2p-5'UTR-GFP* strain, showing some basal level of transcription; however, this appears to be an artefact that was observed for both the *MAL2p-5'UTR-WOR1-HA* and *MAL2p-WOR1-HA* strains (Figure 3.6). In white cells, Western blots probing for GFP showed that higher protein levels were reached more quickly upon induction with *MAL2p-myc-GFP* than with *MAL2p-5'UTR-GFP*, demonstrating that the *WOR1* 5'UTR is sufficient for reducing translational efficiency. Notably, opaque cells of *MAL2p-5'UTR-GFP* expressed more GFP protein than their corresponding white cells upon maltose induction (Figure 3.5B). Thus, the difference in translational efficiency imparted by the 5'UTR is less stark in opaque cells, suggesting less regulation by the 5'UTR in this state. Similar results were seen by observing GFP fluorescence using fluorescence-activated cell sorting (not shown).

Finally, we investigated whether there is a difference in translational efficiency reduction by the 5'UTR at higher temperatures. Some bacterial 5'UTRs are known to contain temperature-sensing hairpin structures that regulate heat response (Kortmann & Narberhaus, 2012). To investigate whether the *WOR1* 5'UTR has similar temperature-sensing properties, we expressed *MAL2p-myc-GFP* and *MAL2p-5'UTR-GFP* at room temperature (25^{o}C) and 37^{o}C, then quantified GFP

mRNA level through qPCR and protein level through FACS. Normalizing protein to transcript level, we found that while the translation of *5'UTR-GFP* is lower than that of GFP alone at both temperatures, at 37^{o}C the difference was greater, with a twofold decrease of *5'UTR-GFP* from room temperature (Figure 3.5C). Thus, the translational impairment conferred by the 5'UTR is even greater at 37^{o}C and may contribute to the 37^{o}C phenotype of lowered *WOR1* expression and mass switching of opaque cells to white.

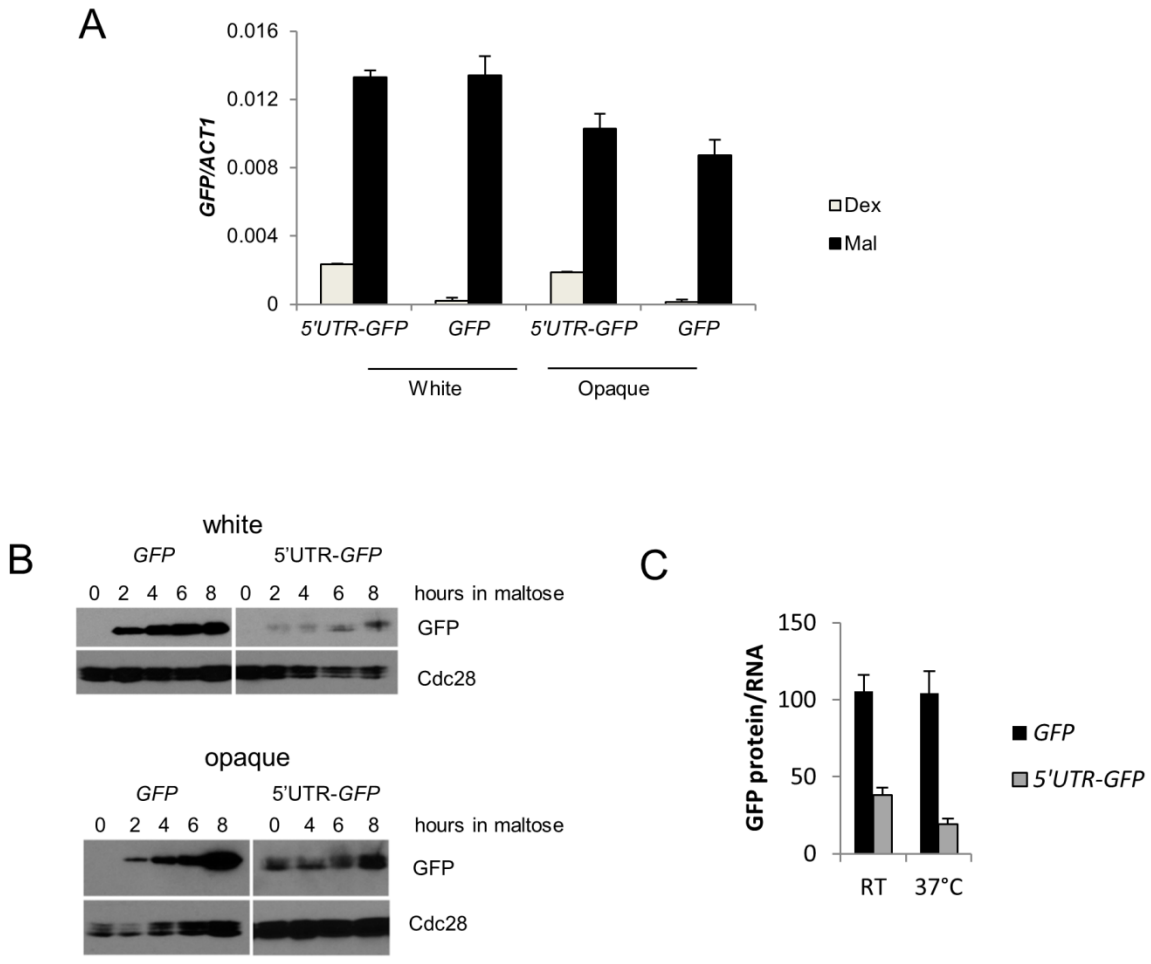

Figure 3.5. The *WOR1* 5'UTR can represses translation of a downstream reporter. (A) RT-qPCR of *GFP* and (B) Western blot detecting GFP in white and opaque cells of WT + *MAL2p-WOR1 5'UTR-GFP* (HLY4216) and WT + *MAL2p-myc-GFP* (HLY4217) . (C) Ratio of GFP protein as detected by FACS, to *GFP* mRNA level as detected by qPCR, of white cells of WT + *MAL2p-WOR1 5'UTR-GFP* (HLY4216) and WT + *MAL2p-myc-GFP* (HLY4217), at room temperature or 37℃ . Strains were grown to log phase in YEP + dextrose, then inoculated to YEP + maltose at RT or 37℃ to induce expression from the *MAL2* promoter. Samples were collected after 4 hours. qPCR was performed in triplicate and values were normalized to *ACT1*.

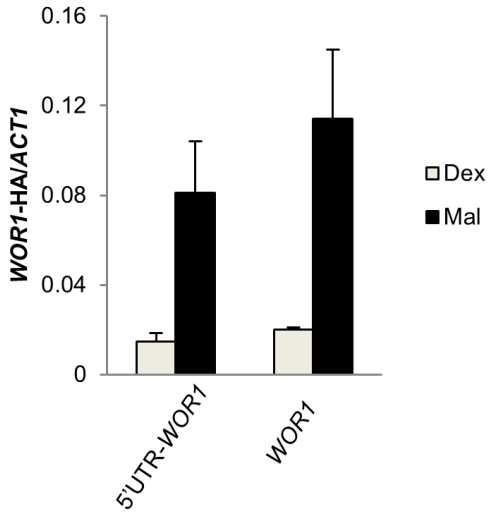

Figure 3.6. Transcriptional analysis of *MAL2* promoter driven 5'UTR-*WOR1* or *WOR1*. RT-qPCR of HA-tagged *WOR1* in white cells of WT + *MAL2p-5'UTR-WOR1-HA* or WT + *MAL2p-WOR1-HA*. Strains were grown to log phase in YEP + dextrose, then transferred to YEP + dextrose or maltose for 4 hours. Values were normalized to *ACT1*.

Argonaute, Ssd1, and uncapped 5'UTR-*WOR1* transcripts are not involved in translational regulation at the *WOR1* 5'UTR

Several possibilities exist for the mechanism of translational regulation by the *WOR1* 5'UTR. One such possibility is through micro-RNA-directed translational repression. It has been demonstrated that translational repression by miRNAs interacts with the 5'UTR of genes through the initiation factor eIF4A2, which unwinds 5'UTR structure to allow binding of the 60S ribosomal subunit (Meijer *et al.*, 2013). While RNAi is absent from *S. cerevisiae*, many other budding yeasts, including *C. albicans*, have functional Argonaute and Dicer proteins as well as small nocoding RNAs, suggesting a possible RNAi system (Drinnenberg *et al.*, 2009, Liu *et al.*, 1996) To test the possibility of translational repression of RNA transcripts by Argonaute. we examined whether *WOR1* 5'UTR-associated translational repression is present in the absence of Argonaute (*AGO1*). An *ago1* mutant was constructed and transformed with *MAL2p-5'UTR-GFP* or *MAL2p-myc-GFP*. GFP protein levels after maltose induction of the *MAL2* promoter were assayed by Western blotting. We found that in an *ago1* background, GFP protein level was still greatly reduced in the *MAL2p-5'UTR-GFP* strain compared to *MAL2p-myc-GFP* absent the *WOR1* 5'UTR, similar to results observed for wild type (Figure 3.7). This result is corroborated by fluorescence activated cell sorting (FACS) measuring GFP fluorescence in the cell population after induction of the *MAL2* promoter (Figure 3.8). Therefore, Argonaute is not necessary for translational repression by the *WOR1* 5'UTR. This is consistent with our observeration of the lack of an effect by *AGO1* deletion on white-opaque switching (not shown).

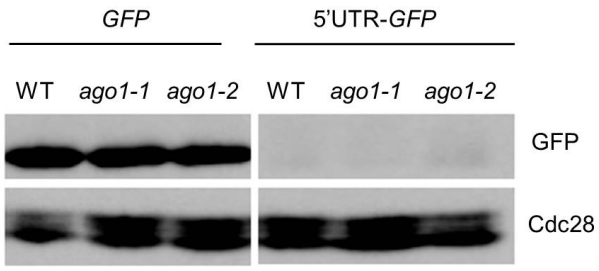

Figure 3.7. Ago1 is not required for the translational repression by the *WOR1* 5'UTR. Western blot detecting GFP in WT carrying *MAL2p-WOR1 5'UTR-GFP* (HLY4216), WT carrying *MAL2p-myc-GFP* (HLY4217), *ago1* (HLY3673) carrying *MAL2p-WOR1 5'UTR-GFP* (HLY4218), or *ago1* carrying *MAL2p-myc-GFP* (HLY4219). Strains were grown to log phase in YEP + dextrose, then inoculated to YEP + maltose for 4 hours at 37℃ to induce transcription from the *MAL2* promoter. GFP was detected with Clontech Living Colors anti-GFP antibody.

To examine alternate mechanisms of translational regulation, we considered the role of RNA-binding proteins that may potentially interact with the *WOR1* 5'UTR. In *S. cerevisiae*, Ssd1 is known to bind at the 5' and 3'UTR of specific mRNAs, reducing their translational efficiency (Cao *et al.*, 2006). Ssd1 activity is repressed by Cbk1, which is part of the RAM network critical for the regulation of cellular morphogenesis, polarized growth and septum destruction (Lopes da Rosa *et al.*, 2010, Kolonko *et al.*, 2010, Brooks & Jackson, 1994). Homologues of Cbk1, Ssd1 and downstream genes are present in *C. albicans*, where they are also critical for cell morphogenesis and mother-daughter separation (Lopes da Rosa *et al.*, 2013, Jackson *et al.*, 1994, Watanabe *et al.*, 2013). Considering that opaque cells are better separated than white cells between mother and daughters, the Cbk1-Ssd1 pathway could potentially be differentially regulated between white and opaque cells, and Ssd1 could be a candidate for translational repression at the *WOR1* 5'UTR. If translational repression through the *WOR1* 5'UTR is indeed regulated through Ssd1, deletion of *SSD1* should reduce this repression. To investigate this, we transformed a *ssd1* deletion mutant (Zentner & Henikoff, 2013) with *MAL2p-myc-GFP* or *MAL2p-UTR-GFP*. After the *MAL2* promoter was activated by growth of cells in maltose-containing medium, FACS was performed to assess population-level GFP flourescence as a reporter of translation. We find that fluorescence of *MAL2p-5'UTR-GFP* is lower than that of *MAL2p-myc-GFP* in both *ssd1* and WT. Expression levels of either GFP construct in *ssd1* is nearly indistinguishable from its level in a wild-type background (Figure 3.8). Thus, it appears that translational regulation through the *WOR1* 5'UTR is not regulated by Ssd1.

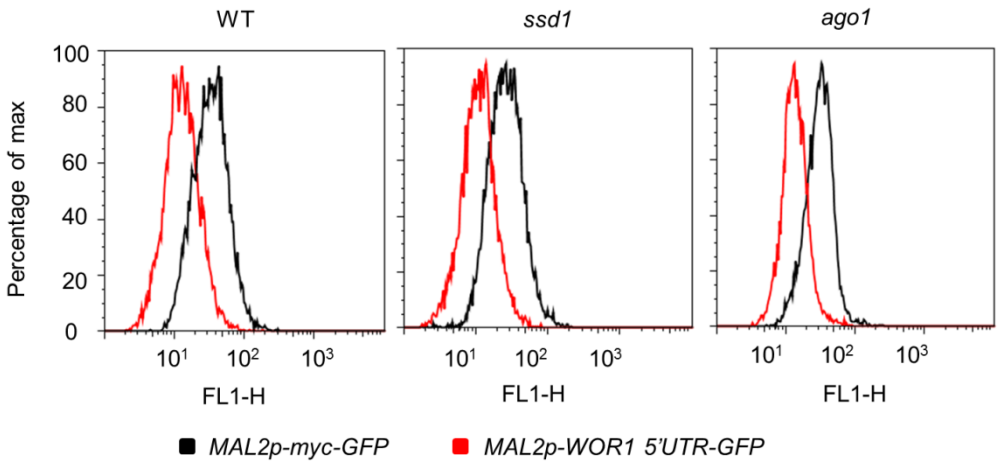

Figure 3.8. *SSD1* and *AGO1* are not involved in the translational repression by the *WOR1* 5'UTR. FACS histogram profiles showing GFP fluorescence from *MAL2p-myc-GFP* or *MAL2p-WOR1 5'UTR-GFP* in a background of WT+*MAL2p-myc-GFP*, WT+*MAL2p-WOR1 5'UTR-GFP*, *ssd1* + *MAL2p-myc-GFP* (HLY4221), *ssd1* + *MAL2p-WOR1 5'UTR-GFP* (HLY4222), *ago1* + *MAL2p-WOR1 5'UTR-GFP* (HLY4218). Expression from the MAL2 promoter was induced in all samples by growth in YEP + maltose for 4 hours.

Another possible mechanism driving differential translational efficiency of 5'UTR-*WOR1* and Δ5'-*WOR1* is the existence of cap-independent translation initiating through the *WOR1* 5'UTR. To explore this possibility, we sought to determine whether uncapped 5'UTR-*WOR1* transcripts are normally found in the cell, and at what levels. The splint-ligation-based, qSL-RT-PCR method described by Blewett et al was used uncapped mRNA (Blewett *et al.*, 2011). RNA was extracted from wild-type opaque cells, and ligation reactions performed to ligate the 5'UTR-*WOR1* RNA to an RNA anchor oligo, facilitated by a DNA splint homologous to both. Only RNA transcripts without the 5' cap would be ligated to the anchor. RT-qPCR was then performed to detect both an amplicon within the original transcript (*WOR1* 5'UTR), and one spanning the anchor and 5'UTR. Detection of the second amplicon is indicative of successful ligation of an uncapped transcript. A ligase-free reaction was performed as a control. We find that with the addition of ligase, the detection of uncapped 5'UTR-*WOR1* transcripts are 0.58 fold of ligase-free reaction, indicating that few, if any, 5'UTR-*WOR1* transcripts exist in uncapped form. In comparison, detection of uncapped *ACT1* increases by 9.13 fold when ligase is added, demonstrating that the ligation reaction proceeds efficiencly when uncapped transcripts exist (Table 3.1). While the high level of uncapped *ACT1* transcript appears reflective of non-specific background decapping activity, this level of decapping is not seen for 5'UTR-*WOR1* transcripts. These results indicate that the mechanism behind the lower translational efficiency of the *WOR1* 5'UTR does not involve translation of uncapped transcripts. We also tested the possibility of alternative transcription originating within the *WOR1* 5'UTR, resulting in shorter *WOR1* transcripts lacking all or part of the 5'UTR. To assess whether these transcripts were produced, and whether they appeared transiently during switching or in stable opaque cells, we used the WT + *WOR1p-GFP* + *MAL2p-WOR1* strain, in which *GFP* is under the *WOR1* promoter and

5’UTR. This would allow for induction of white-opaque switching by ectopically expressing *WOR1* under the *MAL2* promoter, while transcription from the *WOR1* promoter could be assayed through *GFP* RNA levels, without interference from ectopically expressed *WOR1*. Northern blotting was conducted to probe for *GFP*-containing RNA. As expected, the appearance of *WOR1p-GFP* RNA was correlated with switching to opaque. While alternate transcription would have produced both a long (5’UTR-*GFP*) and short (*GFP* only) transcript, we found *GFP* transcript of only one size, correlating to 5’UTR-*GFP* at 2.7 kbp (Figure 3.9). Thus, alternative transcription does not appear to initiate in the *WOR1* 5’UTR.

Table 3.1: Absence of uncapped 5'UTR-*WOR1* transcripts as detected by qSL-RT-PCR.

		Ct transcript only	Ct anchor-transcript	Fold above background
ACT1	ligase	14.08	32.15	9.13
	no ligase	15.08	36.34	
5'UTR-*WOR1*	ligase	20.02	34.98	0.58
	no ligase	19.64	33.81	

Splint ligation was performed on RNA extracted from opaque wild-type cells, using DNA splints that facilitate the ligation of an RNA anchor oligo to uncapped *ACT1* or 5'UTR-*WOR1* RNA transcript. Reactions for which ligase was omitted were used as control for background. RNA was purified from ligation reactions and used for RT-PCR. Ct values for the transcript of interest, and for the ligated anchor-transcript region, were taken as mean from triplicate. Fold change above background was calculated as ΔCt.

Figure 3.9. RNA level of *WOR1*-promoter-driven *GFP* during white-opaque switching. Northern blot probing for 500bp regions of *GFP* and *WOR1* in the WT + *WOR1p-GFP* + *MAL2p-WOR1* strain (HLY4055). *GFP* was expressed under the *WOR1* promoter and 5'UTR. Two *WOR1* bands were detected, a 5'UTR-*WOR1* transcript from the *WOR1* locus, and a *WOR1* transcript under the *MAL2* promoter. Switching was induced by growing white cells in YEP + maltose at 25℃. White-opaque phenotype was assessed by removing cells to SCD plates and scoring after 4 days.

Monosome association of 5'UTR-containing transcripts extends to other key regulators of morphology in *C. albicans*

While long 5'UTRs are uncommon in *C. albicans*, they are notably present on a handful of genes regulating morphological switches. Key regulators of the yeast-hyphal transition, such as *NRG1* and *FLO8*, and of the white-opaque circuitry, such as *CZF1* and *EFG1* (also a hyphal regulator), all have 5'UTRs in excess of several hundred to several thousand base pairs (Table 3.2) (Tuch *et al.*, 2010) . The length of the 5'UTR in these genes raises the question of whether they possess a translational repressive activity like the *WOR1* 5'UTR. To address this question, we conducted a polysome profile assay on wild-type opaque cells (Figure 3.10A). The identification of 80S and polysomal fractions were corroborated by 40S and 60S subunit content in each fraction as measured by RT-qPCR. A fraction containing predominantly 40S subunit was also identified (Figure 3.10B). Further RT-qPCR revealed that transcripts with long 5'UTRs were consistently enriched in those fractions containing predominantly 40S ribosomal subunit or 80S monosome, but not polysomes, suggesting many of these transcripts are stalled in translational initiation or otherwise less efficiently translated. *ACT1*, which is actively translated and has a short 5'UTR, displayed the opposite pattern and was enriched in polysomes (Figure 3.10C). This result demonstrates that a long 5'UTR is associated with reduced translational efficiency in numerous other genes regulating morphology in *C. albicans*. Whether the mechanisms of translational regulation through the 5'UTR are similar for these genes has yet to be determined.

Table 3.2: 5’UTR length of key regulatory genes in *C. albicans*.

Gene name	5'UTR length (bp)
CZF1	2071
WOR1	1978
RFG1	1267
EFG1	1139
FLO8	835
NRG1	466
ACT1	72

5’UTR length was calculated based on transcriptome analysis by Tuch *et al.*, 2010.

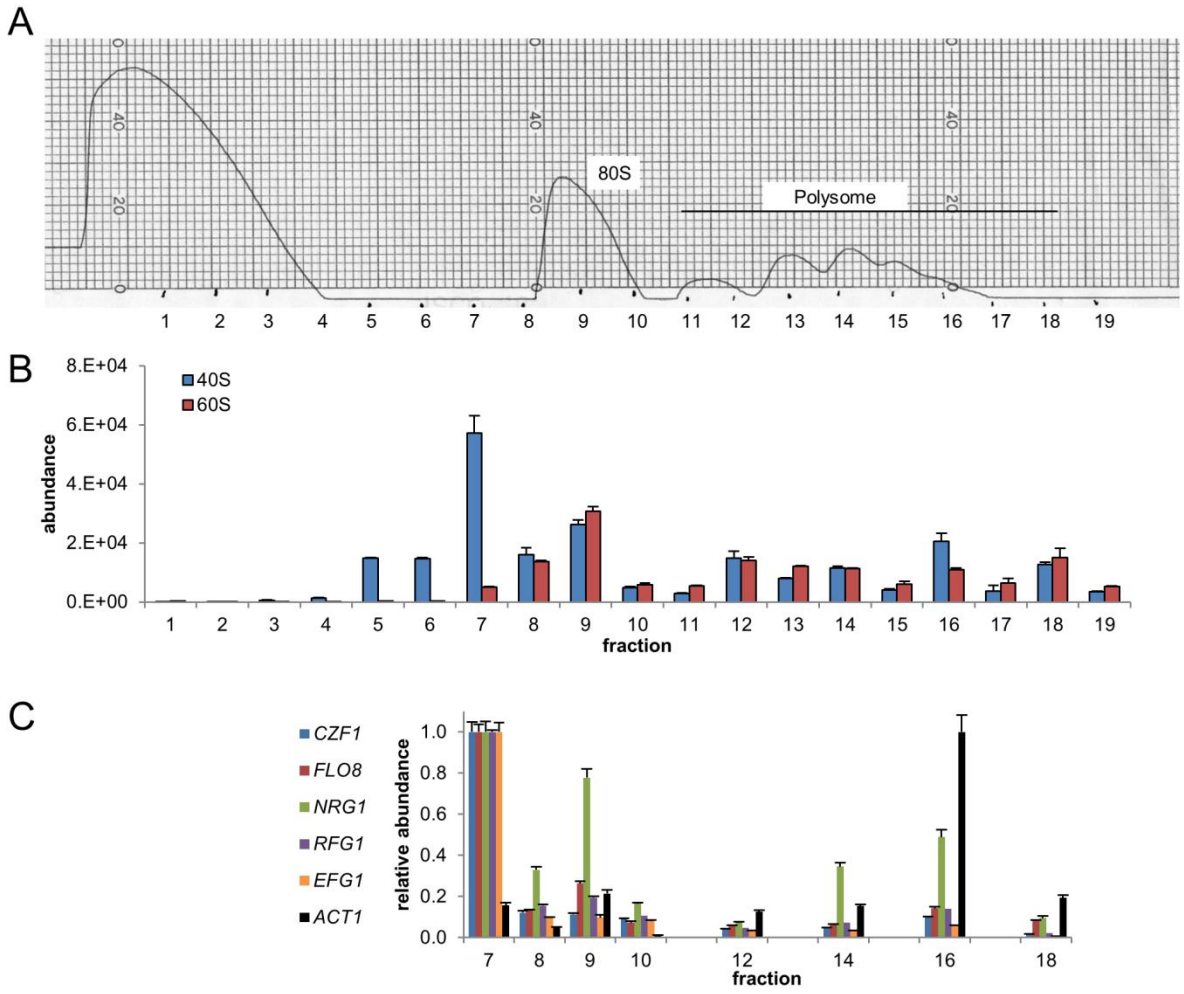

Figure 3.10. Transcripts with long 5'UTR are associated with monosome in *C. albicans*. (A) Polysome profile of wild type (JYC5) opaque cells grown to log phase at room temperature.(B) 40S and 60S ribosomal subunit abundance in each fraction as determined by RT-qPCR. (C) Relative abundance in each fraction of transcripts of white-opaque regulatory genes *CZF1, FLO8, NRG1, RFG1, EFG1*, and *ACT1* as determined by RT-qPCR. Abundance of each transcript was normalized to the fraction containing the highest value.

Discussion

Extensive work has been done to characterize the network governing white-opaque switching in *Candida albicans*, involving the master regulator *WOR1* and numerous other transcriptional regulators. However, much remains to be understood regarding the regulation of white-opaque switching at the translational level, in particular the translational regulation of *WOR1*. In this study, we identify the *WOR1* 5'UTR as a regulator of white-opaque switching through reducing the translational efficiency of *WOR1*. The *WOR1* 5'UTR negatively regulates white-opaque switching and reduces the stability of the opaque cell state. We show evidence of reduced translational efficiency of 5'UTR-*WOR1* both through polysome analysis, in which 5'UTR-*WOR1* transcripts are more enriched in monosomes than polysomes, and through assays which demonstrate lower protein being translated from 5'UTR-*WOR1* than Δ5'-*WOR1* transcripts, even as transcription of the two remain the same. This effect is independent of the *WOR1* promoter, and also of the *WOR1* coding region; placing the *WOR1* 5'UTR upstream of another gene under an ectopic promoter produce the same reduction in translation. Therefore, *WOR1* 5'UTR is sufficient for the observed translational repression.

The mechanisms by which the *WOR1* 5'UTR regulates translation leave ample room to be explored. There are numerous known mechanisms through which a 5'UTR may affect translational efficiency. Within 5'UTR regions themselves, upstream ORFS (uORFs) and upstream AUGs (uAUGs) have been identified as a mechanism for translational regulation. Work in yeast has demonstrated that out-of-frame uAUGs can significantly alter the translational efficiency of a gene (Dvir *et al.*, 2013). However, the *WOR1* 5'UTR contains no uORFs or

uAUGs, so this possibility was eliminated. Secondary structures in the 5'UTR are also known to negatively regulate translational efficiency, as stable structures can inhibit translational initiation. The secondary structure of the *WOR1* 5'UTR and its effects on translation has yet to be determined due to the length of the 5'UTR. Additional work has shown that the length and structure of the 5'UTR impacts translational repression by miRNAs through RNA interference [27]. *C. albicans* potentially has an intact RNAi system, (Briggs *et al.*, 1989). We tested the effect of Argonaute on 5'UTR translational regulation and found that deletion of *AGO1* did not increase the translational efficiency of transcripts bearing the *WOR1* 5'UTR. Thus regulation through Argonaute appears an unlikely mechanism. It should be noted that Argonaute and Dicer appear insufficient for RNA interference in *C. albicans* (Liu *et al.*, 1996), and other components of RNA silencing pathways may still have effect on *WOR1* transcript regulation.

Cap-independent translation initiating in the 5'UTR provides an alternate mechanism for translational regulation. It is possible that cap-independent translation of 5'UTR-*WOR1* occurs at a slower rate than cap-dependent translation, and that this may be a dominant means of *WOR1* translation under some conditions. As a preliminary test, we assayed whether uncapped 5'UTR-*WOR1* transcripts exist in opaque cells. We find that such transcripts are low, if not undetectable. Thus, the translation of uncapped RNAs does not appear to be a major mechanism regulating translation of 5'UTR-*WOR1*.

Finally, RNA-binding protein activity at the 5'UTR is another mechanism for translational regulation. One such example is Ssd1, which has been demonstrated to repress translation of specific genes by binding to their 5'UTR and 3'UTR in *S. cerevisiae* (Cao *et al.*, 2006). Notably,

Ssd1 represses translation of a specific subset of genes involved in cell morphogenesis and mother-daughter separation (Brooks & Jackson, 1994). Ssd1 targets are expected to be highly expressed in opaque cells, so Ssd1 is a candidate for regulation at the *WOR1* 5'UTR. We find that translational efficiency is reduced by the *WOR1* 5'UTR in *ssd1* deletion mutant in a similar extent to WT, so Ssd1 does not appear to regulate translation through the *WOR1* 5'UTR. However, the role of numerous other RNA-binding proteins on the *WOR1* 5'UTR remain to be tested. Whether the observed translational regulation at the 5'UTR occurs through one of these proteins will require further exploration.

The identification of the *WOR1* 5'UTR as a translational regulator of *WOR1* raises many questions for further investigation. The role of the 5'UTR in translational regulation in higher eukaryotes has been extensively characterized, and in recent years various studies in yeast have been done exploring instances of UTR-mediated regulation as well. However, in *C. albicans*, the characterization of the effect on translation by 5'UTRs has only begun to be explored. Recent work has shown that the *UME6* 5'UTR, which is long and has predicted complex structure, reduces the translational efficiency of *UME6* and thereby negatively regulates filamentation (Childers *et al.*, 2014). RNAseq studies in *C. albicans* have identified long 5'UTRs on genes regulating white-opaque switching, hyphal morphogenesis, and key processes in pathogenesis and commensalism. Our findings on *WOR1* identifies a novel level of regulation for white-opaque switching through translation, and lends support to the possibility that key regulators of cell fate and cell morphology in *C. albicans* are translationally regulated through their 5'UTRs. Further work may demonstrate roles for 5'UTR on numerous other genes, through similar or perhaps disparate mechanisms.

Chapter 4

Overlapping functions between *SWR1* deletion and H3K56 acetylation in *Candida albicans*

Introduction

Chromatin-level changes, such as histone modifications, variants, and nucleosome remodeling, have been implicated in the epigenetic regulation of gene expression in many systems. In recent years, focus has shifted toward the role of nucleosome dynamics in epigenetic regulation, in particular the importance of nucleosome destabilization in the establishment and inheritance of active chromatin states (Henikoff, 2008). Increasing evidence has shown that numerous histone modifications affect nucleosome stability and dynamics by altering rate of nucleosome turnover and DNA access (Zentner & Henikoff, 2013).

One such example of a histone modification altering nucleosome dynamics is the acetylation of H3 lysine 56. H3K56 acetylation occurs during S phase on newly synthesized histones, and facilitates histone deposition onto replicating DNA, as well as nucleosome assembly (Masumoto *et al.*, 2005). Consequently, H3K56ac is found highly on newly synthesized chromatin, and is involved in chromatin packing after DNA replication and repair in *S. cerevisiae* (Masumoto *et al.*,

2005, Li *et al.*, 2008, Chen *et al.*, 2008). During transcriptional activation, H3K56ac promotes chromatin disassembly (Williams *et al.*, 2008, Xu *et al.*, 2005). Replication-independent deposition of histones is also associated with H3K56ac (Rufiange *et al.*, 2007). In addition, H3K56 is located near the DNA entry and exit points on the nucleosome core particle (Luger *et al.*, 1997), further implicating its role in nucleosome dynamics. In yeast, the acetylation of H3K56 is performed by the histone acetyltransferase Rtt109 (Driscoll *et al.*, 2007, Han *et al.*, 2007), and deacetylation occurs by the sirtuin class HDACs, Hst3 and Hst4 (Celic *et al.*, 2006, Maas *et al.*, 2006).

H3K56 acetylation has been shown to regulate the epigenetic process of white-opaque switching in *Candida albicans*. As in *S. cerevisiae*, H3K56 acetylation in *C. albicans* is regulated by Rtt109 and Hst3 (Lopes da Rosa *et al.*, 2010, Wurtele *et al.*, 2010). Deletion of *RTT109* in *C. albicans*, which prevents acetylation of H3K56, has been shown to impair white-opaque switching, while the *HST3/hst3* mutant promotes switching. Treatment with nicotinamide, which increases H3K56ac, also promotes switching to opaque, and this activity has also been shown to be dependent on *RTT109* (Stevenson & Liu, 2011). Furthermore, hyperacetylation of H3K56 is toxic to *C. albicans* (Stevenson & Liu, 2013, Wurtele *et al.*, 2010) .

In *S. cerevisiae*, high H3K56ac has been shown to reduce chromatin levels of the histone variant H2A.Z, and increase the eviction of H2A.Z-containing nucleosomes (Watanabe *et al.*, 2013). This is notable as H2A.Z itself has been implicated in altering nucleosome dynamics and stability. H2A.Z is a highly conserved variant of H2A, and is essential in a number of eukaryotic organisms but not in yeast (Jackson & Gorovsky, 2000, Liu *et al.*, 1996, van Daal & Elgin, 1992).

H2A.Z is enriched in euchromatin at the promoters of both actively expressed and repressed genes, and prevents the spread of heterochromatin (Raisner *et al.*, 2005, Meneghini *et al.*, 2003, Guillemette *et al.*, 2005). Nucleosomes containing H2A.Z are enriched at the nucleosome-free regions (NFR) adjacent to the +1/-1 nucleosomes at the transcriptional start site of genes (Raisner *et al.*, 2005). H2A.Z-containing nucleosomes have been noted to have altered stability; however, separate studies have shown H2A.Z nucleosomes to be either more or less stable than those with H2A (Dion *et al.*, 2007, Park *et al.*, 2004). Of particular note is the finding that nucleosomes containing both H3.3, the variant of H3 which is the canonical H3 in yeast, and H2A.Z, are more labile (Henikoff, 2009). In multicellular organisms, H2A.Z has been associated with cellular differentiation and reprogramming (Creyghton *et al.*, 2008). H2A.Z is deposited by the Swi/Snf family chromatin remodeling complex SWR1 through ATP-dependent exchange of H2A.Z-H2B dimers with H2A-H2B (Kobor *et al.*, 2004, Mizuguchi *et al.*, 2004). Neither H2A.Z nor SWR1 are essential in yeast; however, SWR1 activity causes genetic instability in the absence of H2A.Z (Morillo-Huesca *et al.*, 2010). The acetylation of canonical histone H2 and H4 tails by the NuA4 complex has been shown to recruit SWR1 to deposit H2A.Z (Altaf *et al.*, 2010). In yeast, NuA4 and SWR1 share 4 subunits, including YAF9 which is critical for SWR1 deposition of H2A.Z; functions of the two in higher eukaryotes are shared by the NuA4/Tip60 complex (Zhang *et al.*, 2004). However, NFRs are dominant over histone acetylation in targeting SWR1 activity (Ranjan *et al.*, 2013). The localization and effect on nucleosomal dynamics by H2A.Z make it a promising subject for the study of epigenetic regulation.

In this study, we find that deposition of H2A.Z by SWR1 is crucial in regulating the white-opaque transition in *C. albicans*. Abrogation of H2A.Z deposition through deletion of *SWR1*, the major subunit of the SWR1 complex, results in a phenotype that favors switching to opaque and stability of opaque phase. We find that nucleosome dynamics on the promoter of *WOR1*, the master regulator of switching (Huang *et al.*, 2006, Srikantha *et al.*, 2006, Zordan *et al.*, 2006), differs between white and opaque phase, and that deletion of *SWR1* changes this dynamic. Furthermore, H2A.Z is present on the *WOR1* promoter at higher levels in white phase than in opaque, suggesting that its absence destabilizes white cells. We find that deletion of *YNG2*, a subunit of the NuA4 complex, produces a similar white-opaque phenotype to *swr1*. Furthermore, we find that *swr1* deletion mutant displays a synthetic lethality with nicotinamide but no heightened sensitivity to DNA damage, suggesting a close functional relationship between H2A.Z and H3K56ac in *C. albicans*.

Results

The *swr1* deletion mutant increases white-to-opaque switching frequency and stabilizes opaque phase

To investigate the role of chromatin remodeling by SWR1 on white-opaque switching, we deleted *SWR1* in *C. albicans* using homologous recombination to replace with auxotrophic markers described by Noble and Johnson (Noble & Johnson, 2005). In the resulting *swr1* deletion mutant, chromatin immunoprecipitation confirmed that deposition of H2A.Z into chromatin was abrogated (not shown). High rates of spontaneous switching to opaque in white colonies of *swr1* was observed at room temperature, often occurring as multiple opaque sectors per white colony (Figure 4.1A). The switching percentage of *swr1* at room temperature (25 ℃) is 82%, compared to 2-4% for wild type. Opaque cells of *swr1* are more stable than wild type, with 100% remaining opaque after 7 days of growth at RT, compared to 66% for WT (Figure 4.1B). To test the ability of *SWR1* re-expression to complement the *swr1* switching phenotype, we used a conditional *swr1* mutant from the *C. albicans* GRACE (gene replacement and conditional expression) library (Roemer *et al.*, 2003). The sole copy of *SWR1* in the conditional mutant is regulated by a TET-inducible system. Cells are *SWR1/swr1* in the absence of doxycycline and effectively *swr1/swr1* in its presence. In the absence of doxycycline, *swr1 + SWR1* showed white-opaque and opaque-white switching behavior similar to that of wild-type, while on doxycycline, the strain behaved similarly to the *swr1* deletion mutant we generated (Figure 4.2). We next sought to determine the effect of temperature on the *swr1* white-opaque phenotype. At higher temperatures of 30 ℃ to 37 ℃, white-opaque switching of *swr1* increases to 100% and

97%, respectively, while WT cells no longer switch. *swr1* opaque stability is reduced but still greater than WT, remaining at 86% (30 ℃) or 30% (37 ℃) opaque while all WT cells switch to white (Figure 4.1C). We also compared the phenotype of *swr1* to *efg1*, the deletion mutant of the transcriptional regulator *EFG1*, which is known to be highly white-opaque switching. Unlike *swr1*, *efg1* is not able to switch to opaque and *efg1* opaque cells are unstable at high temperatures (Figure 4.1B-C). From these results, we find that the white-opaque switching and opaque stability are enhanced in *swr1*, even at higher temperature.

We proceeded to investigate whether deletion of *SWR1* promotes switching downstream of known pathways. It has been documented that low concentrations of CO_2, as well as utilization of N-acetyl-glucosamine (GlcNAc) as the main carbon source, promote white-opaque switching, and these two pathways show a synergistic effect with each other (Huang *et al.*, 2009, Huang *et al.*, 2010). To assay whether SWR1 acts downstream either of these pathways, we cultured white cells of WT and *swr1* in air or 5% CO_2, on Lee's medium with dextrose or GlcNAc as the carbon source, and tracked switching to opaque over the course of 14 days. In WT, as previously documented, both CO_2 and GlcNAc promoted white-opaque switching and showed synergy with each other. In the *swr1* mutant, we observed higher spontaneous switching than WT even in the control condition of growth in air on dextrose. Notably, switching of *swr1* was elevated in the presence of CO_2 regardless of carbon source, showing a synergy similar to that of GlcNAc and CO_2 (Figure 4.1D). Thus, *SWR1* deletion appears to drive white-opaque switching in a pathway separate from the Flo8-mediated CO_2-sensing pathway, and may instead act downstream of the GlcNAc signaling pathway. Although wild-type opaque cells switch to white at 37 ℃ under most conditions, it has been noted that GlcNAc as a carbon source increases switching in a manner

synergistic with higher temperature as well (Huang *et al.*, 2010). This is consistent with the observation of white-to-opaque switching at high temperature in the *swr1* mutants.

We then explored the mechanisms behind the white-opaque phenotype of *swr1* through regulation of *WOR1*, the master regulator of switching. First, we investigated whether *swr1* had higher expression from the *WOR1* promoter by using WT and *swr1* strains transformed with the p*WOR1-GFP* plasmid, which expresses *GFP* from the native *WOR1* promoter. After 4 days of growth on solid SCD media starting from white cells, *swr1* showed numerous instances of darker colonies and sectors compared to WT, indicative of the expression of *pWOR1-GFP* in cells that had become opaque (Figure 4.1E). This further supports elevated white-to-opaque switching in *swr1*. To determine *WOR1* expression levels in white and opaque cells, fluorescence activated cell sorting (FACS) was performed on WT, *swr1* and *efg1* cells carrying *pWOR1-GFP*. As seen by histograms of population-wide fluorescence, transcription from the *WOR1* promoter in white cells was not greater in *swr1* than WT. In opaque cells, GFP in *swr1* was slightly elevated from WT, but not as much as in *efg1* (Figure 4.1F). Thus, the major regulation behind the white-opaque phenotype of *swr1* does not appear to be through increased expression of *WOR1*.

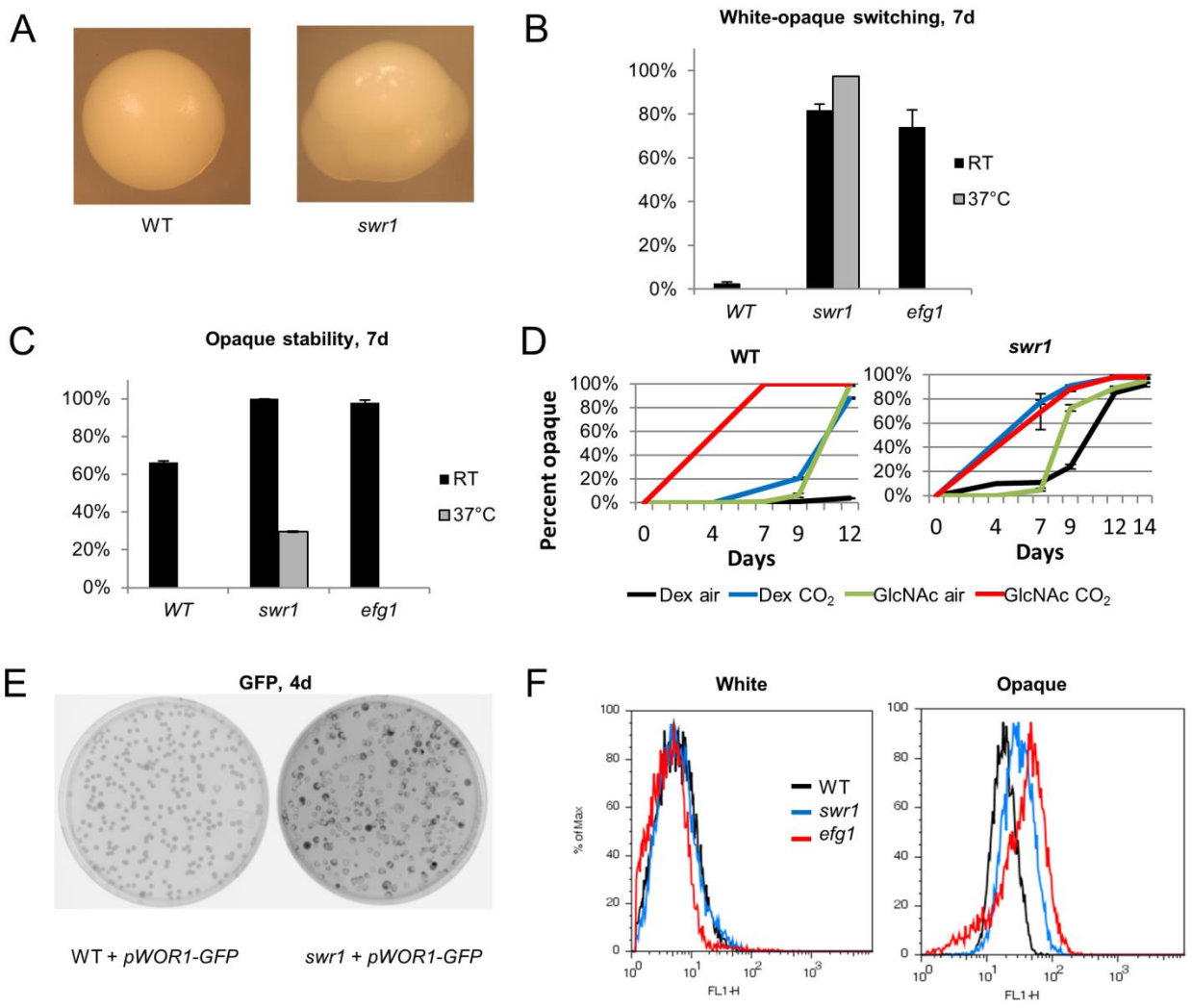

Figure 4.1. Elevated white-opaque switching and opaque stability, switching synergy with CO_2, and *WOR1* expression in the *swr1* deletion mutant. (A) Single colonies of white WT (JYC1) and *swr1* (HLY4233) cells after 7 days of growth at room temperature (25 ℃) on YPD. The *swr1* colony displays multiple opaque sectors typical of the strain. (B) Spontaneous white-to-opaque and (C) opaque-to-white switching rate of *swr1* compared to WT at varying temperatures of RT (25 ℃), 30 ℃, and 37 ℃ after 7 days of growth on SCD. (D) Percentage spontaneous switching to opaque of white cells of WT, *swr1*, and *efg1* after 12 days of growth on Lee's media with 1.25% dextrose or 1.25% N-acetyl-glucosamine (GlcNAc) as the carbon source, in air or 5% CO_2, at RT. (E) Fluorescence image of colonies of WT + *WOR1p-GFP* (HLY3555) and *swr1* + *WOR1p-GFP* (HLY4234) after 4 days of growth on SCD at RT. Opaque colonies and sectors, expression more GFP, appear darker. (F) Fluorescence activated cell sorting (FACS) profiles of GFP fluorescence in a population of 10,000 cells of white or opaque WT + *pWOR1-GFP* (HLY3555), *swr1* + *pWOR1-GFP* (HLY4234), and *efg1* + pWOR1-GFP (HLY3600). Cells were from log phase liquid culture at RT.

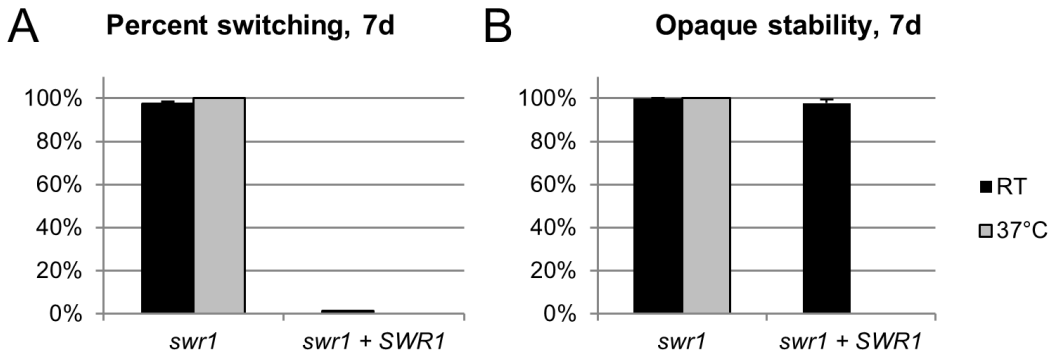

Figure 4.2. The *swr1* switching phenotype is complemented by re-expression of *SWR1*. (A) Spontaneous white-to-opaque and (B) opaque-to-white switching rate of *swr1* (GRACE#2061 + doxy) compared to *swr1 + SWR1* (GRACE#2061 – doxy) at RT (25 ℃) and 37 ℃ after 7 days of growth on SCD +/- 50 µM doxycycline. A GRACE conditional mutant was used for which the expression profile of the strain was *swr1* in the presence of doxycycline and *swr1 + SWR1* in its absence.

Nucleosome positioning on the *WOR1* promoter differs between white and opaque cells, and is altered in *swr1*

We next sought to investigate whether deletion of *SWR1* altered the white-opaque phenotype by changing regulation of *WOR1* through chromatin remodeling at the *WOR1* promoter. As *WOR1* has a long 8kb promoter as well as long 5'UTR, nucleosomal dynamics upstream of *WOR1* may be crucial to the regulation of its transcription. Since H2A.Z-containing nucleosomes have been shown to have altered stability and dynamics (Dion *et al.*, 2007, Henikoff, 2009, Mizuguchi *et al.*, 2004, Park *et al.*, 2004), we proceeded with a nucleosome map of the *WOR1* promoter in WT and *swr1* cells, both of which carry HA-tagged *HTA3* (H2A.Z) to facilitate further studies. To obtain nucleosomal DNA, *Staphylococcus aureus* micrococcal nuclease digestion was performed in order to cleave non-nucleosome-bound DNA, while leaving nucleosome-bound DNA intact. Then, qPCR was performed on the nucleosomal DNA, amplifying for staggered 100 bp regions along the *WOR1* promoter, providing a map of nucleosomal enrichment in this region. We find that even in WT, white and opaque cells show a difference in nucleosome occupancy and positioning along the *WOR1* promoter. While regular nucleosome peaks are observed in both, notably, nucleosome positioning is more defined in white cells. In particular, this is true of the +1/-1 nucleosomes adjacent to the transcriptional start site -1997 bp upstream of the *WOR1* ATG. In white cells, there is also a nucleosome-free region (NFR) approximately 2550 to 2350 bp upstream of the *WOR1* ATG, absent in opaque cells. In *swr1*, we see a marked change in nucleosome positions on the *WOR1* promoter compared to WT. Nucleosome positioning is greatly altered from wild type, particularly in white cells and the NFR is abolished. The highly elevated levels of nucleosome occupancy at NFRs of the *WOR1* promoter in white *swr1* cells

likely reflect slower nucleosome turnover, which is consistent with the known function of H2A.Z. In contrast, nucleosome occupancy at the NFRs of *WOR1* promoter is much lower in opaque *swr1* cells than wild-type white or opaque cells (Figure 4.3). The lower level of nucleosome occupation in the opaque *swr1* cells indicates decreased nucleosome stability at the *WOR1* promoter. The mechanism of the differential effects of *swr1* on nucleosome occupation at the same promoter in different cell types is not known. But this more "open" chromatin conformation on the *WOR1* promoter in opaque *swr1* cells may contribute to persistent *WOR1* transcription and opaque stability. Overall, nucleosome mapping suggests that SWR1 is required for proper nucleosome positioning and stability at the *WOR1* promoter. Our data, therefore, support the importance of SWR1 and deposition of H2A.Z in epigenetic regulation of transcription in cell fate determination.

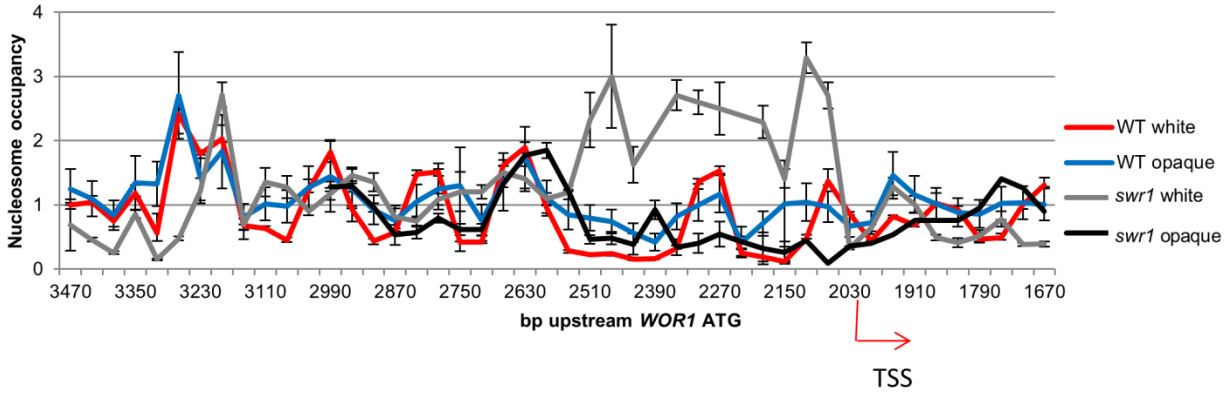

Figure 4.3. Nucleosome map of the *WOR1* promoter shows white-opaque differences in wild type, and altered nucleosome positioning and occupancy in *swr1*. Nucleosomal DNA was isolated from WT+*HTA3*-HA (HLY4238) or *swr1*+*HTA3*-HA (HLY4236) after removing non-nucleosome-bound DNA with micrococcal nuclease digestion. Mapping was performed with qPCR using primers amplifying 100 bp regions along the *WOR1* promoter.

H2A.Z is enriched at the *WOR1* promoter in white cells

H2A.Z is known to be enriched at developmentally regulated regions. To further investigate nucleosomal H2A.Z content, we mapped H2A.Z enrichment along the *WOR1* promoter in white and opaque WT cells. In addition, *swr1* cells were used as control. H2A.Z was HA-tagged in all strains used. H2A.Z enrichment was assayed by immunoprecipitation of H2A.Z-containing nucleosomes using anti-HA on micrococcal nuclease treated nucleosomes from Fig. 2, followed by qPCR using the same *WOR1* primers used for nucleosome mapping to provide coverage along the *WOR1* promoter. As expected, H2A.Z levels on promoter chromatin are very low in the *swr1* mutant. In wild type, notably, H2A.Z is higher in white cells than in opaque cells. Particularly of interest is that H2A.Z is enriched in the -2 and -1 nucleosomes at two NFRs on the *WOR1* promoter (Figure 4.4). The location of H2A.Z-enriched nucleosomes at NFRs is consistent with its role in promoting nucleosome dynamics, as shown in yeast and high eukaryotes (Teves *et al.*). Elevated H2A.Z deposition by SWR1 at the *WOR1* promoter in white cells indicates a role for H2A.Z in stabilizing the repressive chromatin state in white cells.

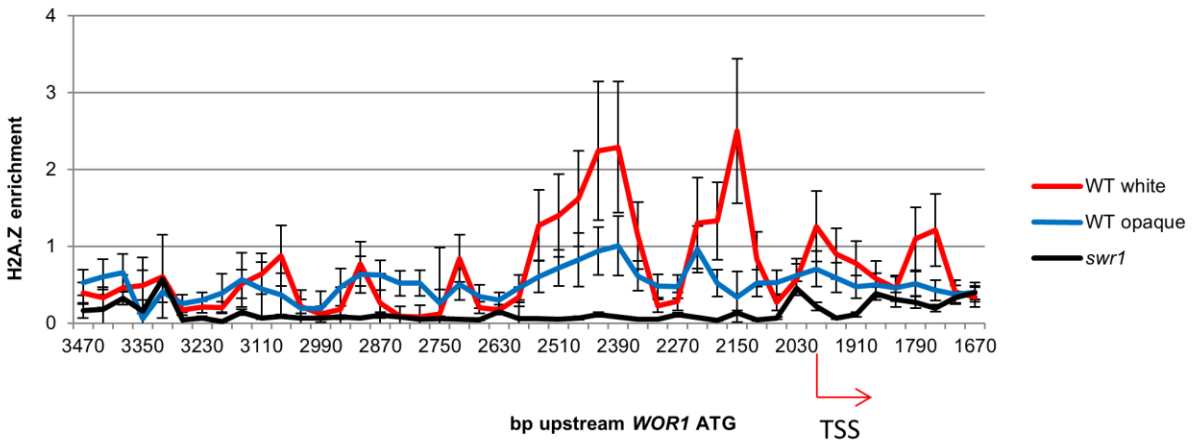

Figure 4.4. Differential enrichment of H2A.Z at the *WOR1* promoter is seen in white and opaque cells. Chromatin immunoprecipitation of HA-tagged H2A.Z was performed on nucleosomal DNA isolated from WT+*HTA3*-HA white and opaque cells, and *swr1*+*HTA3*-HA opaque cells. qPCR was performed using primers used to map the *WOR1* promoter. Results are normalized to total nucleosome level.

Deletion mutant of *yng2*, a subunit of the NuA4 complex, produces similar white-opaque switching phenotype and synergy with CO_2 as *swr1*

In exploring the regulation of H2A.Z deposition, we considered the recruitment of SWR1 by NuA4 acetylation of H2 and H4, and the substantial overlap in subunits between the SWR1 and NuA4 complexes. Yng2 is a subunit of the NuA4 HAT module, deletion of which we have shown severely impairs H4 acetylation (Lu *et al.*, 2008). Thus, we investigated whether deletion of *YNG2* would produce a white-opaque phenotype similar to *swr1*. We found that at room temperature, white cells of the *yng2* mutant switched to opaque at a much high frequency compared to wild type, while opaque cells of *yng2* were highly stable (Figure 4.5A). In addition, opaque *yng2* cells were stable at 30^{o}C but not at 37^{o}C (not shown). Because of the relation between NuA4 acetylation of histones and SWR1 deposition of H2A.Z in the same nucleosome, we speculated that *yng2* and *swr1* produced their high-switching phenotype through the same pathways, and would respond similarly to CO_2 and GlcNAc. To test this, white cells of *yng2* were grown at room temperature in air or 5% CO_2 with dextrose or GlcNAc as a carbon source, and switching was assessed. We found that *yng2* began switching to opaque sooner when incubated in CO_2, preceding switching in air by several days. This behavior is similar to that of *swr1*, though the complete conversion of white *yng2* colonies to opaque occurs sooner than *swr1*. Notably, *yng2* switches more slowly when the carbon source is GlcNAc than when grown on dextrose, showing a more complete lack of synergy with GlcNAc than *swr1* does (Figure 4.5B). Therefore, like SWR1, Yng2/NuA4 also functions downstream of the GlcNAc signaling pathway, separate from the CO_2 regulated pathway. This is consistent with the known function of NuA4 in histone acetylation, which in turn allows SWR1 recruitment and H2A.Z deposition.

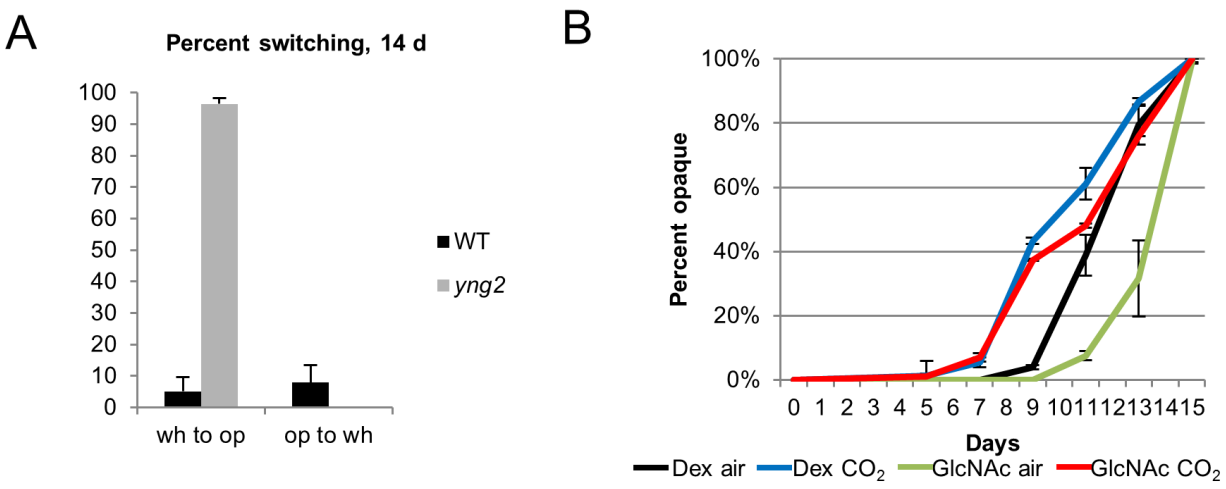

Figure 4.5. White-opaque switching of *yng2* is elevated and shows synergy with CO_2. (A) Spontaneous white-to-opaque and opaque-to-white switching rate of *yng2* (CLY4) compared to WT after 14 days at room temperature on SCD medium. (B) Percentage spontaneous switching to opaque of white cells of *yng2* after 15 days of growth on Lee's media with 1.25% dextrose or 1.25% N-acetyl-glucosamine (GlcNAc) as the carbon source, in air or 5% CO_2, at RT.

***swr1* is highly sensitive to nicotinamide (NAM)**

In addition to epigenetic regulation of white-opaque switching, we also sought to investigate the effects of *swr1* deletion on additional cellular functions. H2A.Z is enriched in nucleosomes surrounding TSSs and is involved in gene expression (Weber & Henikoff, 2014) . Proper deposition of H2A.Z has been linked to numerous global effects, such as euchromatin-heterochromatin boundary establishment, centromeric functions, and DNA repair (Meneghini *et al.*, 2003, Greaves *et al.*, 2007, Xu *et al.*, 2012, Kalocsay *et al.*, 2009). Recent work in *S. cerevisiae* has demonstrated that heightened acetylation of H3K56 is associated with reduced deposition and increased eviction of H2A.Z from chromatin by SWR1, with significant overlap in gene expression profiles between cells with constitutively acetylated H3K56 and *htz1* (H2A.Z) deletion (Watanabe *et al.*, 2013). It is known that NAM inhibits *C. albicans* growth by elevation of H3K56ac levels through inhibition of the HDAC Hst3 (Stevenson & Liu, 2011, Wurtele *et al.*, 2010). To further explore the functional relationship between H3K56ac and H2A.Z deposition, we examined sensitivity of WT, *SWR1/swr1*, *swr1*, *HST3*/*hst3*, and *rtt109* strains to NAM by a spot assay for growth on solid medium in the presence of nicotinamide (NAM). Cells were grown for 3 days at 30℃. As reported, *HST3*/*hst3* was highly sensitive to NAM and barely grew at 4 mM NAM, while *rtt109* was more resistant to NAM than WT at 4 mM, consistent with previously reported results (Stevenson & Liu, 2011). Interestingly, *swr1* was even more sensitive to NAM than *HST3*/*hst3*, barely growing even on 2mM NAM (Figure 4.6A). Unlike *HST3*/*hst3*, NAM sensitivity was not observed in *SWR1/swr1*. The lack of haploid insufficiency indicates that NAM probably does not directly act on Swr1. In contrast to NAM sensitivity, *swr1* and *HST3*/*hst3* did not show any increased sensitivity to the DNA-damaging agent methyl

methanesulfonate (MMS), while *rtt109* was sensitive (Figure 4.6A). In addition, *swr1* showed no increased growth sensitivity to hydroxyurea, or heat and osmotic stress (not shown). We have previously shown that *rtt109* mutant has increased rate of generating aneuploidy (Stevenson & Liu, 2013). To assess whether *swr1* also had an increase in aneuploidy, we assayed its ability to survive utilizing L-sorbose as a carbon source, which requires monosomy of chromosome 5 in *C. albicans* (Janbon *et al.*, 1998). However, we did not observe any elevation in aneuploidy formation in *swr1* compared to WT after growth on L-sorbose medium (Figure 4.7.). Therefore, *rtt109* (or blocking H3K56 acetylation) is associated with aneuploidy and sensitivity to DNA damage, while H3K56Ac and *swr1* are associated with sensitivity to NAM. From our genetic studies, we suggest that the NAM sensitivity of *swr1* and H3K56Ac is associated with their roles in gene expression. If the NAM sensitivity of *swr1* is through regulation of gene expression, we expect to see NAM functioning synergistically with *swr1* in *WOR1* expression, and therefore, white-to-opaque switching. To test this, white cells of WT, *SWR1/swr1*, and *swr1* strains were grown on solid SCD media containing varying concentrations of NAM for 7 days to observe spontaneous switching. The switching rate of *SWR1/swr1* did not differ from wild-type when exposed to NAM, while *swr1* displayed increased switching to opaque at concentrations of NAM where growth was still able to occur (Figure 4.6B). The increase in switching frequency by NAM is limited because *swr1* already has over 80% switching rate. Thus, deletion of *SWR1* and NAM act in parallel in white-opaque switching (Figure 4.6B), and NAM acts via Hst3 to increase level of H3K56Ac in white-opaque switching (Stevenson & Liu, 2011).

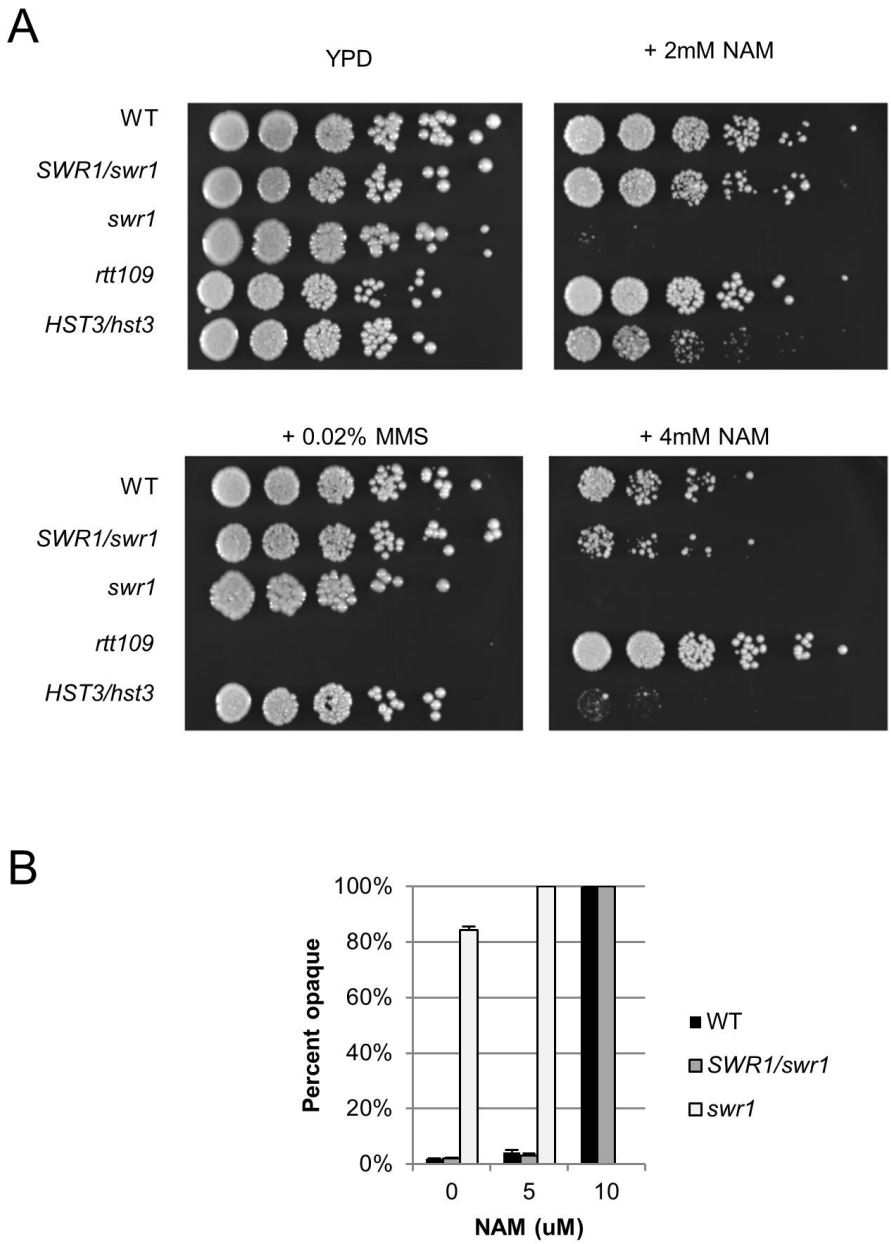

Figure 4.6. *swr1* displays synthetic sensitivity to nicotinamide but not to methyl monosulfonate. Spot assay of WT, *SWR1/swr1*, *swr1*, *HST3/hst3* (HLY3993) and *rtt109* (HLY3997) strains on YPD, YPD + 2% methyl monosulfonate (MMS), or YPD + 2mM or 4mM NAM. 5-fold serial dilutions from cultures with OD_{600} = 0.1 were made on agar media plates and incubated 3 days at 30 ℃ prior to imaging.

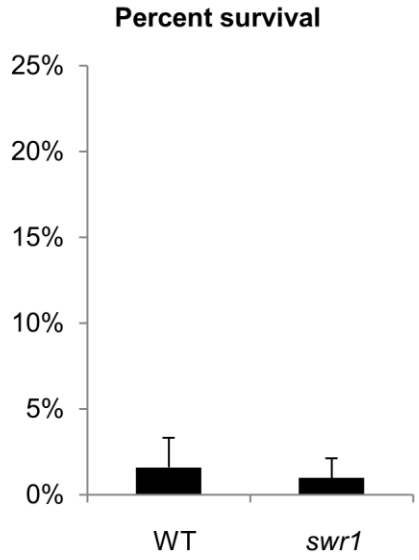

Figure 4.7. *swr1* does not display increased aneuploidy. Percentage survival of WT and *swr1* cells after 6 days of growth on Lee's medium + 2% sorbose as a fraction of colonies formed on 2% dextrose.

Supplemental Results

H2A phosphorylation is not elevated in *swr1* mutant

One early response to DNA damage is the phosphorylation of H2A by Mec1(Lu *et al.*, 2011). In *Drosophila*, the phosphorylated form of the histone variant H2Av is evicted from and exchanged for unphosphorylated form of the variant by the chromatin remodeling complex Tip60, which shares subunits and similar functions with the SWR1 complex (Kent & Mellor, 1995). Furthermore, the chromatin remodeling complex INO80, which acts in opposition to SWR1 by replacing H2A.Z with H2A, has been shown to affect H2A-γ levels in yeast. Deletion of *INO80* is correlated with lower chromatin levels of H2A-γ, as H2A can be phosphorylated but H2A.Z cannot, suggesting an interplay of INO80 and SWR1 in regulation of H2A, H2A-γ, and H2A.Z in chromatin. (Bai *et al.*, 2010, Su *et al.*, 2013). Together, these findings raised the possibility that SWR1 functions to remove H2A-γ from chromatin by exchanging it for H2A.Z. We tested whether deletion of *SWR1* impacts global H2A-γ levels in the event of DNA damage. WT and *swr1* cells were treated with MMS or NAM for one hour, and Western blotting performed for H2A-γ. We find that H2A-γ increases to similar levels in both WT and *swr1* after treatment with either drug (Figure 4.8A). While MMS has long been demonstrated to induce DNA damage and H2A phosphorylation, the documentation of H2A phosphorylation in response to NAM is novel. However, deletion of *SWR1* does not appear to alter the level of H2A phosphorylation response. We next tested whether clearance of H2A-γ after the DNA damaging agent is removed would be affected in *swr1*, if it is unable to replace H2A-γ with H2A.Z. Cells were treated with MMS, washed, and cultured in fresh YPD medium before collection for Western blot. Again, no

difference was observed in H2A-γ levels for WT and *swr1* (Figure 4.8B). Thus, we find that SWR1 does not play a significant role in the H2A phosphorylation response to DNA damage. While nicotinamide does elicit this response, its synthetic lethality with *swr1* appears to be through other mechanisms.

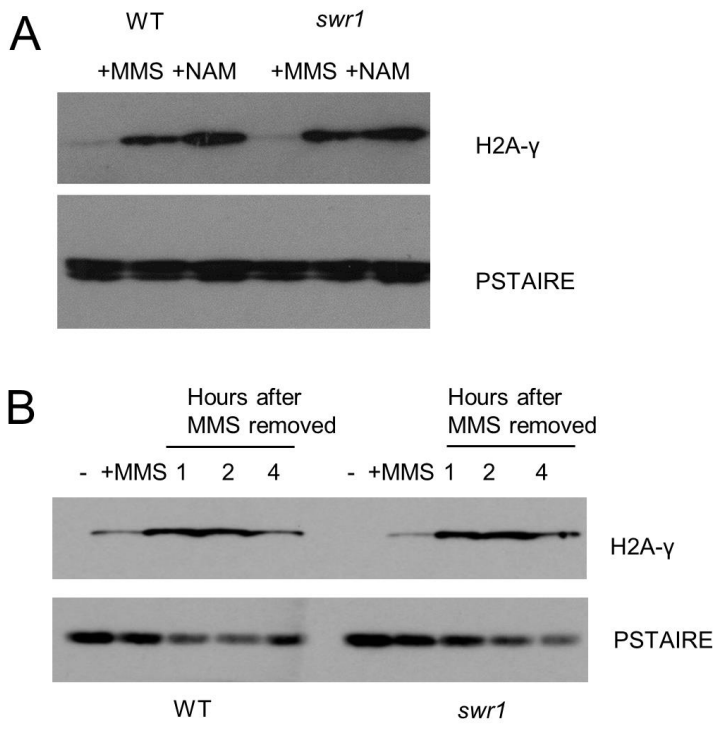

Figure 4.8. H2A phosphorylation in response to MMS is not altered by *swr1* deletion, but is elevated in response to nicotinamide. (A) Western blot against H2A-γ in WT and *swr1* cells grown in YPD and treated with 0.2% MMS or 50mM NAM for 1 hour. (B) Western blot against H2A-γ in WT and *swr1* cells before, during, and after treatment with 0.2% MMS. Cells were washed after 1 hour of treatment and inoculated to fresh media.

Discussion

The role of histone variants and modifications on nucleosomal stability is a promising angle for the investigation of epigenetic regulation. In particular, the histone variant H2A.Z, as well as the acetylation of H3K56, have been linked to changes in nucleosomal dynamics. Previous studies in this lab have demonstrated the effect of H3K56 acetylation on epigenetic regulation of white-opaque switching in *C. albicans*(Stevenson & Liu, 2011, Stevenson & Liu, 2013). In this study we show that epigenetic switching is also regulated by chromatin deposition of H2A.Z by SWR1. Both chromatin modifications affect the switching frequency and stability of cell fates, but do not dramatically affect transcriptional levels of key cell fate regulators. Additionally, we find a synergy between *swr1* deletion and H3K56ac in *C. albicans*.

H2A.Z enrichment at promoter regions is often associated with both active and inactive transcription (Raisner *et al.*, 2005, Meneghini *et al.*, 2003, Guillemette *et al.*, 2005). Many studies find H2A.Z nucleosomes enriched on the promoters of repressed state, and H2A.Z deposition is important for proper induction of gene expression. Our study finds an example of these properties in demonstrating that H2A.Z is enriched at the *WOR1* promoter in white cells, and that white-to-opaque switching is enhanced in *swr1*. Thus, H2A.Z is repressive to *WOR1* expression or opaque state. How does H2A.Z exert both positive and negative effects on transcription? One attractive model is that H2A.Z facilitates the binding of either activating or repressive complexes by keeping regions of promoters accessible (Teves *et al.*, 2014) We find that nucleosome occupancy at the *WOR1* promoter in white cells is elevated when *SWR1* is deleted. The higher nucleosome occupancy at the *WOR1* promoter in *swr1*, in comparison to WT in white cells, is expected to reflect reduced nucleosome dynamics, making the promoter

less accessible to transcription regulators, and in this case, probably negative regulators of white-to-opaque switching. This can lead to an increased switching frequency from white-to-opaque in *swr1*. Future work is needed to examine this model of reduced accessibility of the *WOR1* promoter to negative regulators of white-opaque switching in *swr1*.

In exploring the functional relation of SWR1 with known white-opaque signaling pathways, we also find that the high-switching phenotype of *swr1* show synergy with CO_2 in promoting white-opaque switching. This synergy with CO_2 is similar to that of GlcNAc with CO_2. In addition, *swr1* shows no additional synergy with GlcNAc. Based on these data, we suggest that SWR1 functions downstream of the GlcNAc signaling pathway. A similar high-switching phenotype and synergy with CO_2 is seen in the deletion mutant of *yng2*, a subunit of the NuA4 complex that shares subunits with SWR1 and recruits SWR1 through histone H2 and H4 acetylation. Thus, it is likely that reduced histone acetylation in the *yng2* mutant in turn reduces SWR1 deposition of H2A.Z, producing a similar phenotype to *swr1*. Our genetic data indicate that the GlcNAc signaling in white-opaque switching is likely to regulate *WOR1* promoter chromatin in white cells by down regulating NuA4 and SWR1. In contrast, the major function of the CO_2 signaling pathway in white-opaque switching is not via chromatin remodeling.

A recent study has shown that high H3K56ac reduces nucleosome incorporation of H2A.Z (Watanabe *et al.*, 2013). Not only is H2A.Z deposition greatly reduced on H3K56ac-containing nucleosomes, but the presence of nucleosomal H3K56ac also alters the activity of SWR1, increasing its reverse-reaction activity of eviction of H2A.Z from nucleosomes. While nucleosomes containing both H3K56ac and H2A.Z are not less stable than those with H2A.Z

alone, this increased exchange by H3K56ac can promote nucleosome turnover in H2A.Z-rich regions (Watanabe *et al.*, 2013). On the other hand, can H2A.Z deposition promote the turnover of H3K56ac-nucleosomes? We find in this study that *swr1* deletion mutant is highly sensitive to NAM. As hyperacetylation of H3K56 in chromatin is toxic to *C. albicans*, the high sensitivity of *swr1* to NAM in growth could be due to reduced nucleosome turnover in the absence of H2A.Z deposition and slowed removal of H3K56ac from chromatin. It is interesting to note that while H2A.Z is enriched at the *WOR1* promoter in white cells, H3K56 acetylation is found enriched at the *WOR1* promoter in opaque cells (Stevenson & Liu, 2011).This difference in levels of H3K56ac may explain the differential effects on nucleosome occupation on the *WOR1* promoter between white and opaque *swr1* cells. Future research is needed to examine whether the reduced nucleosome occupancy at the *WOR1* promoter in opaque *swr1* cells is linked to H3K56ac level.

Chapter 5

The full *WOR1* promoter is required for opaque formation but not opaque-specific expression

Introduction

In addition to having a long 5' untranslated region, as discussed in Chapter 3, *WOR1* also has a remarkably long promoter region. While most promoters in yeasts, including *C. albicans*, are a few hundred base pairs or less in length, the *WOR1* promoter is over 8 kb. Wor1 protein is known to positively regulate its own transcription by binding to the *WOR1* promoter. Previous studies using chromatin immunoprecipitation has identified several peaks of Wor1 binding along its own promoter (Zordan *et al.*, 2007). In addition, the *WOR1* promoter is bound by other transcriptional regulators in the white-opaque circuit, such as Efg1, Czf1, and Wor2 (Sonneborn *et al.*, 1999, Srikantha *et al.*, 2000, Zordan *et al.*, 2007). In Chapter 4 of this dissertation, we found differences in nucleosome positioning between white and opaque state between -3 kb and -2kb of the *WOR1* promoter, and this region was also most affected by deletion of *SWR1*. In addition, we found high levels of H2A.Z in this region of the promoter in white cells as well. Thus, the -3 kb to -2 kb region of the *WOR1* promoter may have particular importance in chromatin-level regulation of *WOR1* and binding of regulatory factors.

We sought to investigate the significance of this region of the *WOR1* promoter and its effects on *WOR1* expression, as well as the effects of regions further upstream. To this end, we assayed whether truncation of the *WOR1* promoter to 3 kb upstream of the start codon would lead to reduced output, and also whether this would reduce rate or efficiency of white-opaque switching. Using a GFP reporter under a truncated *WOR1* promoter, as well as the *WOR1* coding region itself under this promoter, we demonstrate that the -3 kb region of the *WOR1* promoter is sufficient to drive some level of opaque-specific expression, with higher expression correlated to promoter length. We further demonstrate that the -3 kb region is not sufficient for levels of *WOR1* expression necessary to sustain opaque phase.

Results and Discussion

Truncation of the *WOR1* promoter reduces opaque-specific expression levels

We sought to test the regulatory effects of *WOR1* promoter length on *WOR1* expression, and in particular whether the -3 kb region was sufficient robust expression. We used *GFP* under the as a reporter for expression from the promoter to reduce the effects of positive feedback from Wor1 protein. *GFP* was cloned either under the full *WOR1* promoter at its native locus, or under 3 kb and 2.4 kb truncated versions of the promoter, in a wild-type (JYC5) background (Figure 5.1A). We expected GFP fluorescence levels to be reduced under the 3 kb promoter compared to full-length if this region was not sufficient for wild-type expression, and equivalent if it was. In addition, the 2.4 kb promoter-*GFP* was expected to have reduced expression if positive *cis*-

regulatory elements between -3 and -2.4 kb exist. All differences in expression were expected to be observed only in opaque cells, as *WOR1* expression is opaque-specific. Indeed, we see that in white cells, no fluorescence is seen in any of the strains (Figure 5.1B). In opaque cells, all strains had markedly higher GFP fluorescence than white cells. In cells carrying GFP under the full-length *WOR1* promoter, fluorescence was highest in the whole population, as shown by histogram. GFP signal was reduced when it was expressed under the 3kb *WOR1* promoter, though still above white-state levels, and even lower under the 2.4kb promoter (Figure 5.1C). These results indicate that the -3 kb to -2kb region is enough to drive some opaque-specific expression, but a full-length *WOR1* promoter is necessary for wild-type levels of expression. Positive cis-regulatory elements driving *WOR1* expression exist both upstream of -3kb, and within the -3 kb to -2.4 kb in the *WOR1* promoter.

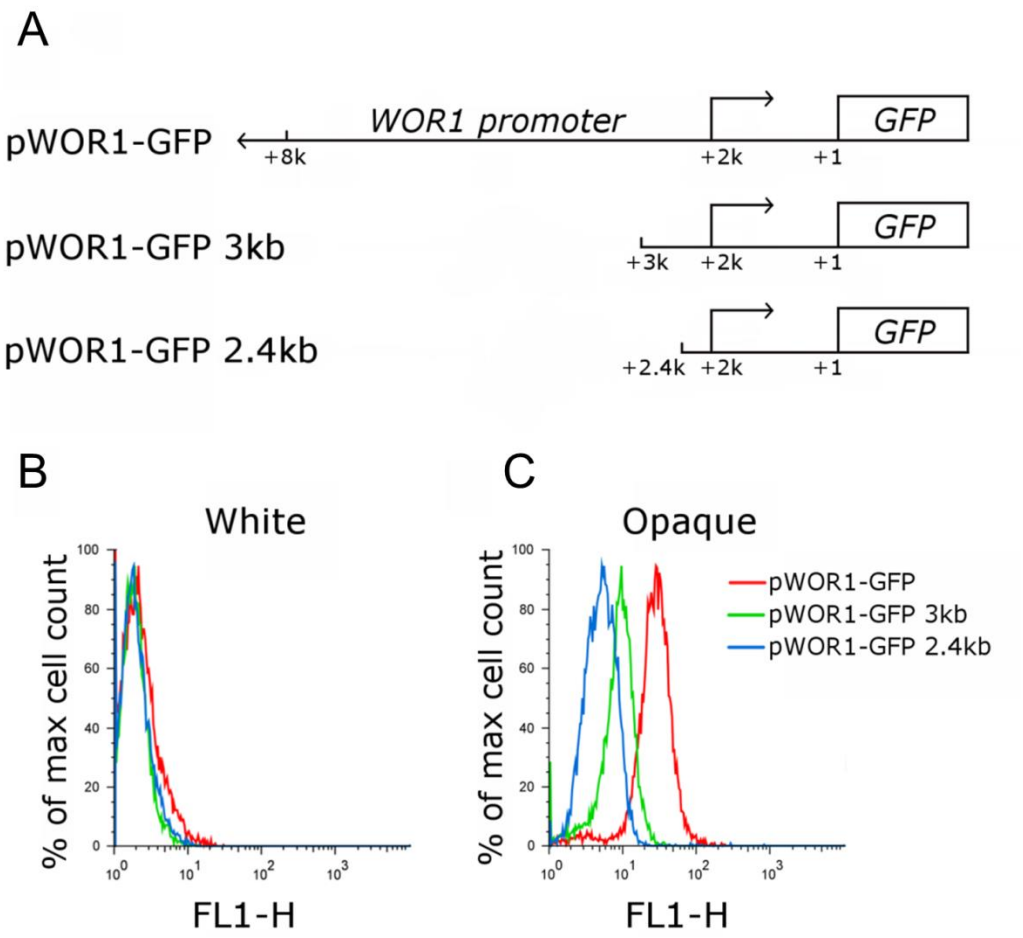

Figure 5.1 Truncation of the *WOR1* promoter reduces expression in opaque cells. (A) Schematic of the full promoter, 3 kb, and 2.4 kb p*WOR1-GFP* reporter constructs. (B) GFP fluorescence from white cells and C. opaque cells of a WT (JYC5) background carrying the full p*WOR1-GFP* (HLY3555), 3 kb p*WOR1-GFP* (HLY3550), or 2.4 kb p*WOR1-GFP* (HLY3895), as a histogram of 10,000 cells.

The 3kb *WOR1* promoter is insufficient to drive white-opaque switching

We further examined the effects of a truncated *WOR1* promoter on white-opaque switching, predicting that switching would be reduced when *WOR1* was solely expressed under the 3 kb promoter. To this end, the sole copy of *WOR1* in a *WOR1/wor1* heterozygous deletion mutant was placed under the 3kb *WOR1* promoter. This was accomplished by integrating the 3kb promoter-GFP construct at a restriction site 1.4 kb upstream of the *WOR1* coding sequence. Integration of the cassette at the intact copy of *WOR1* would result in a strain in which the 3 kb promoter now drove the sole copy of *WOR1*, with GFP under the full *WOR1* promoter (Figure 5.2). An additional strain resulted from the integration of the cassette upstream of the deleted copy of *wor1*. As the intact copy of *WOR1* remained under the full promoter in this strain, it was used as a control. White cells of both strains were grown on solid SCD medium at room temperature for 10 days to assay spontaneous white-opaque switching. No switching was observed for 3kb-promoter-*WOR1/wor1* cells, while spontaneous switching occurred at 4% for full promoter-*WOR1/wor1*, a rate similar to wild-type (Figure 5.3A). As both strains carried p*WOR1-GFP*, opaque sectors could be visualized under fluorescence for the full promoter-*WOR1/wor1* strain but not 3kb promoter-*WOR1/wor1* (Figure 5.3B). This indicated that expression of Wor1 from the truncated promoter had been reduced to such an extent that opaque state could not form.

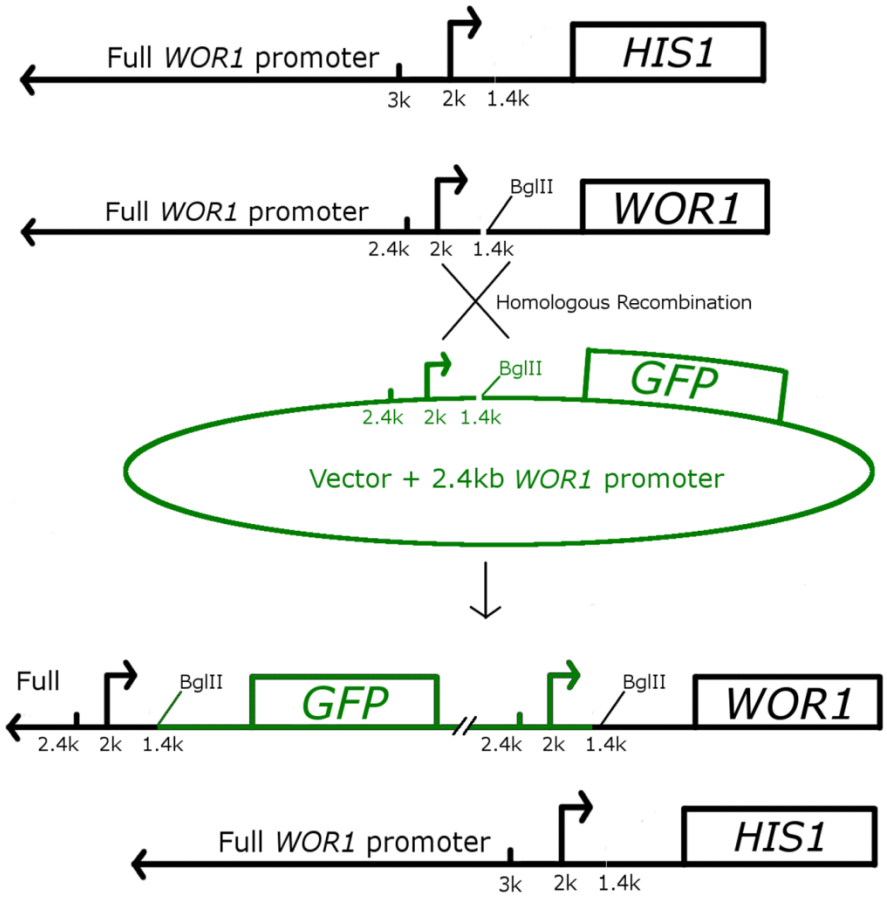

Figure 5.2. Construction of the 3kb promoter-*WOR1/wor1* strain. Schematic shows integration of the 3kb *WOR1* promoter from the p*WOR1-GFP-URA* plasmid to replace the full-length promoter upstream of *WOR1* in the *WOR1/wor1* background strain, resulting in the 3kb *WOR1* promoter-*WOR1/wor1* + p*WOR1-GFP* strain (HLY4239).

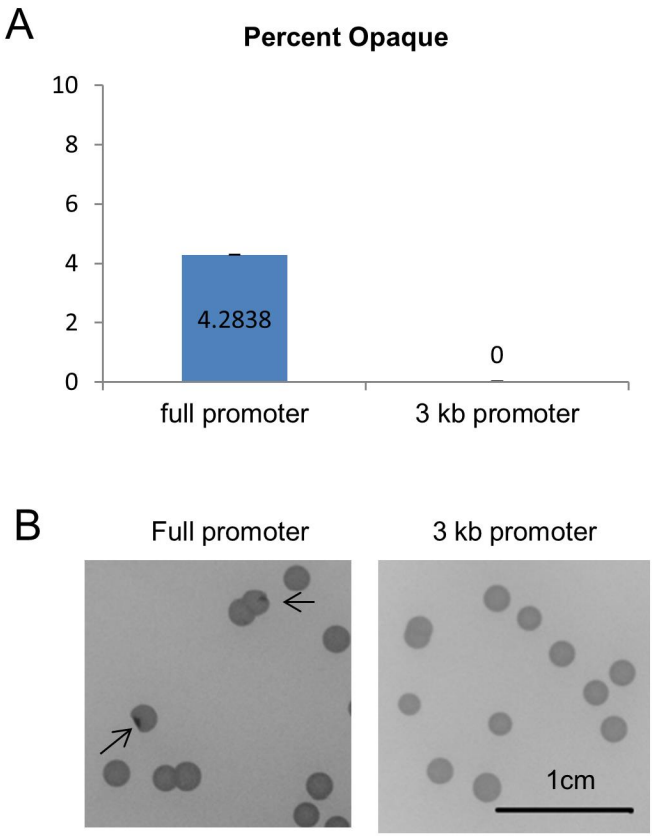

Figure 5.3. Insufficiency of 3kb-promoter-*WOR1* to drive switching. (A) Spontaneous white-to-opaque switching rates of full-promoter-*WOR1/wor1* (HLY4240) and 3kb promoter-*WOR1/wor1* (HLY4239) strains on SCD medium at RT after 7 days. (B) Formation of opaque sectors in white colonies of full-promoter-*WOR1/wor1* but not 3kb promoter-*WOR1/wor1* after 7 days of growth. Opaque sectors are visualized by the presence of p*WOR1-GFP*.

We further investigated the ability of the *WOR1* promoter to respond to positive feedback from Wor1 protein by introducing an ectopic tetracycline- and doxycycline-inducible copy of *WOR1*. The *TET1-WOR1* cassette was transformed into both strains. Induction of ectopic *WOR1* expression by growth in doxycycline-containing medium was expected to drive positive feedback of Wor1 on its own promoter and give rise to an increase in white-opaque switching. White cells of the full promoter-*WOR1/wor1* + *TET1-WOR1* strain and 3kb promoter-*WOR1/wor1*+*TET1-WOR1* strains were incubated at room temperature in liquid YPD culture with 50 μM doxycycline for 48 hours. Cells were removed and plated to solid YPD medium, and colony phenotype subsequently observed. We found that the full promoter-*WOR1/wor1* + *TET1-WOR1* strain showed moderate levels of white-opaque switching, but in the 3kb promoter-*WOR1/wor1*+*TET1-WOR1* strain, again no opaque colonies arose (Figure 5.4A). In addition, cells taken from mid-induction showed greater GFP fluorescence and more opaque-like elongation in the full promoter-*WOR1/wor1* + *TET1-WOR1* strain than the 3kb promoter-*WOR1/wor1*+*TET1-WOR1*strain (Figure 5.4B). These findings indicate that the full length *WOR1* promoter, including regions upstream of -3 kb, is necessary for opaque state and sustained *WOR1* expression through positive feedback, and critical regulatory elements are not limited to the -3 kb region.

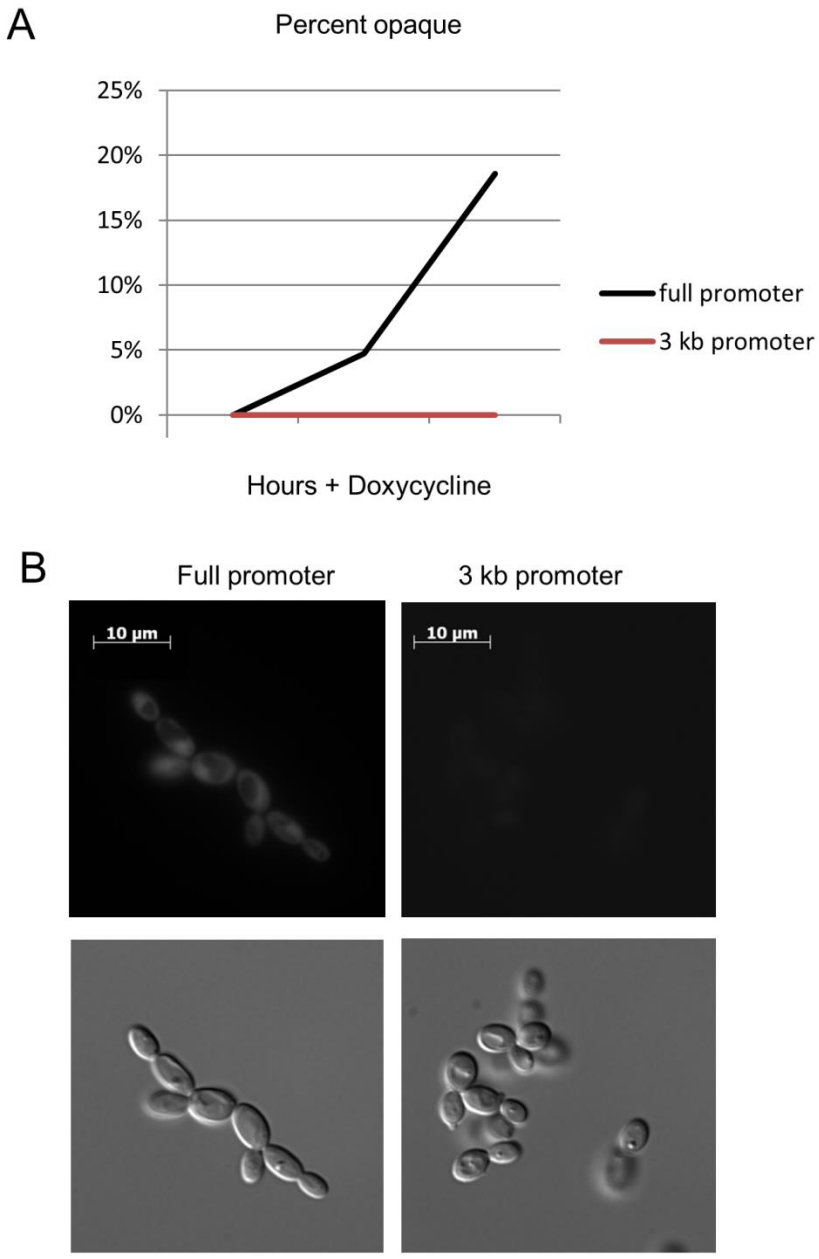

Figure 5.4. 3kb-promoter-*WOR1/wor1* is unable to form opaque even under ectopic expression of *WOR1*. (A) Percent white-opaque switching of full-promoter-*WOR1/wor1* + *TET1-WOR1* (HLY4242) and 3kb promoter-*WOR1/wor1* + *TET1-WOR1* (HLY4241) strains after 48 hours of induction of *WOR1* expression from the TET1 promoter via incubation in YPD + 50 µM doxycycline at RT. Switching was assessed by colony phenotype of cells removed from doxycycline to solid YPD medium. (B) p*WOR1-GFP* fluorescence in full-promoter-*WOR1/wor1* + *TET1-WOR1* and 3kb promoter-*WOR1/wor1* + *TET1-WOR1* strains after 48 hours of induction of *WOR1* expression from the *TET1* promoter.

Chapter 6

Summary and Conclusions

White-opaque switching in *Candida albicans* provides an excellent system for the study of epigenetic regulation of gene expression and phenotype. The master regulator of switching, *WOR1*, is crucial for switching to opaque as well as maintenance of opaque state. *WOR1* and its transcriptional regulators form an interlocking feedback network that has been studied extensively, but many blanks remain to be filled in terms of translational and chromatin-level studies. Studies on epigenetic regulation by upstream elements, and by nucleosome-level elements such as histone variants, have in recent years been carried out in numerous eukaryotic organisms, but rarely in *C. albicans.* Identifying additional regulators of *WOR1* not only furthers understanding of gene regulation in an epigenetic system, but also sheds light on the ability of *C. albicans* to adapt to environmental conditions. The dramatic phenotypic and transcriptional differences between white and opaque phase, the low frequency of switching and the slowness of the transition, all suggest that there is a benefit to a switch-like but rare commitment to phase change. This dissertations explores some of the additional mechanisms of regulation of *WOR1* and epigenetic switching. First, the *WOR1* long 5'UTR is identified as a translational regulator of *WOR1* and of the white-opaque phenotype. Second, deposition of the histone variant H2A.Z by SWR1 is shown to regulate switching by alter nucleosome stability at the *WOR1* promoter, and

to interact with Histone H3 K56 acetylation. Finally, the long *WOR1* promoter is shown to regulate *WOR1* expression, with regions upstream of -3 kb required for opaque formation. The implications of these findings go beyond white-opaque switching and extends to other epigenetic regulations.

Translational regulation of *WOR1* by its 5'UTR

WOR1 and other genes in the transcriptional regulatory network of white-opaque switching have unusually long 5' untranslated regions. In yeasts and higher eukaryotes, long 5'UTRs have been characterized to regulate translation through a number of mechanisms. Recent work in *C. albicans* has also identified examples of regulation by 5'UTR (Childers *et al.*, 2014, Sundaram & Grant, 2014). This study identified the *WOR1* 5'UTR as a translational repressor of *WOR1*, and thus also a repressor of white-opaque switching. Deletion of the 5'UTR led to elevated switching and opaque state stability. 5'UTR-*WOR1* transcripts were more associated with monosome than polysome, in contrast to the polysome-enriched Δ5'-*WOR1* transcripts, indicating lowered translational efficiency. In addition, expression of *WOR1* or a GFP reporter was reduced when the sequence was placed downstream of the *WOR1* 5'UTR, and this was determined to be translational but not transcriptional. The mechanism behind this regulation by the 5'UTR remains to be explored. We have eliminated the possibilities of IRES and uORF/uATG sequences, RNA interference, cap-independent translation, and at least one RNA-binding protein. The length of the *WOR1* 5'UTR makes prediction of its secondary structures quite challenging. Notably, the recent study on the *UME6* 5'UTR in *C. albicans* also did not identify a specific mechanism for its translational regulatory role, but noted that numerous mechanisms were

possible (Childers *et al.*, 2014). Future work on the *WOR1* 5'UTR, including identification of RNA-binding proteins that interact with it, and prediction of its structure, may shed light on the processes through which it regulates translation.

Notably, the monosomal association of 5'UTR-*WOR1* was observed for several other key regulators of white-opaque as well as yeast-hyphal morphogenesis in *C. albicans*, all of which have a long 5'UTR (Bruno *et al.*, 2010, Tuch *et al.*, 2010). Our initial results suggest that long 5'UTRs may play a significant role in the translational regulation of all key regulators of morphological transitions in *C. albicans*, making it an important regulatory mechanism in the epigenetic properties of this organism. Future investigation on the 5'UTR of these genes can provide further illumination on the adaptation of *C. albicans* to host environments and its virulence properties. the role of the 5'UTR of these genes may be characterized as was done for *WOR1*, and polysome association or lack thereof can also be confirmed *in vivo* with an MS2-GFP reporter system.

SWR1 deposition of H2A.Z regulates *WOR1* expression on a nucleosomal level

The role of chromatin, and in particular that of nucleosomes and histones, in epigenetic regulation is a topic that has been much explored and debated over the past several decades. The regulation of epigenetic gene expression through histone modifications, in a sort of "histone code", is one often-suggested mechanism of regulation. However, the transience of most histone modifications points to the importance of additional chromatin-level epigenetic regulations. Alteration of chromatin dynamics through changes in nucleosome stability and turnover appears to be a promising mechanism. Histone modifications as well as histone variants have been shown

to play a role in changing nucleosomal dynamics, positioning, and stability. In this study, the histone variant H2A.Z was demonstrated to play a role in the regulation of *WOR1* expression and white-opaque switching. Abrogation of chromatin incorporation of H2A.Z, through the deletion of *SWR1*, promotes high-frequency white-opaque switching and opaque stability. The *swr1* mutant also shows altered nucleosome positioning and stability on the *WOR1* promoter, as seen by nucleosome mapping. Notably, these effects differ between white and opaque cells, and indeed the nucleosome map in wild-type cells on *WOR1* promoter differ between the two states as well. In addition, we found H2A.Z more enriched on the *WOR1* promoter in white cells, particularly adjacent to nucleosome-free regions. These results suggest that in white cells, the presence of H2A.Z on the *WOR1* promoter stabilizes nucleosome positioning and contributes to a repressive chromatin state, while the reduced H2A.Z on the promoter in opaque cells leads to a more open conformation conducive to expression of *WOR1*. Future work can explore whether other epigenetically regulated genes in *C. albicans* display this regulation by H2A.Z as well. Furthermore, we find that *yng2* produces an opaque-favoring phenotype similar to *swr1*, and both mutants are synergistic with CO_2 but not N-acetyl-glucosamine. Yng2 is a subunit of the NuA4 complex, which recruits SWR1 activity through histone H2 and H4 acetylation. In future work, we expect to see reduced H2A.Z incorporation on the *WOR1* promoter in *yng2* mutant. Further investigation of the interaction of the NuA4 and SWR1 complexes, and the correlation between H2/H4 acetylation and H2A.Z, may provide additional information on epigenetic regulation in *C. albicans*.

SWR1 deposition of H2A.Z interacts with H3K56ac

The role of H2A.Z in *C. albicans* is not limited to regulation of white-opaque switching. While switching was the common theme that prompted investigation of the relationship between H2A.Z and H3K56ac, which previous work in this lab has shown to promote opaque state, the findings in this study indicated more far-reaching consequences of their interaction. Nicotinamide (NAM) elevates H3K56ac and promotes white-opaque switching, and is known to be moderately toxic to *C. albicans* (Stevenson & Liu, 2011, Wurtele *et al.*, 2010). We find that *swr1* mutant is extremely sensitive to NAM, though not to other genotoxic stresses. Indeed, H2A phosphorylation, an indicator of first response to DNA damage, is not altered in *swr1* at all. These results point to unique global effects of interaction between H2A.Z and H3K56ac. In *S. cerevisiae*, high K56ac leads to reduced H2A.Z incorporation, and heightened eviction of H2A.Z-containing nucleosomes by SWR1 (Watanabe *et al.*, 2013). It is then possible that the elevation of H3K56ac in *swr1* mutant leads to growth defect by impaired turnover of H3K56ac-containing nucleosomes, as SWR1 activity is no longer extant. Additionally, *swr1* and H3K56ac have a synergistic effect on white-opaque switching, and this may also be explained by the effects of their interaction on nucleosome turnover. Genome-wide nucleosome mapping can be used in future studies to determine whether NAM-treated *swr1* cells show reduced nucleosome occupation at known H2A.Z-enriched regions. The interaction between H2A.Z deposition and H3K56ac may also exist in multicellular organisms.

The long *WOR1* promoter and phase-specific expression

The regulatory role of the *WOR1* promoter is of particular interest due to its length, as well as our findings in Chapter 4 that critical variations in nucleosome peaks between white and opaque were found on the -3 kb to -2 kb region of the promoter, where Wor1 protein is known to bind. We tested the sufficiency of this region of the *WOR1* promoter to drive expression in opaque cells, and found that while a 3 kb promoter (including the 5'UTR) was able to drive phase-specific expression of a GFP reporter, levels were lower than when a full-length promoter was used. In addition, truncating the promoter to 2.4 kb reduced expression even further. We further investigated the sufficiency of the 3 kb region to drive white-opaque switching by assaying the switching phenotype of a strain in which the sole copy of *WOR1* was under the 3 kb promoter. This strain was unable to form opaque cells through spontaneous switching, and even when *WOR1* was ectopically expressed for 48 hours. Thus, sequences upstream of -3 kb in the *WOR1* promoter are necessary to drive and maintain *WOR1* expression to such levels as to form and sustain opaque phase. Future studies can be done to correlate the binding sites of Wor1, as well as other positive and negative regulators of the *WOR1* circuity, to the regions of the *WOR1* promoter and map them to known nucleosome positions and NFRs. In particular, identification of binding sites for negative regulators at sites made inaccessible by high nucleosome occupancy in white cells, as shown in Chapter 4, can further illuminate the regulation of white-opaque switching through the *WOR1* promoter. As Wor1 binds to the promoters of other regulators of switching, similar studies on the promoters of these genes can be conducted as well to further characterize the white-opaque regulatory circuit.

Contribution of newly identified regulators to the dynamics of the white-opaque transition

The discovery of novel regulatory mechanisms of white-opaque switching also raises questions on their biological significance. In particular, the impact of these regulations on the timescale of switching and the processes behind cell fate determination. White-opaque switching is slow, stochastic, and occurs infrequently. Even with ectopic expression of *WOR1*, many hours still pass before endogenous Wor1 protein is expressed at high levels, and switching is able to occur. The *WOR1* 5'UTR provides one means through which opaque phase commitment is delayed. The reduced translational efficiency of *WOR1* conferred by the 5'UTR may be a mechanism for preventing rapid switching to opaque during transient increases of *WOR1* transcription, such that commitment to opaque only occurs when long-term conditions are favorable to opaque state. In this study, we also find that the translational regulation by the *WOR1* 5'UTR is more pronounced in white than opaque cells. In addition, the *WOR1* 5'UTR reduces stability of opaque state, which may also help cells more readily adjust to conditions that no longer favor opaque. We also note that the *WOR1* 5'UTR has effects extending beyond translational regulation. Within the 5'UTR-*WOR1*/ Δ 5'-*WOR1* strain, 5'UTR-*WOR1* transcript is present at higher levels than Δ 5'-*WOR1* for opaque cells at room temperature, indicating that transcript stability is increased by the 5'UTR. Finally, the 5'UTR is even less translationally-efficient at 37℃, promoting a more rapid transition to white phase at high temperature. Thus, the 5'UTR provides multiple regulations that help *C. albicans* adapt to environmental changes without responding inappropriately to environmental fluctuations. Regulation by the *WOR1* 5'UTR promotes white phase stability and opaque-to-white switching, adding a layer of regulation to *WOR1*, which itself promotes opaque. It will be intriguing to investigate whether 5'UTR of other genes serve to regulate cell fate, and reduce or delay switching and cell fate commitment. Nucleosome-level

regulations, such as those by H2A.Z and H3K56ac at the *WOR1* promoter, are also expected to occur on a longer timescale. The dynamic changes of H2A.Z and H3K56ac during the slow white-to-opaque transition are yet another topic to be further explored.

In summary, this work has identified novel regulators of white-opaque switching in *Candida albicans*, centering on the master regulator of switching, *WOR1*. The findings of this study contribute to a more comprehensive understanding of epigenetic regulation in *C. albicans*, particularly at the chromatin and translational levels, with implications for the regulation of other morphological transitions in *C. albicans*, as well as epigenetic regulation in other organisms.

Bibliography

Alby, K. & R.J. Bennett, (2009) Stress-induced phenotypic switching in Candida albicans. *Mol Biol Cell* **20**: 3178-3191.

Altaf, M., A. Auger, J. Monnet-Saksouk, J. Brodeur, S. Piquet, M. Cramet, N. Bouchard, N. Lacoste, R.T. Utley, L. Gaudreau & J. Cote, (2010) NuA4-dependent acetylation of nucleosomal histones H4 and H2A directly stimulates incorporation of H2A.Z by the SWR1 complex. *J Biol Chem* **285**: 15966-15977.

Bai, L., G. Charvin, E.D. Siggia & F.R. Cross, (2010) Nucleosome-depleted regions in cell-cycle-regulated promoters ensure reliable gene expression in every cell cycle. *Dev Cell* **18**: 544-555.

Berchowitz, L.E., A.S. Gajadhar, F.J. van Werven, A.A. De Rosa, M.L. Samoylova, G.A. Brar, Y. Xu, C. Xiao, B. Futcher, J.S. Weissman, F.M. White & A. Amon, (2013) A developmentally regulated translational control pathway establishes the meiotic chromosome segregation pattern. *Genes Dev* **27**: 2147-2163.

Bergen, M.S., E. Voss & D.R. Soll, (1990) Switching at the cellular level in the white-opaque transition of Candida albicans. *J Gen Microbiol* **136**: 1925-1936.

Blewett, N., J. Coller & A. Goldstrohm, (2011) A quantitative assay for measuring mRNA decapping by splinted ligation reverse transcription polymerase chain reaction: qSL-RT-PCR. *RNA* **17**: 535-543.

Briggs, D., D. Jackson, E. Whitelaw & N.J. Proudfoot, (1989) Direct demonstration of termination signals for RNA polymerase II from the sea urchin H2A histone gene. *Nucleic Acids Res* **17**: 8061-8071.

Brooks, W. & V. Jackson, (1994) The rapid transfer and selective association of histones H2A and H2B onto negatively coiled DNA at physiological ionic strength. *J Biol Chem* **269**: 18155-18166.

Bruno, V.M., Z. Wang, S.L. Marjani, G.M. Euskirchen, J. Martin, G. Sherlock & M. Snyder, (2010) Comprehensive annotation of the transcriptome of the human fungal pathogen Candida albicans using RNA-seq. *Genome Res* **20**: 1451-1458.

Calderone, R.A. & W.A. Fonzi, (2001) Virulence factors of Candida albicans. *Trends Microbiol* **9**: 327-335.

Cao, F., S. Lane, P.P. Raniga, Y. Lu, Z. Zhou, K. Ramon, J. Chen & H. Liu, (2006) The Flo8 transcription factor is essential for hyphal development and virulence in Candida albicans. *Mol Biol Cell* **17**: 295-307.

Celic, I., H. Masumoto, W.P. Griffith, P. Meluh, R.J. Cotter, J.D. Boeke & A. Verreault, (2006) The sirtuins hst3 and Hst4p preserve genome integrity by controlling histone h3 lysine 56 deacetylation. *Curr Biol* **16**: 1280-1289.

Chen, C.C., J.J. Carson, J. Feser, B. Tamburini, S. Zabaronick, J. Linger & J.K. Tyler, (2008) Acetylated lysine 56 on histone H3 drives chromatin assembly after repair and signals for the completion of repair. *Cell* **134**: 231-243.

Chen, J., S. Lane & H. Liu, (2002) A conserved mitogen-activated protein kinase pathway is required for mating in Candida albicans. *Mol Microbiol* **46**: 1335-1344.

Childers, D.S., V. Mundodi, M. Banerjee & D. Kadosh, (2014) A 5' UTR-mediated translational efficiency mechanism inhibits the Candida albicans morphological transition. *Mol Microbiol* **92**: 570-585.

Creyghton, M.P., S. Markoulaki, S.S. Levine, J. Hanna, M.A. Lodato, K. Sha, R.A. Young, R. Jaenisch & L.A. Boyer, (2008) H2AZ is enriched at polycomb complex target genes in ES cells and is necessary for lineage commitment. *Cell* **135**: 649-661.

Dion, M.F., T. Kaplan, M. Kim, S. Buratowski, N. Friedman & O.J. Rando, (2007) Dynamics of replication-independent histone turnover in budding yeast. *Science* **315**: 1405-1408.

Downs, J.A., S. Allard, O. Jobin-Robitaille, A. Javaheri, A. Auger, N. Bouchard, S.J. Kron, S.P. Jackson & J. Cote, (2004) Binding of chromatin-modifying activities to phosphorylated histone H2A at DNA damage sites. *Mol Cell* **16**: 979-990.

Drinnenberg, I.A., D.E. Weinberg, K.T. Xie, J.P. Mower, K.H. Wolfe, G.R. Fink & D.P. Bartel, (2009) RNAi in budding yeast. *Science* **326**: 544-550.

Driscoll, R., A. Hudson & S.P. Jackson, (2007) Yeast Rtt109 promotes genome stability by acetylating histone H3 on lysine 56. *Science* **315**: 649-652.

Dvir, S., L. Velten, E. Sharon, D. Zeevi, L.B. Carey, A. Weinberger & E. Segal, (2013) Deciphering the rules by which 5'-UTR sequences affect protein expression in yeast. *Proc Natl Acad Sci U S A* **110**: E2792-2801.

Gilbert, W.V., K. Zhou, T.K. Butler & J.A. Doudna, (2007) Cap-independent translation is required for starvation-induced differentiation in yeast. *Science* **317**: 1224-1227.

Gray, N.K. & M.W. Hentze, (1994) Regulation of protein synthesis by mRNA structure. *Mol Biol Rep* **19**: 195-200.

Greaves, I.K., D. Rangasamy, P. Ridgway & D.J. Tremethick, (2007) H2A.Z contributes to the unique 3D structure of the centromere. *Proc Natl Acad Sci U S A* **104**: 525-530.

Guillemette, B., A.R. Bataille, N. Gevry, M. Adam, M. Blanchette, F. Robert & L. Gaudreau, (2005) Variant histone H2A.Z is globally localized to the promoters of inactive yeast genes and regulates nucleosome positioning. *PLoS Biol* **3**: e384.

Han, J., H. Zhou, B. Horazdovsky, K. Zhang, R.M. Xu & Z. Zhang, (2007) Rtt109 acetylates histone H3 lysine 56 and functions in DNA replication. *Science* **315**: 653-655.

Hellen, C.U. & P. Sarnow, (2001) Internal ribosome entry sites in eukaryotic mRNA molecules. *Genes Dev* **15**: 1593-1612.

Henikoff, S., (2008) Nucleosome destabilization in the epigenetic regulation of gene expression. *Nat Rev Genet* **9**: 15-26.

Henikoff, S., (2009) Labile H3.3+H2A.Z nucleosomes mark 'nucleosome-free regions'. *Nat Genet* **41**: 865-866.

Hernday, A.D., M.B. Lohse, P.M. Fordyce, C.J. Nobile, J.L. DeRisi & A.D. Johnson, (2013) Structure of the transcriptional network controlling white-opaque switching in Candida albicans. *Mol Microbiol* **90**: 22-35.

Huang, G., T. Srikantha, N. Sahni, S. Yi & D.R. Soll, (2009) CO(2) regulates white-to-opaque switching in Candida albicans. *Curr Biol* **19**: 330-334.

Huang, G., H. Wang, S. Chou, X. Nie, J. Chen & H. Liu, (2006) Bistable expression of WOR1, a master regulator of white-opaque switching in Candida albicans. *Proc Natl Acad Sci U S A* **103**: 12813-12818.

Huang, G., S. Yi, N. Sahni, K.J. Daniels, T. Srikantha & D.R. Soll, (2010) N-acetylglucosamine induces white to opaque switching, a mating prerequisite in Candida albicans. *PLoS Pathog* **6**: e1000806.

Jackson, J.D., V.T. Falciano & M.A. Gorovsky, (1996) A likely histone H2A.F/Z variant in Saccharomyces cerevisiae. *Trends Biochem Sci* **21**: 466-467.

Jackson, J.D. & M.A. Gorovsky, (2000) Histone H2A.Z has a conserved function that is distinct from that of the major H2A sequence variants. *Nucleic Acids Res* **28**: 3811-3816.

Jackson, S., W. Brooks & V. Jackson, (1994) Dynamics of the interactions of histones H2A,H2B and H3,H4 with torsionally stressed DNA. *Biochemistry* **33**: 5392-5403.

Jackson, V., (1987) Deposition of newly synthesized histones: new histones H2A and H2B do not deposit in the same nucleosome with new histones H3 and H4. *Biochemistry* **26**: 2315-2325.

Janbon, G., F. Sherman & E. Rustchenko, (1998) Monosomy of a specific chromosome determines L-sorbose utilization: a novel regulatory mechanism in Candida albicans. *Proc Natl Acad Sci U S A* **95**: 5150-5155.

Kalocsay, M., N.J. Hiller & S. Jentsch, (2009) Chromosome-wide Rad51 spreading and SUMO-H2A.Z-dependent chromosome fixation in response to a persistent DNA double-strand break. *Mol Cell* **33**: 335-343.

Kent, N.A. & J. Mellor, (1995) Chromatin structure snap-shots: rapid nuclease digestion of chromatin in yeast. *Nucleic Acids Res* **23**: 3786-3787.

Kobor, M.S., S. Venkatasubrahmanyam, M.D. Meneghini, J.W. Gin, J.L. Jennings, A.J. Link, H.D. Madhani & J. Rine, (2004) A protein complex containing the conserved Swi2/Snf2-related ATPase Swr1p deposits histone variant H2A.Z into euchromatin. *PLoS Biol* **2**: E131.

Kolonko, E.M., B.N. Albaugh, S.E. Lindner, Y. Chen, K.A. Satyshur, K.M. Arnold, P.D. Kaufman, J.L. Keck & J.M. Denu, (2010) Catalytic activation of histone acetyltransferase Rtt109 by a histone chaperone. *Proc Natl Acad Sci U S A* **107**: 20275-20280.

Kortmann, J. & F. Narberhaus, (2012) Bacterial RNA thermometers: molecular zippers and switches. *Nat Rev Microbiol* **10**: 255-265.

Kvaal, C., S.A. Lachke, T. Srikantha, K. Daniels, J. McCoy & D.R. Soll, (1999) Misexpression of the opaque-phase-specific gene PEP1 (SAP1) in the white phase of Candida albicans

confers increased virulence in a mouse model of cutaneous infection. *Infect Immun* **67**: 6652-6662.

Lachke, S.A., S.R. Lockhart, K.J. Daniels & D.R. Soll, (2003) Skin facilitates Candida albicans mating. *Infect Immun* **71**: 4970-4976.

Levchenko, V., B. Jackson & V. Jackson, (2005) Histone release during transcription: displacement of the two H2A-H2B dimers in the nucleosome is dependent on different levels of transcription-induced positive stress. *Biochemistry* **44**: 5357-5372.

Levchenko, V. & V. Jackson, (2004) Histone release during transcription: NAP1 forms a complex with H2A and H2B and facilitates a topologically dependent release of H3 and H4 from the nucleosome. *Biochemistry* **43**: 2359-2372.

Li, Q., H. Zhou, H. Wurtele, B. Davies, B. Horazdovsky, A. Verreault & Z. Zhang, (2008) Acetylation of histone H3 lysine 56 regulates replication-coupled nucleosome assembly. *Cell* **134**: 244-255.

Liu, X., B. Li & GorovskyMa, (1996) Essential and nonessential histone H2A variants in Tetrahymena thermophila. *Mol Cell Biol* **16**: 4305-4311.

Lo, H.J., J.R. Kohler, B. DiDomenico, D. Loebenberg, A. Cacciapuoti & G.R. Fink, (1997) Nonfilamentous C. albicans mutants are avirulent. *Cell* **90**: 939-949.

Lohse, M.B., A.D. Hernday, P.M. Fordyce, L. Noiman, T.R. Sorrells, V. Hanson-Smith, C.J. Nobile, J.L. DeRisi & A.D. Johnson, (2013) Identification and characterization of a previously undescribed family of sequence-specific DNA-binding domains. *Proc Natl Acad Sci U S A* **110**: 7660-7665.

Lohse, M.B. & A.D. Johnson, (2008) Differential phagocytosis of white versus opaque Candida albicans by Drosophila and mouse phagocytes. *PLoS One* **3**: e1473.

Lohse, M.B., R.E. Zordan, C.W. Cain & A.D. Johnson, (2010) Distinct class of DNA-binding domains is exemplified by a master regulator of phenotypic switching in Candida albicans. *Proc Natl Acad Sci U S A* **107**: 14105-14110.

Lopes da Rosa, J., V. Bajaj, J. Spoonamore & P.D. Kaufman, (2013) A small molecule inhibitor of fungal histone acetyltransferase Rtt109. *Bioorg Med Chem Lett* **23**: 2853-2859.

Lopes da Rosa, J., V.L. Boyartchuk, L.J. Zhu & P.D. Kaufman, (2010) Histone acetyltransferase Rtt109 is required for Candida albicans pathogenesis. *Proc Natl Acad Sci U S A* **107**: 1594-1599.

Lu, Y., C. Su, X. Mao, P.P. Raniga, H. Liu & J. Chen, (2008) Efg1-mediated recruitment of NuA4 to promoters is required for hypha-specific Swi/Snf binding and activation in Candida albicans. *Mol Biol Cell* **19**: 4260-4272.

Lu, Y., C. Su, A. Wang & H. Liu, (2011) Hyphal development in Candida albicans requires two temporally linked changes in promoter chromatin for initiation and maintenance. *PLoS Biol* **9**: e1001105.

Luger, K., A.W. Mader, R.K. Richmond, D.F. Sargent & T.J. Richmond, (1997) Crystal structure of the nucleosome core particle at 2.8 A resolution. *Nature* **389**: 251-260.

Maas, N.L., K.M. Miller, L.G. DeFazio & D.P. Toczyski, (2006) Cell cycle and checkpoint regulation of histone H3 K56 acetylation by Hst3 and Hst4. *Mol Cell* **23**: 109-119.

Manning, M. & T.G. Mitchell, (1980) Strain variation and morphogenesis of yeast- and mycelial-phase Candida albicans in low-sulfate, synthetic medium. *J Bacteriol* **142**: 714-719.

Masek, T., L. Valasek & M. Pospisek, (2011) Polysome analysis and RNA purification from sucrose gradients. *Methods Mol Biol* **703**: 293-309.

Masumoto, H., D. Hawke, R. Kobayashi & A. Verreault, (2005) A role for cell-cycle-regulated histone H3 lysine 56 acetylation in the DNA damage response. *Nature* **436**: 294-298.

McQuillen, K., R.B. Roberts & R.J. Britten, (1959) Synthesis of Nascent Protein by Ribosomes in Escherichia Coli. *Proc Natl Acad Sci U S A* **45**: 1437-1447.

Meijer, H.A., Y.W. Kong, W.T. Lu, A. Wilczynska, R.V. Spriggs, S.W. Robinson, J.D. Godfrey, A.E. Willis & M. Bushell, (2013) Translational repression and eIF4A2 activity are critical for microRNA-mediated gene regulation. *Science* **340**: 82-85.

Meimoun, A., T. Holtzman, Z. Weissman, H.J. McBride, D.J. Stillman, G.R. Fink & D. Kornitzer, (2000) Degradation of the transcription factor Gcn4 requires the kinase Pho85 and the SCF(CDC4) ubiquitin-ligase complex. *Mol Biol Cell* **11**: 915-927.

Meneghini, M.D., M. Wu & H.D. Madhani, (2003) Conserved histone variant H2A.Z protects euchromatin from the ectopic spread of silent heterochromatin. *Cell* **112**: 725-736.

Miller, M.G. & A.D. Johnson, (2002) White-opaque switching in Candida albicans is controlled by mating-type locus homeodomain proteins and allows efficient mating. *Cell* **110**: 293-302.

Mizuguchi, G., X. Shen, J. Landry, W.H. Wu, S. Sen & C. Wu, (2004) ATP-driven exchange of histone H2AZ variant catalyzed by SWR1 chromatin remodeling complex. *Science* **303**: 343-348.

Morillo-Huesca, M., M. Clemente-Ruiz, E. Andujar & F. Prado, (2010) The SWR1 histone replacement complex causes genetic instability and genome-wide transcription misregulation in the absence of H2A.Z. *PLoS One* **5**: e12143.

Morris, D.R. & A.P. Geballe, (2000) Upstream open reading frames as regulators of mRNA translation. *Mol Cell Biol* **20**: 8635-8642.

Nagalakshmi, U., Z. Wang, K. Waern, C. Shou, D. Raha, M. Gerstein & M. Snyder, (2008) The transcriptional landscape of the yeast genome defined by RNA sequencing. *Science* **320**: 1344-1349.

Noble, S.M. & A.D. Johnson, (2005) Strains and strategies for large-scale gene deletion studies of the diploid human fungal pathogen Candida albicans. *Eukaryot Cell* **4**: 298-309.

Odds, F.C., (1987) Candida infections: an overview. *Crit Rev Microbiol* **15**: 1-5.

Pande, K., C. Chen & S.M. Noble, (2013) Passage through the mammalian gut triggers a phenotypic switch that promotes Candida albicans commensalism. *Nat Genet* **45**: 1088-1091.

Park, Y.J., P.N. Dyer, D.J. Tremethick & K. Luger, (2004) A new fluorescence resonance energy transfer approach demonstrates that the histone variant H2AZ stabilizes the histone octamer within the nucleosome. *J Biol Chem* **279**: 24274-24282.

Pickering, B.M. & A.E. Willis, (2005) The implications of structured 5' untranslated regions on translation and disease. *Semin Cell Dev Biol* **16**: 39-47.

Raisner, R.M., P.D. Hartley, M.D. Meneghini, M.Z. Bao, C.L. Liu, S.L. Schreiber, O.J. Rando & H.D. Madhani, (2005) Histone variant H2A.Z marks the 5' ends of both active and inactive genes in euchromatin. *Cell* **123**: 233-248.

Ramirez-Zavala, B., O. Reuss, Y.N. Park, K. Ohlsen & J. Morschhauser, (2008) Environmental induction of white-opaque switching in Candida albicans. *PLoS Pathog* **4**: e1000089.

Ranjan, A., G. Mizuguchi, P.C. FitzGerald, D. Wei, F. Wang, Y. Huang, E. Luk, C.L. Woodcock & C. Wu, (2013) Nucleosome-free region dominates histone acetylation in targeting SWR1 to promoters for H2A.Z replacement. *Cell* **154**: 1232-1245.

Rikkerink, E.H., B.B. Magee & P.T. Magee, (1988) Opaque-white phenotype transition: a programmed morphological transition in Candida albicans. *J Bacteriol* **170**: 895-899.

Roemer, T., B. Jiang, J. Davison, T. Ketela, K. Veillette, A. Breton, F. Tandia, A. Linteau, S. Sillaots, C. Marta, N. Martel, S. Veronneau, S. Lemieux, S. Kauffman, J. Becker, R. Storms, C. Boone & H. Bussey, (2003) Large-scale essential gene identification in Candida albicans and applications to antifungal drug discovery. *Mol Microbiol* **50**: 167-181.

Rufiange, A., P.E. Jacques, W. Bhat, F. Robert & A. Nourani, (2007) Genome-wide replication-independent histone H3 exchange occurs predominantly at promoters and implicates H3 K56 acetylation and Asf1. *Mol Cell* **27**: 393-405.

Slutsky, B., M. Staebell, J. Anderson, L. Risen, M. Pfaller & D.R. Soll, (1987) "White-opaque transition": a second high-frequency switching system in Candida albicans. *J Bacteriol* **169**: 189-197.

Sonneborn, A., B. Tebarth & J.F. Ernst, (1999) Control of white-opaque phenotypic switching in Candida albicans by the Efg1p morphogenetic regulator. *Infect Immun* **67**: 4655-4660.

Srikantha, T., A.R. Borneman, K.J. Daniels, C. Pujol, W. Wu, M.R. Seringhaus, M. Gerstein, S. Yi, M. Snyder & D.R. Soll, (2006) TOS9 regulates white-opaque switching in Candida albicans. *Eukaryot Cell* **5**: 1674-1687.

Srikantha, T., L.K. Tsai, K. Daniels & D.R. Soll, (2000) EFG1 null mutants of Candida albicans switch but cannot express the complete phenotype of white-phase budding cells. *J Bacteriol* **182**: 1580-1591.

Stevenson, J.S. & H. Liu, (2011) Regulation of white and opaque cell-type formation in Candida albicans by Rtt109 and Hst3. *Mol Microbiol* **81**: 1078-1091.

Stevenson, J.S. & H. Liu, (2013) Nucleosome assembly factors CAF-1 and HIR modulate epigenetic switching frequencies in an H3K56 acetylation-associated manner in Candida albicans. *Eukaryot Cell* **12**: 591-603.

Su, C., Y. Lu & H. Liu, (2013) Reduced TOR signaling sustains hyphal development in Candida albicans by lowering Hog1 basal activity. *Mol Biol Cell* **24**: 385-397.

Sundaram, A. & C.M. Grant, (2014) A single inhibitory upstream open reading frame (uORF) is sufficient to regulate Candida albicans GCN4 translation in response to amino acid starvation conditions. *RNA* **20**: 559-567.

Teves, S.S., C.M. Weber & S. Henikoff, Transcribing through the nucleosome. *Trends in Biochemical Sciences* **39**: 577-586.

Teves, S.S., C.M. Weber & S. Henikoff, (2014) Transcribing through the nucleosome. *Cell* **39**: 577-586.

Tuch, B.B., Q.M. Mitrovich, O.R. Homann, A.D. Hernday, C.K. Monighetti, F.M. De La Vega & A.D. Johnson, (2010) The transcriptomes of two heritable cell types illuminate the circuit governing their differentiation. *PLoS Genet* **6**: e1001070.

van Daal, A. & S.C. Elgin, (1992) A histone variant, H2AvD, is essential in Drosophila melanogaster. *Mol Biol Cell* **3**: 593-602.

Wang, H., W. Song, G. Huang, Z. Zhou, Y. Ding & J. Chen, (2011) Candida albicans Zcf37, a zinc finger protein, is required for stabilization of the white state. *FEBS Lett* **585**: 797-802.

Warner, J.R., P.M. Knopf & A. Rich, (1963) A multiple ribosomal structure in protein synthesis. *Proc Natl Acad Sci U S A* **49**: 122-129.

Watanabe, S., M. Radman-Livaja, O.J. Rando & C.L. Peterson, (2013) A histone acetylation switch regulates H2A.Z deposition by the SWR-C remodeling enzyme. *Science* **340**: 195-199.

Weber, C.M. & S. Henikoff, (2014) Histone variants: dynamic punctuation in transcription. *Genes Dev* **28**: 672-682.

Wey, S.B., M. Mori, M.A. Pfaller, R.F. Woolson & R.P. Wenzel, (1988) Hospital-acquired candidemia. The attributable mortality and excess length of stay. *Arch Intern Med* **148**: 2642-2645.

Williams, S.K., D. Truong & J.K. Tyler, (2008) Acetylation in the globular core of histone H3 on lysine-56 promotes chromatin disassembly during transcriptional activation. *Proc Natl Acad Sci U S A* **105**: 9000-9005.

Wunsch, A. & V. Jackson, (2005) Histone release during transcription: acetylation stabilizes the interaction of the H2A-H2B dimer with the H3-H4 tetramer in nucleosomes that are on highly positively coiled DNA. *Biochemistry* **44**: 16351-16364.

Wurtele, H., S. Tsao, G. Lepine, A. Mullick, J. Tremblay, P. Drogaris, E.H. Lee, P. Thibault, A. Verreault & M. Raymond, (2010) Modulation of histone H3 lysine 56 acetylation as an antifungal therapeutic strategy. *Nat Med* **16**: 774-780.

Xie, J., L. Tao, C.J. Nobile, Y. Tong, G. Guan, Y. Sun, C. Cao, A.D. Hernday, A.D. Johnson, L. Zhang, F.Y. Bai & G. Huang, (2013) White-opaque switching in natural MTLa/alpha isolates of Candida albicans: evolutionary implications for roles in host adaptation, pathogenesis, and sex. *PLoS Biol* **11**: e1001525.

Xu, F., K. Zhang & M. Grunstein, (2005) Acetylation in histone H3 globular domain regulates gene expression in yeast. *Cell* **121**: 375-385.

Xu, Y., M.K. Ayrapetov, C. Xu, O. Gursoy-Yuzugullu, Y. Hu & B.D. Price, (2012) Histone H2A.Z controls a critical chromatin remodeling step required for DNA double-strand break repair. *Mol Cell* **48**: 723-733.

Zentner, G.E. & S. Henikoff, (2013) Regulation of nucleosome dynamics by histone modifications. *Nat Struct Mol Biol* **20**: 259-266.

Zhang, H., D.O. Richardson, D.N. Roberts, R. Utley, H. Erdjument-Bromage, P. Tempst, J. Cote & B.R. Cairns, (2004) The Yaf9 component of the SWR1 and NuA4 complexes is required for proper gene expression, histone H4 acetylation, and Htz1 replacement near telomeres. *Mol Cell Biol* **24**: 9424-9436.

Zordan, R.E., D.J. Galgoczy & A.D. Johnson, (2006) Epigenetic properties of white-opaque switching in Candida albicans are based on a self-sustaining transcriptional feedback loop. *Proc Natl Acad Sci U S A* **103**: 12807-12812.

Zordan, R.E., M.G. Miller, D.J. Galgoczy, B.B. Tuch & A.D. Johnson, (2007) Interlocking transcriptional feedback loops control white-opaque switching in Candida albicans. *PLoS Biol* **5**: e256.